SAND REPORT

SAND2003-3410
Unlimited Release
Printed September 2003

Chemiresistor Microsensors for In-Situ Monitoring of Volatile Organic Compounds: Final LDRD Report

Clifford K. Ho, Lucas K. McGrath, Chad E. Davis, Michael L. Thomas, Jerome L. Wright, Ara S. Kooser, and Robert C. Hughes

Prepared by
Sandia National Laboratories
Albuquerque, New Mexico 87185 and Livermore, California 94550

Sandia is a multiprogram laboratory operated by Sandia Corporation, a Lockheed Martin Company, for the United States Department of Energy under Contract DE-AC04-94AL85000.

Issued by Sandia National Laboratories, operated for the United States Department of Energy by Sandia Corporation.

Available to DOE and DOE contractors from
U.S. Department of Energy
Office of Scientific and Technical Information
P.O. Box 62
Oak Ridge, TN 37831

Telephone: (865)576-8401
Facsimile: (865)576-5728
E-Mail: reports@adonis.osti.gov
Online ordering: http://www.doe.gov/bridge

Available to the public from
U.S. Department of Commerce
National Technical Information Service
5285 Port Royal Rd
Springfield, VA 22161

Telephone: (800)553-6847
Facsimile: (703)605-6900
E-Mail: orders@ntis.fedworld.gov
Online order: http://www.ntis.gov/help/ordermethods.asp?loc=7-4-0#online

SAND2003-3410
Unlimited Release
Printed September 2003

Chemiresistor Microsensors for In-Situ Monitoring of Volatile Organic Compounds: Final LDRD Report

Clifford K. Ho,[1] Lucas K. McGrath,[1] Chad E. Davis,[2] Michael L. Thomas,[2] Jerome L. Wright,[1] Ara S. Kooser,[1] and Robert C. Hughes[2]

[1]Geohydrology Department
[2]Microsensors Science & Technology Department

Sandia National Laboratories
P.O. Box 5800, MS-0735
Albuquerque, NM 87185-0735
Contact: (505) 844-2384; ckho@sandia.gov

Abstract

This report provides a summary of the three-year LDRD (Laboratory Directed Research and Development) project aimed at developing microchemical sensors for continuous, in-situ monitoring of volatile organic compounds. A chemiresistor sensor array was integrated with a unique, waterproof housing that allows the sensors to be operated in a variety of media including air, soil, and water. Numerous tests were performed to evaluate and improve the sensitivity, stability, and discriminatory capabilities of the chemiresistors. Field tests were conducted in California, Nevada, and New Mexico to further test and develop the sensors in actual environments within integrated monitoring systems. The field tests addressed issues regarding data acquisition, telemetry, power requirements, data processing, and other engineering requirements. Significant advances were made in the areas of polymer optimization, packaging, data analysis, discrimination, design, and information dissemination (e.g., real-time web posting of data; see www.sandia.gov/sensor).

This project has stimulated significant interest among commercial and academic institutions. A CRADA (Cooperative Research and Development Agreement) was initiated in FY03 to investigate manufacturing methods, and a Work for Others contract was established between Sandia and Edwards Air Force Base for FY02-FY04. Funding was also obtained from DOE as part of their Advanced Monitoring Systems Initiative program from FY01 to FY03, and a DOE EMSP contract was awarded jointly to Sandia and INEEL for FY04-FY06. Contracts were also established for collaborative research with Brigham Young University to further evaluate, understand, and improve the performance of the chemiresistor sensors.

Acknowledgments

The authors thank the following individuals for their contributions to various aspects of this project:

Chemiresistor/Preconcentrator Technology & Fabrication:

- Graham Yelton, Mark Jenkins, John Lucero, Tina Petersen, Gayle Schwartz, Jonathan Blaich, Cathy Nowlen, Cathy Reber, Steve Showalter, Richard Kottenstette, Ron Manginell (SNL)

Packaging:

- Paul Reynolds (Team Specialty Products)

Testing, Calibration, and Data Acquisition:

- Irene Ma, Angela McLain (SNL Student Interns), Dan Lucero, Jeff Zirzow (SNL)

Data Analysis:

- Dion Rivera, Kathy Alam (SNL)

Field Testing:

- James May, Mary Spencer, Irene Nester (Edwards AFB)
- Charles Lohrstorfer (Bechtel NV), Warren Cox (SNL) (Nevada Test Site)
- Sue Collins, Robert Ziock, Henry Bryant, Sharissa Young, David Miller (Chemical Waste Landfill, SNL)

This work was funded by Sandia's Laboratorary Directed Research and Development Project 26553. Sandia is a multiprogram laboratory operated by Sandia Corporation, a Lockheed Martin Company, for the United States Department of Energy under Contract DE-AC04-94AL85000.

Contents

List of Figures

List of Tables

1. Executive Summary

The objective of this LDRD project was to develop a microchemical sensor system for unattended real-time monitoring and characterization of volatile organic compounds (VOCs) in soil and groundwater. The intent was to reduce the high costs associated with manual sampling methods while improving public and stakeholder confidence in long-term monitoring and environmental stewardship activities.

An in-situ chemiresistor sensor probe was developed that can continuously monitor VOCs in a variety of media including air, soil, and water. The chemiresistor itself consists of a conductive polymer deposited onto a microfabricated circuit. The polymer swells reversibly in the presence of VOCs as vapor-phase molecules absorb into the polymer, causing a change in the electrical resistance of the circuit that can be calibrated to known concentrations of analytes. An array of four chemiresistors has been fabricated on a single chip to aid in discrimination, and many polymers were tested and evaluated to yield an optimized array of chemiresistors to detect the subsurface contaminants of interest. Data analysis methods employing pattern recognition techniques (e.g., VERI) and statistical methods (e.g., partial-least squares) were investigated and evaluated using data obtained from the chemiresistor array when exposed to a variety of environmental conditions and analytes. Preconcentrators were also investigated as a means of increasing the sensitivity of the chemiresistor sensors, and automated on-chip temperature control methods were developed to produce more stable responses.

In addition to laboratory testing and evaluation of the chemiresistor sensors, a complete in-situ chemiresistor monitoring system was developed for field applications. A rugged, waterproof housing was constructed that allows the chemiresistor to be emplaced in monitoring wells or immersed in water. A cable connects the sensor to a surface-based solar-powered data logger employing wireless telemetry. Data can be collected automatically and uploaded to a web site (e.g., see www.sandia.gov/sensor/cwl). Field tests of the in-situ chemiresistor sensor system were conducted at Edwards Air Force Base, CA, the Nevada Test Site, and the Chemical Waste Landfill, NM. Results of these field tests show that the in-situ chemiresistor sensor shows promise for use in long-term monitoring activities for trichloroethylene and other VOCs in the subsurface.

New and alternative designs and applications for the chemiresistor sensor (e.g., concentric spiral configuration, Chemicouples,™ ChemSticks,™ Bioresistors,™ automated monitoring and remediation systems) have been developed as part of this LDRD project. These new concepts and applications have led to seven patent applications and eight technical advances, a dozen scientific publications, nearly 20 invited and contributed presentations, media coverage in over 30 magazines and news publications, a CRADA, Work for Others contracts, and collaborations with academic universities. Collectively, nearly $700K of external revenue has been generated as a result of this LDRD project, and additional collaborations are currently being initiated.

This page intentionally left blank.

2. Introduction

Thousands of sites containing toxic chemical spills, leaking underground storage tanks, and chemical waste dumps require characterization and long-term monitoring to reduce health risks and ensure public safety (http://www.epa.gov/superfund). In addition, over two million underground storage tanks containing hazardous (and often volatile) contaminants are being regulated by the EPA (U.S. EPA, 1992), and the tanks require some form of monitoring to detect leaks from the tanks and pipe network. However, current methods are costly and time-intensive, and limitations in sampling and analytical techniques exist. Looney and Falta (2000, Ch. 4) report that the Department of Energy (DOE) Savannah River Site requires manual collection of nearly 40,000 groundwater samples per year, which can cost between $100 to $1,000 per sample for off-site analysis. Wilson et al. (1995, Ch. 36) report that as much as 80% of the costs associated with site characterization and cleanup of a Superfund site can be attributed to laboratory analyses. In addition, the integrity of the analyses can be compromised during sample collection, transport, and storage. Clearly, a need exists for accurate, inexpensive, real-time, in-situ analyses using robust sensors that can be remotely operated.

Although a number of chemical sensors are commercially available for field measurements of chemical species (e.g., portable gas chromatographs, surface-wave acoustic sensors, optical instruments, etc.), few have been adapted for use in geologic environments for long-term monitoring or remediation applications.

2.1. Objectives and Scope

The objective of this LDRD (Laboratory Directed Research and Development) project was to develop a microchemical sensor system that can detect and monitor subsurface volatile organic compounds (VOCs) for potentially long-term applications. As part of the first year of the LDRD project, Ho et al. (2001) conducted a survey of sensor technologies and concluded that conductometric (chemiresistor) sensors were strong candidates for long-term in-situ monitoring applications because of their simplicity (no moving parts) and ruggedness. As a result, the bulk of the LDRD project focused on developing, designing, improving, and understanding the technology and performance of the chemiresistor sensors for operation in long-term subsurface monitoring environments. The resulting in-situ chemiresistor sensor system can be applied to other applications requiring real-time in-situ monitoring (e.g., air monitoring, homeland security, etc.).

2.2. Overview of Report

This report first provides a description of the chemiresistor sensor and it's basic operation in Section 3. Laboratory testing and evaluation of the chemiresistor and its components (e.g., polymers and preconcentrators) are discussed in Sections 4 and 5, and data analysis methods are presented in Section 6. Field tests are described in Section 7, and alternative chemiresistor

designs and applications are described in Section 8. A "return on investment" from this project is presented in Section 9, and recommendations for future work are discussed in Section 9.

3. Chemiresistor Sensor

3.1. Description

The chemiresistor sensor is a chemically sensitive resistor comprised of a conductive polymer film deposited on a micro-fabricated circuit. The chemically-sensitive insulating polymer is dissolved in a solvent and mixed with conductive carbon particles. The resulting ink is then deposited and dried onto thin-film, parallel, non-intersecting platinum traces on a solid substrate (chip). When chemical vapors come into contact with the polymers, the chemicals absorb into the polymers, causing them to swell. The swelling changes the physical conformation of the conductive particles in the polymer film, thereby changing the electrical resistance across the platinum-trace electrodes, which can be measured and recorded using a data logger or an ohmmeter (see Figure 1). The swelling is reversible if the chemical vapors are removed, but some hysteresis can occur at high concentration exposures. The amount of swelling corresponds to the concentration of the chemical vapor in contact with the chemiresistor, so these devices can be calibrated by exposing the chemiresistors to known concentrations of target analytes.

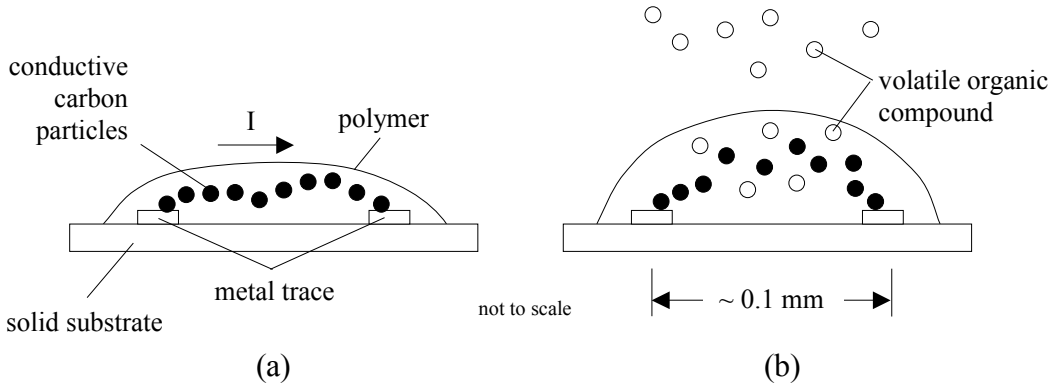

Figure 1. VOC detection by a thin-film chemiresistor: (a) Electrical current (I) flows across a conductive thin-film carbon-loaded polymer deposited on a pair of micro-fabricated electrodes; (b) VOCs absorb into the polymer, causing it to swell (reversibly) and break some of the conductive pathways, which increases the electrical resistance.

Figure 2 shows the architecture of the microsensor, which integrates an array of chemiresistors with a temperature sensor and heating elements (Hughes et al., 2000). The chemiresistor array has been shown to detect a variety of VOCs including aromatic hydrocarbons (e.g., benzene), chlorinated solvents (e.g., trichloroethylene (TCE), carbon tetrachloride), aliphatic hydrocarbons (e.g., hexane, iso-octane), alcohols, and ketones (e.g., acetone). The on-board temperature

sensor comprised of a thin-film platinum trace can be used to not only monitor the in-situ temperature, but it can also be used in a temperature control system. A feedback control system between the temperature sensor and on-board heating elements can allow the chemiresistors to be maintained at a fairly constant temperature, which can aid in the processing of data when comparing the responses to calibrated training sets. In addition, the chemiresistors can be maintained at a temperature above the ambient to prevent condensation of water, which may be detrimental to the wires and surfaces of the chemiresistor.

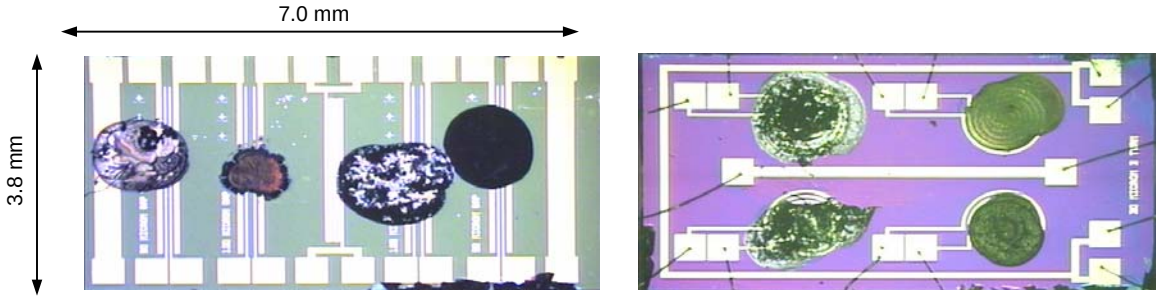

Figure 2. Chemiresistor arrays developed at Sandia with four conductive polymer films (black spots) deposited onto platinum wire traces on a silicon wafer substrate. Left: Linear-electrode design (device #C4) with a temperature sensor in the middle and heating elements on the ends. Right: New spiral-electrode design (device #E2) with temperature sensor on the perimeter and heating element in the middle.

3.2. Fabrication

3.2.1. Chip Fabrication

The chemiresistor chips are created using standard photolithographic methods, similar to the manufacture of microprocessors for PCs. A mask is designed and fabricated to define the metal traces that will be deposited on a silicon wafer. Three-inch and four-inch silicon wafers have been used in this project. A typical process used to fabricate a four-inch silicon chemiresistor wafer is shown below:

1) Solvent clean wafer – acetone, methanol, isopropanol, N2 dry.
2) LFE O2 plasma clean, 5min 10 watts.
3) 790 PECVD deposition: 2000Å SiN.
4) Solvent clean wafer – acetone, methanol, isopropanol, N2 dry.
5) HMDS – 33 minutes.
6) Coat wafer with AZ4330 photoresist.
7) Spin at 4K rpm for 30 seconds.
8) Soft bake at 90°C for 90 seconds.
9) Exposure on MA6 Aligner for 6.5 seconds.
10) Develop in MIF 319 for approx. 2.5 minutes.
11) Ozone clean for 5 minutes.
12) Metal Deposition in Temescal – 100Å Ti and 1000Å Pt. (Note: Make sure to use minute sweep on Pt.)

13) Lift off – Place wafer on texwipe and spray in Acetone for a couple minutes, soak in Acetone for a couple of hours.
14) Solvent clean wafer – acetone, methanol, isopropanol, N2 dry.

Figure 3 shows an image of half of a silicon chemiresistor wafer where some of the chemiresistor dies have been removed.

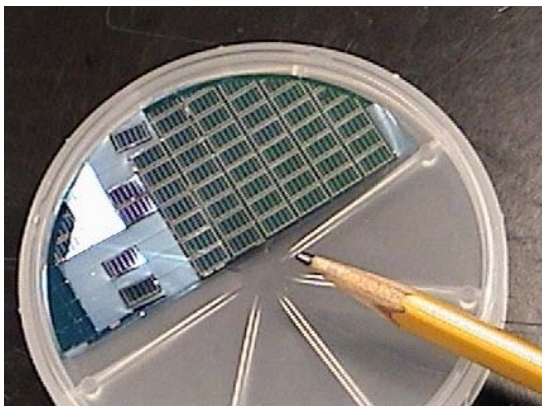

Figure 3. Chemiresistor dies fabricated from half of a silicon wafer.

3.2.2. Ink Creation

The chemiresistor ink is a mixture of a know concentration of polymer, carbon, and solvent. The inks are created by measuring out a known mass of polymer and dissolving it in a solvent. Typically the mass of carbon and polymer totals 0.1 g and is mixed in 5 ml of solvent. The solvent is chosen based on the polymers' solubility. For example, for the polar polymer poly (N-vinyl pyrolidone) (PNVP), water is used as the solvent. For the other three polymers that were selected for our application (poly(epichlorohydrin) (PECH), poly(ethylene-vinyl acetate) (PEVA), and poly(isobutylene) (PIB)), TCE is used to dissolve the polymers (see Section 4.2 for more details on polymer selection). The polymer/solvent mixture is placed on a hotplate set to approximately 40 °C. The polymer will normally go into solution within an hour with heating. After the polymer is in solution a measured quantity of carbon is added to the mixture. The vials are then placed in a sonicating bath for an hour to increase the dispersion of the carbon in the solution. The ink is then ready to deposited on the dies. Figure 4 shows an image of three vials of inks.

Surfactants were also investigated as a means to help promote carbon particle dispersion within the dissolved polymer and enhance chemiresistor response stability. Surfactants investigated included Spurso (purchased form OMG Americas, Inc.), Polyglycol EP-530 (purchased from The Dow Chemical Company), and Ralufon DS (purchased from Raschig AG). Results indicated that the inclusion of surfactants in the carbon/polymer mixture increased chemiresistor response stability, but that the response time was also slightly increased.

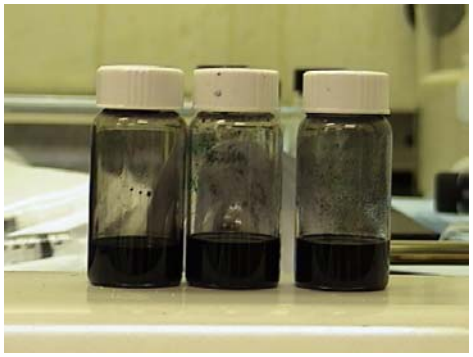

Figure 4. Chemiresistor inks consisting of polymer, carbon, and solvent.

3.2.3. Ink Deposition

The chemiresistor dies are cleaned with acetone and methanol. A micropipette is placed inside the vial that is still in the sonicating bath. A small amount of ink wicks up in the micropipette. The micropipette is placed directly above the area of deposition, and a slight pressure is placed on the top of the micropipette to push a bead of the ink out of the pipette. Then the pipette is placed directly on the chip and pulled up. If a resistance is not measured, more ink can be deposited to the die or the prior deposition can be wiped off with acetone followed by another deposition.

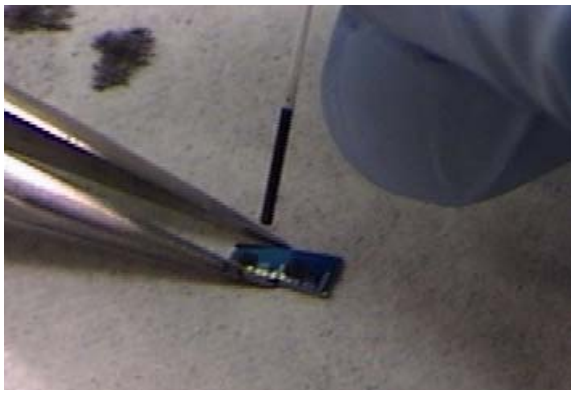

Figure 5. Deposition of inks onto chemiresistor dies using a micropipette and tweezers to hold the chemiresistor die stationary.

The manual deposition methods yields baseline resistances that can vary by 100% or more. However, the yield is excellent compared to automated deposition processes using computer-controlled machines, which are prone to having polymer solutions clog the deposition tips.

3.2.4. Chip Packaging

After the inks are deposited and dried on the die, the die is attached to a 16-pin dual inline package (DIP) with a Hardman 3-minute epoxy (no-heat cure). Then, gold wires are ball-bonded

from the pads of the DIP to the pads of the chemiresistor. Figure 6 shows an example of a wire-bonding template that is used. The numbers on the template correspond to the pads on the DIP.

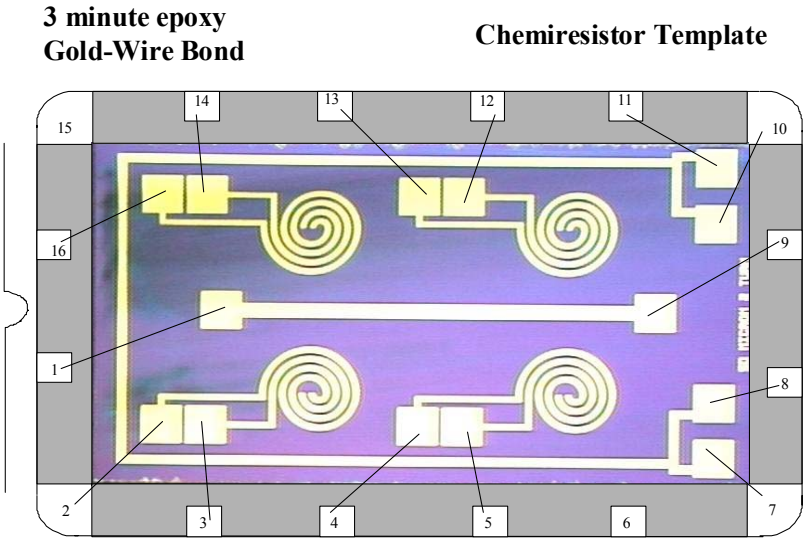

Figure 6. Chemiresistor template for assembly. Note: The notch on the side of the template refers to the notch in the DIP for orientation purposes.

3.3. Waterproof Packaging

A robust package has been designed and fabricated to house the chemiresistor array (Ho and Hughes, 2002). This cylindrical package is small (~ 3 cm diameter) and is constructed of rugged, chemically-resistant material. Early designs have used PEEK (PolyEtherEtherKetone), a semi-crystalline, thermoplastic with excellent resistance to chemicals and fatigue. Newer package designs have been fabricated from stainless steel (Figure 7). The package design is modular and can be easily taken apart (unscrewed like a flashlight) to replace the chemiresistor sensor if desired. Fitted with Viton O-rings, the package is completely waterproof, but gas is allowed to diffuse through a GORE-TEX® membrane that covers a small window to the sensor. Like clothing made of GORE-TEX®, the membrane prevents liquid water from passing through it, but the membrane "breathes," allowing vapors to diffuse through. Even in water, dissolved VOCs can partition across the membrane into the gas-phase headspace next to the chemiresistors to allow detection of aqueous-phase contaminants. The aqueous concentrations can be determined from the measured gas-phase concentrations using Henry's Law. Mechanical protection is also provided via a perforated metal plate that covers the chemiresistors. The chemiresistors on the 16-pin DIP is connected to a weatherproof cable. The cable can be connected to a hand-held multimeter for manual single-channel readings, or it can be connected to a multi-channel data logger for long-term, remote operation.

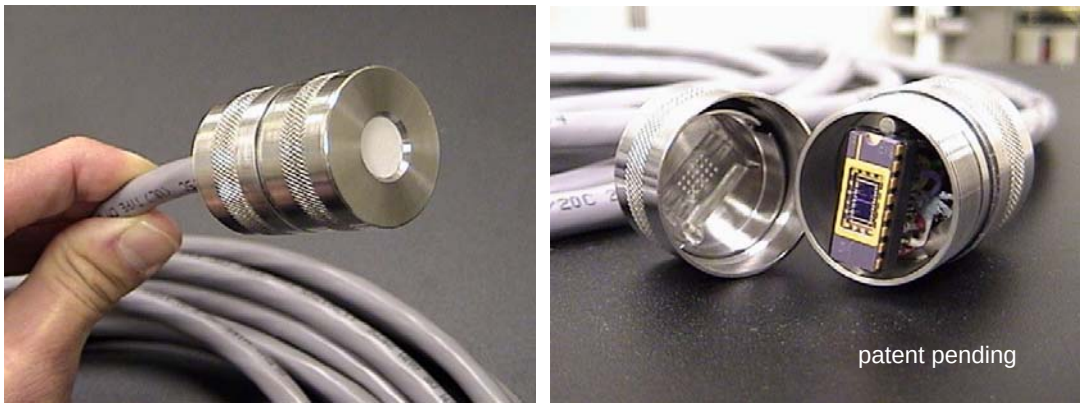

Figure 7. Stainless-steel waterproof package that houses the chemiresistor array. Left: GORE-TEX® membrane covers a small window over the chemiresistors. Right: Disassembled package exposing the 16-pin DIP and chemiresistor chip.

4. Chemiresistor Testing and Development

4.1. Experimental Approach

Throughout the course of this LDRD project, calibrations and experiments were conducted at two facilities at Sandia, New Mexico. The first facility is located in the In-Situ Sensing Lab in the Geoscience and Environment Center, which is operated by staff in the Geohydrology Department (i.e., Cliff Ho, Jerome Wright, Lucas McGrath, and Ara Kooser). The second facility is located in the Integrated Materials Research Laboratory (IMRL) building, which is operated by staff in the Microsensors Science and Technology Department (i.e., Chad Davis, Michael Thomas, and Bob Hughes). The sections below describe the calibration and experimental procedures that were used in each of the facilities.

4.1.1. Calibration and Testing Procedure: In-Situ Sensing Lab

4.1.1.1. Experimental Equipment and Apparatus

The majority of chemiresistor experiments were run using an apparatus that consisted of the chemiresistor being exposed to a known concentration of an analyte of interest. The analyte concentrations were monitored with an MTI M200 micro gas chromatograph. The chemiresistor, in its waterproof packaging, was placed in a sleeve. The sleeve was then placed in a customized steel tube. A customized reservoir that allows the input of a gas line was placed in the opposite end of the steel tube. The sleeve was customized to allow the gas to flow across the sensor and then into the fume hood. Data were recorded with the Agilent 34970A datalogger, a Campbell Scientific CR10X, or Campbell Scientific CR23X datalogger. A schematic of the apparatus used for these experiments is shown in Figure 8.

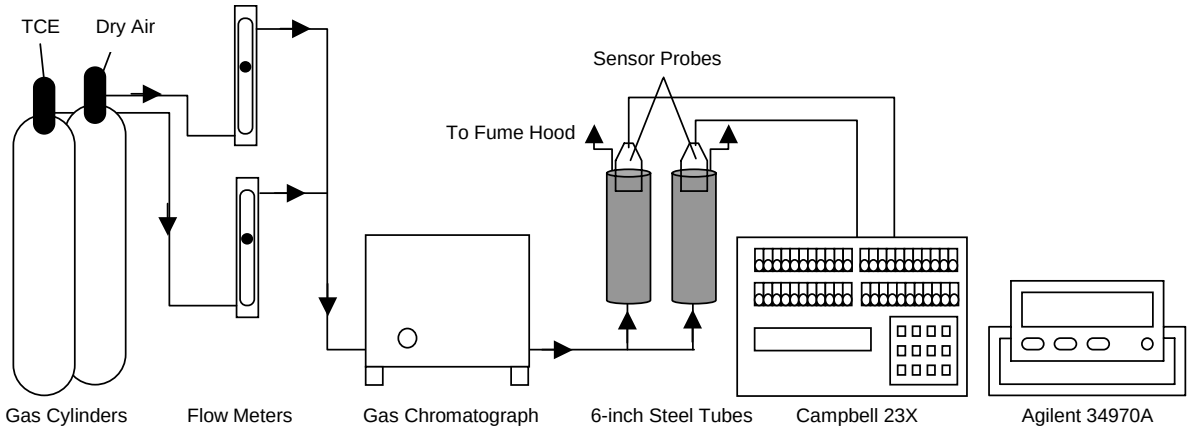

Figure 8. Schematic for chemiresistor experiments in In-Situ Sensing Lab.

An alternative approach to exposing the chemiresistors to know concentrations of analytes employed a customized Nalgene bottle. Holes were drilled into the top of the Nalgene bottle so that the chemiresistor cable could slide through. Then input and output holes were drilled for the addition of a gas line. Figure 9 shows a schematic of a modified Nalgene bottle.

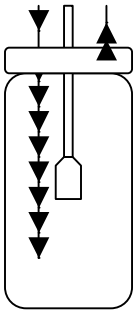

Figure 9. Modified Nalgene bottle for chemiresistor exposures.

4.1.1.2. Calibration Procedure

Each chemiresistor had to be individually calibrated to known concentrations of analyte (TCE was used for most calibration runs). The calibration procedure begins by passing dry air across each sensor in order to remove the ambient water vapor. The sensors are allowed to reach equilibrium in the dry conditions. Equilibrium is determined by visually evaluating the stability of the chemiresistor resistances. If the measured resistances appear to be stable then a steady baseline is recorded. Then known concentrations of TCE are added and the sensors are allowed to stabilize in the TCE environment. Then dry air is added to remove the TCE from the apparatus and reestablish a new baseline for the next TCE exposure. The concentrations of TCE are verified by the micro gas chromatograph. The procedure of adding a known concentration of TCE followed by the addition of dry air was continued for various concentration of TCE. A typical calibration run of the chemiresistor for TCE would use 500, 1000, 5000, 10,000-ppm

TCE. The calibration of the sensors is found by calculating the relative change in resistance for each chemiresistor.

The relative change in resistance for the sensors during an exposure is found by first determining the average of stable baseline values, R_b, for two minutes prior to the exposure of TCE. The baseline values are recalculated prior to each exposure. Next the value of the resistance during an exposure to TCE is calculated by taking an average of the steady resistance values, R, two minutes prior to turning off the TCE. Then the relative change in resistance is calculated using Eq. (1). For simple univariate regression analyses, this relative change is then plotted against the concentration of TCE, and a curve fit (e.g., power law or polynomial) is applied to the data using Microsoft Excel.

$$\frac{\Delta R}{R_b} = \frac{R - R_b}{R_b} \tag{1}$$

As an example, the calibration of chemiresistor array E2 (with polymers PNVP, PECH, PIB, and PEVA) in dry air at room temperature is shown in. Table 1 shows the power functions for each of the polymers with their respective correlation coefficients.

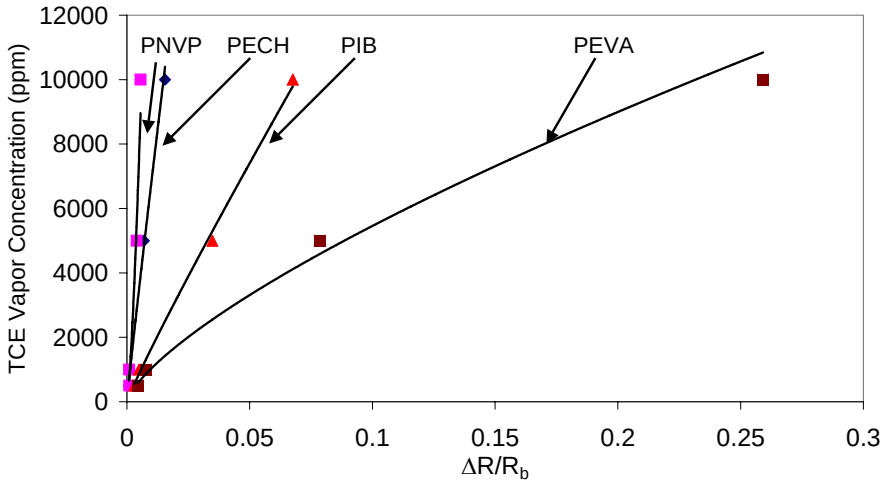

Figure 10. Graph of the calibration of chemiresistors in array E2 to TCE under dry conditions at room temperature, 23 ºC.

Table 1. TCE calibrations for chemiresistor array E2 at room temperature (23 ºC)

	Polymer	Regression Type	Regression (ppm)	R^2
Chemiresistor Array E2	PECH	Power	$y = 5.45E+05x^{9.51E-01}$	0.972
	PNVP	Power	$y = 1.71E+07x^{1.45E+00}$	0.935
	PIB	Power	$y = 1.19E+05x^{9.28E-01}$	0.993
	PEVA	Power	$y = 2.87E+04x^{7.21E-01}$	0.991

y= TCE vapor concentration (ppm)

$x = \Delta R/R_b$

4.1.1.3. Multivariate Analysis

The previous univariate calibration technique assumed that the response of the individual polymers was independent of any other disturbances (e.g., temperature changes, presence of water vapor and other analytes, etc.). In order to calibrate the sensor in the presence of fluctuating environmental variables and/or multiple analytes, multivariate calibration can be performed.

A multivariate calibration procedure consists of exposing several components to the chemiresistor simultaneously and independently. The variables of interest for our applications included water vapor concentration, temperature, and chemical environment (TCE concentration). Statistica™ 6.0 was used to develop a multivariate regression model that incorporated values of the predictor variables (e.g., temperature, water vapor concentration, response of each of the four chemiresistors) into a model that predicted the desired analyte concentration. Different water vapor and TCE concentrations are obtained by dilution using flow meters. Gas bottles of analytes (e.g., TCE) at know concentrations are also used (from Matheson TriGas). The ambient temperature of the chemiresistor is controlled by placing the chemiresistors in an oven or a refrigerator. The chemiresistor is placed in the customized steel tube and a gas line is fed through the reservoir. The gas line is 60 ft of 1/8 inch copper tubing. The copper tubing in located entirely inside the oven/refrigerator in order to allow the flowing gas to reach the same temperature of the oven/refrigerator. The temperature of the gas flowing over the sensor is monitored with the on-chip temperature sensor (Resistance Temperature Detector or RTD). After the temperature of the system has stabilized, exposure of the chemiresistor to various analytes is applied at that temperature. Numerous calibration runs (or training sets) were performed to generate sufficient data that spanned the range of conditions that were anticipated to be encountered.

A subset of a sample calibration data set used by Statistica™ is shown in Table 2. In this example, chemiresistor array E14 is calibrated to TCE at different temperatures and water vapor concentrations. The first six columns of data are used as predictor variables, and the last column is the dependent variable. Several different multiple regression models (e.g., factor analysis, polynomial, linear, response surface, etc.) can be used in Statistica™.

Table 2. Sample $\Delta R/R_b$ values for chemiresistor array E14. Values are used by Statistica™ to generate a multivariate model.

E14						
$\Delta R/R_b$						
PECH	PNVP	PIB	PEVA	Temp C	Vp (Pa)	TCE (ppm)
4.343E-03	5.528E-01	2.815E-03	4.976E-03	25.18	2153	257
4.353E-03	5.528E-01	2.831E-03	4.979E-03	25.18	2153	257
4.365E-03	5.524E-01	2.820E-03	4.959E-03	25.17	2153	257
4.362E-03	5.523E-01	2.848E-03	4.979E-03	25.18	2153	257
4.343E-03	5.523E-01	2.851E-03	4.976E-03	25.18	2153	257
4.349E-03	5.522E-01	2.848E-03	4.998E-03	25.18	2153	257
4.372E-03	5.521E-01	2.873E-03	5.008E-03	25.18	2153	257
4.356E-03	5.520E-01	2.864E-03	5.028E-03	25.18	2153	257
4.349E-03	5.518E-01	2.892E-03	5.031E-03	25.18	2153	257
3.495E-03	2.476E-01	2.754E-03	5.005E-03	25.22	508	1471
3.505E-03	2.473E-01	2.762E-03	5.002E-03	25.22	508	1471
3.492E-03	2.470E-01	2.762E-03	5.002E-03	25.22	508	1471
3.511E-03	2.467E-01	2.776E-03	5.018E-03	25.22	508	1471
3.476E-03	2.463E-01	2.751E-03	5.011E-03	25.22	508	1471
3.505E-03	2.461E-01	2.762E-03	5.024E-03	25.22	508	1471
3.495E-03	2.458E-01	2.773E-03	5.015E-03	25.22	508	1471
3.482E-03	2.453E-01	2.793E-03	5.024E-03	25.22	508	1471

The resulting factor-analysis multiple regression model for chemiresistor array E14 is shown below:

$$TCE(ppm) = -1.08E+00 - 1.83E+03*\Delta R/R_{bPNVP} + 3.81E+06*\Delta R/R_{bPECH}*\Delta R/R_{bPEVA} + 6.89*\Delta R/R_{bPEVA}*TempC + 4.35E-02*PNVP*TempC*Vp + 6.20E+01*PNVP*PIB*PEVA*Vp - 2.83E+01*PNVP*PIB*TempC*Vp + 3.83E+03*PECH*PNVP*PIB*TempC*Vp$$

Where:

TempC: Chemiresistor temperature (ºC)
Vp: Water Vapor Pressure (Pa)

4.1.1.4. RTD Calibrations

The RTD temperature sensor on the chemiresistor is a thin platinum trace on the chemiresistor die. The RTD can be calibrated to temperature by the following procedure. The chemiresistor is taken out of the its housing and is placed in an oven. A thermocouple is placed as close to the chemiresistors as possible (Figure 11).

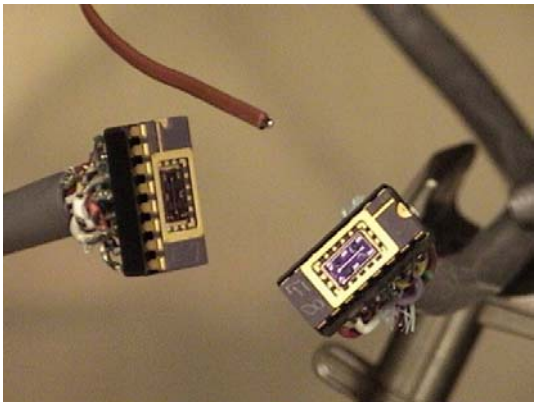

Figure 11. Apparatus inside an oven for RTD calibration (two chemiresistor chips and a thermocouple).

The oven is turned on to an elevated temperature (~ 40ºC) and is allowed to stabilize. Then the oven is turned off and data is recorded for several hours.. The RTD resistance is then plotted against temperature (Figure 12), and a linear regression is fit to the data.

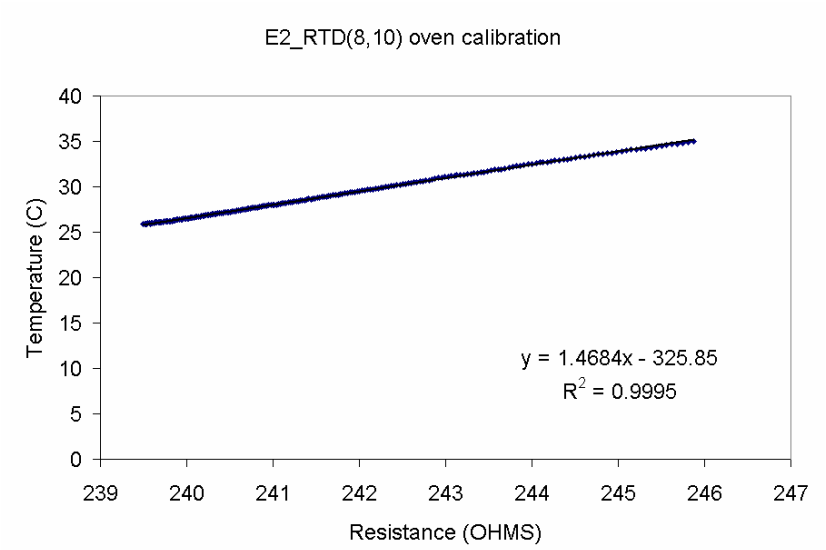

Figure 12. Calibration of the RTD on the chemiresistor die.

4.1.2. Calibration and Testing Procedure: IMRL Facility

Chemiresistors were exposed to chemical analytes in the vapor phase through the use of a custom gas manifold that uses gas cylinders with an analytically verified concentration of the analyte of interest or a nitrogen gas stream passing through gas washing bottles filled with the liquid analyte. A ceramic frit at the bottom of the washing bottle produces a fine stream of nitrogen bubbles. Intimate contact between the liquid analyte and the gas bubbles allows the gas stream to exit the bottle in a saturated condition. Concentration was then controlled by a set of Brooks 5850E mass flow controllers that allow dilution of the gas stream with dry nitrogen to

lower concentrations. Valves and flow controllers were set and continuously monitored by the use of a LabVIEW® controlling program. Concentrations were periodically verified near the exposure cell through the use of a RAE systems ToxiRAE or ppbRAE photo-ionization detector. Once analyte concentrations were established, the total gas stream could be sent directly to the exposure cell or through a final gas washing bottle filled with water to provide a background of 100% relative humidity to simulate typical subsurface conditions.

Chemiresistors, mounted in 16 pin DIPs, were inserted into exposure cells made from PEEK that directed the gas stream across the face of the DIP. An O-ring sealed the face of the DIP to the cell preventing any of the gas stream from escaping. This also allowed downstream measurement of the flow to ensure the total gas stream and desired concentration was passing over the chemiresistor. For consistency all exposures were regulated at 1 SLPM total flow regardless of the concentration or analyte, and tests were conducted in an insulated oven chamber.

For each calibration sequence, a set of chemiresistors were exposed simultaneously to an individual analyte in concentrations of 1, 3, 5, or 10 percent of the saturated vapor pressure at room temperature. An exposure at a given concentration was maintained for ten minutes across the chemiresistors before purging the system with a clean nitrogen stream for ten minutes. Consistency in chemiresistor response was noted by repeating each concentration at least once before proceeding to the next concentration.

Chemiresistor response to an exposure was noted by recording the changes in two-wire electrical resistance across two of the four electrodes (traditional linear electrode design). For all experiments, electrical resistances and thermocouple measurements were taken using a Hewlett Packard 34970A digital multimeter and recorded by a LabVIEW® program on an Apple Macintosh® computer.

4.2. Polymer Selection

Initial work on the project included identification of an optimized set of polymers to include in chemiresistor array fabrication. For this particular project, analytes of interest were identified as isooctane, m-xylene, and trichloroethylene, three different common environmental contaminants representing three distinctly different classes of chemicals (aliphatic, aromatic, and chlorinated hydrocarbons, respectively). In addition, the particular application area of in-situ sensing introduced the element of variable relative humidity that would have some impact on all polymers selected for use. Therefore, ideally either one of the four polymers or the combined results of would provide a signal that would allow determination of the relative humidity for any necessary signal correction. Through the course of our testing, we examined the following polymers: ethyl cellulose, poly(chloroprene), poly(dimethylsiloxane), poly(diphenoxyphosphazine), poly(epichlorohydrin) (or PECH), poly(ethylene), poly(ethylene-vinyl acetate) (or PEVA), poly(isobutylene) (or PIB), poly(n-vinyl pyrrolidone) (or PNVP), poly(styrene), poly(vinyl acetate), and poly(vinyl alcohol).

Evaluation of the polymers for suitability in this program was based on a series of calibration sets. First, each of the candidate polymers was subjected to each of the three VOCs of interest

individually in concentrations of 1, 3, 5, and 10% of the saturated vapor pressure of the particular analyte, with four exposures at a given concentration. The polymers were then similarly exposed to water vapor in the amounts of 1, 3, 5, and 10% relative humidity (at room temperature, ~23°C). Finally, the polymers were exposed to each of the three VOCs for a second time, but in a constant background of 100% relative humidity (at room temperature). Chemiresistor devices were maintained at an elevated temperature of 30°C to prevent condensation of water vapor on the substrates. All polymers were examined for stability and consistency of baseline resistance under unexposed conditions, speed of response to exposure to a particular chemical, consistency of elevated resistance to a particular chemical exposure, and consistency of overall response (measured as the increase in resistance divided by the baseline resistance) to a particular chemical over a series of repeats. Examples of overall resistance measurements and overall response values are shown in Figure 13 and Figure 14, respectively. Based on these experiments and overall combined sensitivity to the analytes and interferant of interest, we selected PECH, PEVA, PIB, and PNVP as our best four polymer candidates for inclusion in a chemiresistor array.

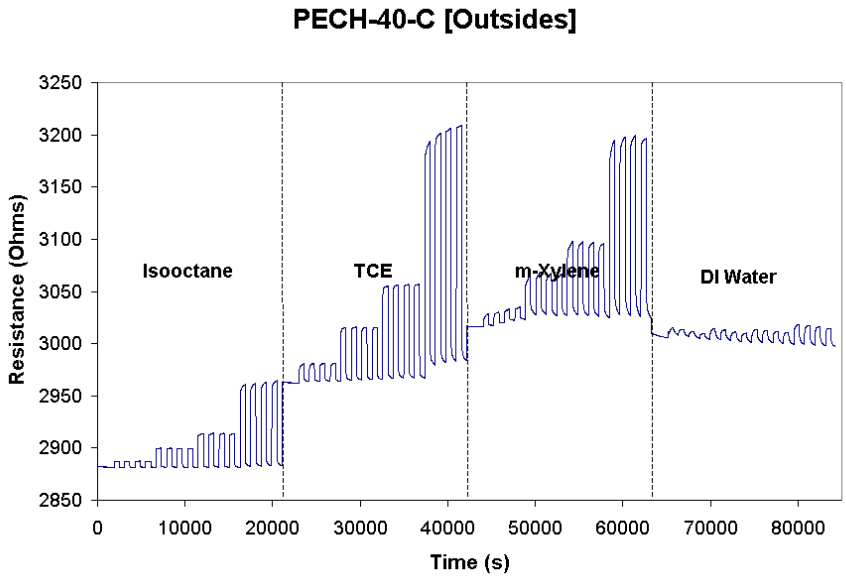

Figure 13. Example plot of raw resistances for PECH-40-C (40% carbon to polymer by mass) chemiresistor exposed to isooctane, TCE, m-xylene, and water at 1, 3, 5, and 10% of the saturated vapor pressure at room temperature, with four exposures at each concentration.

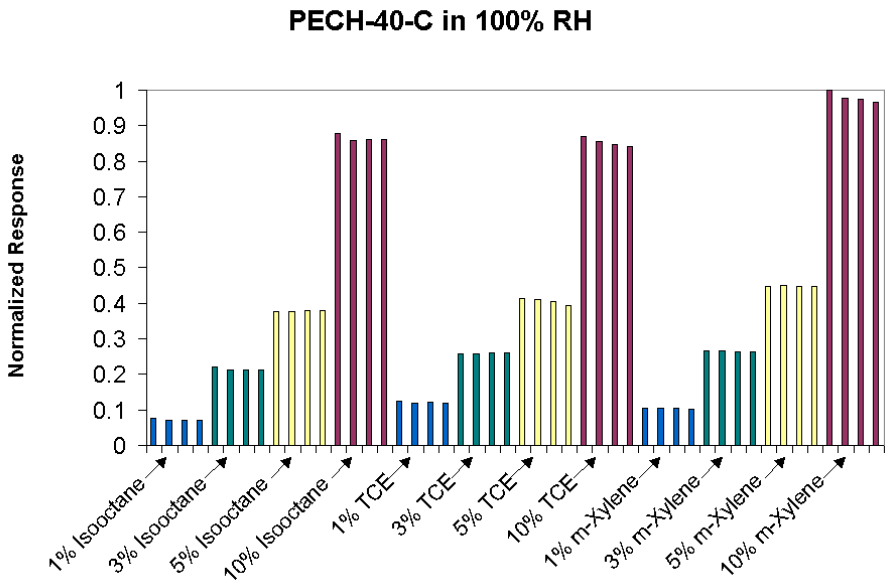

Figure 14. Bar plot of normalized chemiresistor response values to VOC exposures under 100% relative humidity (derived from data similar to that shown in Figure 13). Normalization divides each relative response by the largest response in a particular study, producing values scaled between 0 and 1.

4.3. Temperature Control Analysis

Each chemiresistor has a resistance temperature detector (RTD), which can be calibrated for temperature. The RTD is a thin platinum trace on the chemiresistor die that has a resistance that is linearly dependent on temperature. The RTD is calibrated using the procedure in Section 4.1.1.4. The polymers on the sensor are sensitive to changes in the ambient environment, such as temperature, humidity, and chemical environment. Figure 15 shows the response of the polymer PEVA on chemiresistor array C5 to changes in temperature.

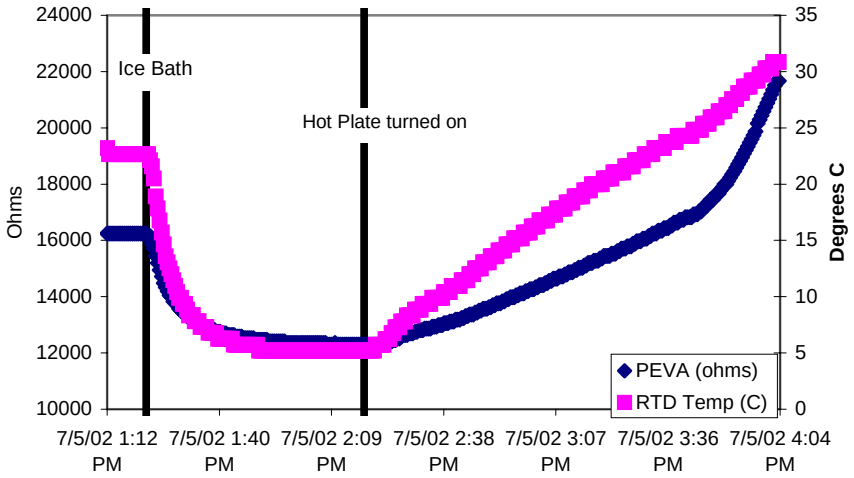

Figure 15. Chemiresistor (C5) response to change in temperature.

Fluctuations in temperature can cause swelling or contraction of the polymers that is similar to the polymer's response during the absorption or desorption of chemicals. This may lead to incorrect predicted concentrations of VOCs. Condensation from water vapor can also lead to spurious readings from the chemiresistor. Maintaining the local temperature above the dew point can prevent the ambient water vapor from condensing on the sensor substrate. Therefore, maintaining the chemiresistor's local temperature at a constant value should provide more accurate predictions of VOC concentration.

Local temperature control is obtained by use of the heating element, or heater bar, on the chemiresistor (see Figure 2). The heating element is simply a low impedance platinum trace on the surface of the chip. Once voltage is applied to the trace, resistive heating will increase the local temperature of the chip. Three different methods were attempted to utilize temperature control on the chemiresistor sensors. These include 1) a feedback loop programmed into the datalogger, 2) use of a constant voltage supply to the heater bar, and 3) use of an external temperature-compensation circuit.

4.3.1. Experimental Approach

4.3.1.1. Programmable Feedback Loop

The Campbell dataloggers can be programmed with the Campbell PC208W software. Programs are comprised of three tables—two programs and one subroutine. Table one contains the program that reads all of the polymers on the chemiresistor as well as the RTD. Table two contains the program instructions for applying voltage to the heater bar as well as the instructions to read the RTD again.

The first attempt at utilizing the heater bar was made with the CR10X. The CR10X is able to supply 12V, 5V, and 2.5V on defined intervals. The switched 12V supply was tried first by

writing a program that turned on the switched 12V for 5 seconds when the resistance was lower than 1.03 kΩ. It was determined that 12 volts being applied for a full 5 seconds raised the temperature from 23°C to approximately 80°C. Since the increase in temperature was too great, we began to evaluate lower voltages. Next, we evaluated the 2.5V supply on the CR10X. We selected a chip, C1, which had an RTD that was calibrated for temperature. A program was written for C1 that excited the heater bar with 2.5 volts when the local temperature of the chip was below 25°C. If the temperature became higher than 25°C, the datalogger would not supply voltage to the heater bar. The program instructions that are specific to turning on and off the heater bar for the chemiresistor are shown below.

```
12:  If (X<=>F) (P89)
1: 43       X Loc [ HtempC    ]
2: 4        <
3: 30       F
4: 30       Then Do

13:  Excitation with Delay (P22)
1: 3        Ex Channel
2: 1500     Delay W/Ex (units = 0.01 sec)
3: 50       Delay After Ex (units = 0.01 sec)
4: 2500     mV Excitation
```

With the parameters shown above, the temperature was maintained between 24.7°C and 26.4°C, but a smaller range in temperature was desired. So the parameters of delay excite, delay after excite, and mV excitation were changed in order to find the smallest span in temperature obtainable. Table 3 shows the parameters tested along with the results.

Table 3. Span of temperatures obtained using different parameters in the temperature-control feedback loop programmed into the Campbell CR10X datalogger.

Delay Excite	Delay After Excite	mV excitation	Temp Range °C	Difference
1500	50	2500	26.437-24.666	1.771
1500	50	1000	26.437-24.666	1.771
1000	50	1000	26.404-24.633	1.771
500	10	1000	25.214-24.625	.589
400	10	1000	25.157-24.567	.59

We determined that the best parameter combination was the following: 400 delay excite, 10 delay after excite, and 1000mV excitation. The sensor was then placed in an ice bath with a temperature of approximately 0°C. With the program parameters, the heater bar was unable to maintain a stable temperature in the non-ambient conditions. It was determined that the 1000 mV power supply could not deliver enough current into the low-impedance load of the heater element to maintain the rated voltage, and thus not enough power was being supplied to heat the chip in the ice bath. The resistance of the heater bar will naturally decrease when temperature decreases, compounding the problem. In order to correct this issue the 12 volt supply on the Campbell dataloggers was used. The switched 12 volts supply on the Campbell dataloggers will

deliver approximately 600mA, which is sufficient current to heat the chemiresistor under normal conditions. However, too much power will increase the temperature too rapidly. So we began to look for a way to limit the duration of heating.

The Edlog program in PC208W contains an instruction (21), titled "pulse port with duration." With this instruction, it is possible to dictate the amount of time a control port is turned on. Once the control port is turned on, the 12 volts will be applied. A program was written with a pulse duration of 0.01s, the smallest possible interval of time that the 12V can be on. The program instructions that were used to apply a pulse of 12 volts to the heater bar is shown below.

```
9:  If (X<=>F) (P89)
 1: 45       X Loc [ HTempC    ]
 2: 4        <
 3: 30       F
 4: 30       Then Do

10:  Pulse Port w/Duration (P21)
 1: 7        Port
 2: 46       Pulse Length Loc [ pulse7    ]
```

The program was set to maintain the temperature at 30°C. The chemiresistor C1 was placed in ambient conditions of the laboratory and the program was loaded. Evaluation of the pulse port instruction program yielded a temperature range of 3.07°C with a standard deviation of 0.62°C **a**t a room temperature of 23°C. To determine how well the 12V pulsed supply performed in a transient temperature environment, the sensor was placed inside a tall graduated cylinder that was placed inside an ice-filled beaker. The apparatus was then placed on a hot plate. A thermocouple was taped to the outside of the sensor in order to monitor the ambient temperature. Once the temperature of the system had reached a minimum in the ice-filled beaker (~10ºC), the hot plate was turned on. The temperature of the system increased to 30°C and the experiment was turned off. Figure 16 shows the response of the polymer PEVA on chemiresistor C1 to the temperature variations during the heating cycle.

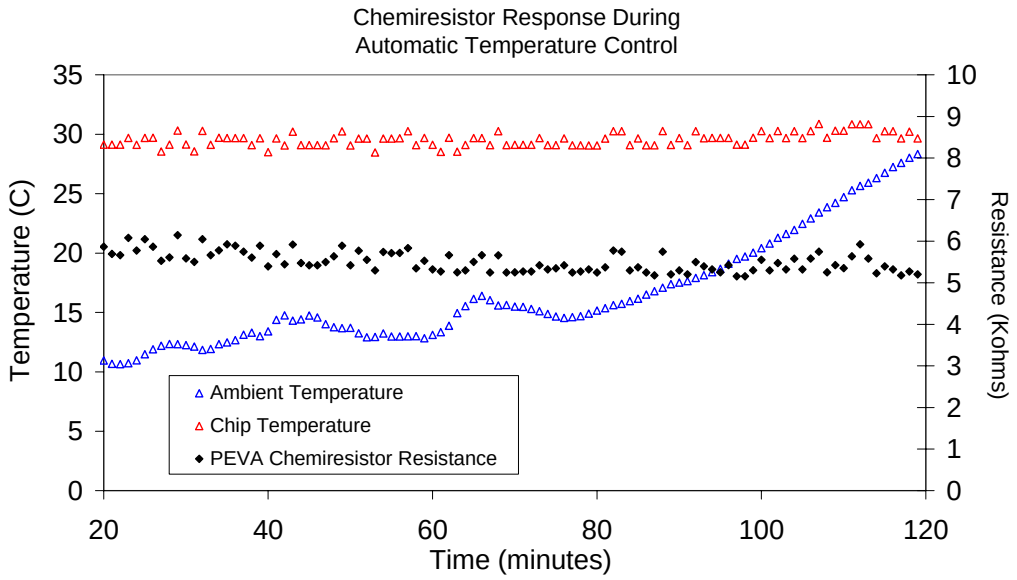

Figure 16. PEVA response to a fluctuating ambient temperature with a programmed feedback loop maintaining the temperature of the chip at ~30ºC.

Figure 16 demonstrates that the resistances of the PEVA did not respond significantly to changes in the ambient temperature when the feedback loop was maintaining the local temperature at ~30ºC. The temperature was maintained within a range of 2.39°C and a standard deviation of 0.64°C. The rather large temperature range results from the large voltage being applied. If the local temperature of the RTD is lower than 30°C, the program applies the full 12 volts to the heater bar. This results in a rapid increase in the chip temperature and chemiresistor response. To address this issue, a more steady supply of voltage was evaluated.

4.3.1.2. Constant Voltage

A constant voltage was applied to the heater bar on the chemiresistor die to determine if a constant temperature could be maintained on the chip. During this test, the stability of the chemiresistor at temperatures elevated just above the dew point was also investigated. The chemiresistor was placed in a 200 mL beaker filled with de-ionized water. The heater bar on the chemiresistor chip was connected to an Agilent E3630A DC power supply, and an Agilent 34970A datalogger recorded the response of the chemiresistor polymers, the RTD temperature, the voltage across the heater bar, and the ambient temperature. The DC power supply was set to supply a constant 2 volts to the heater bar. After the sensor had been in water for a week the power supply was turned off and the chemiresistor remained unheated in the water for an additional week. Then the power supply was turned back on to 2 volts and the sensor remained in the water for two additional weeks. Figure 17 shows the response of the RTD during the experiment.

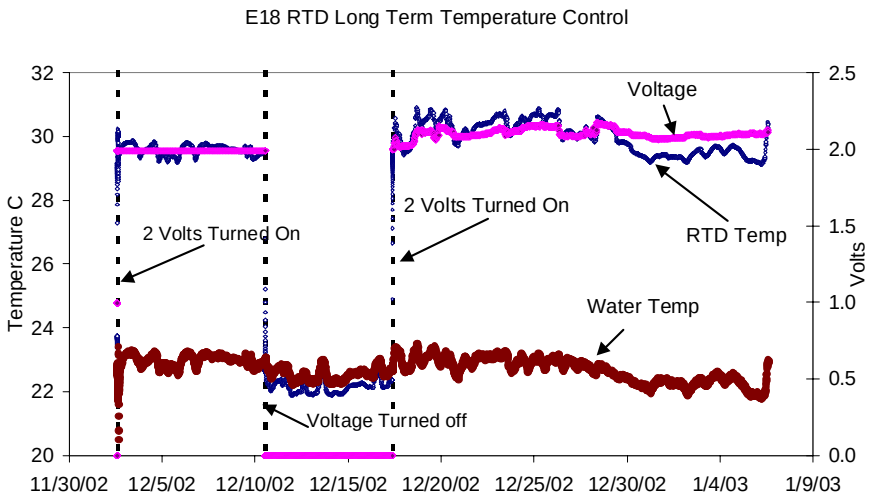

Figure 17. Chemiresistor E18 RTD response with and without a constant-voltage heating.

The constant voltage maintained the temperature within 1.7°C with a standard deviation of 0.31°C. There were no rapid increases in the local temperature of the chip due to the constant voltage supply. However, Figure 17 shows that the local temperature of the chip varied along with changes in the ambient temperature.

The resistances of the polymers were stable during times of heating. The polymer PNVP on E18 demonstrated the most dramatic response to the heating. Figure 18 shows the response of PNVP to the long-term temperature control using a constant voltage supply.

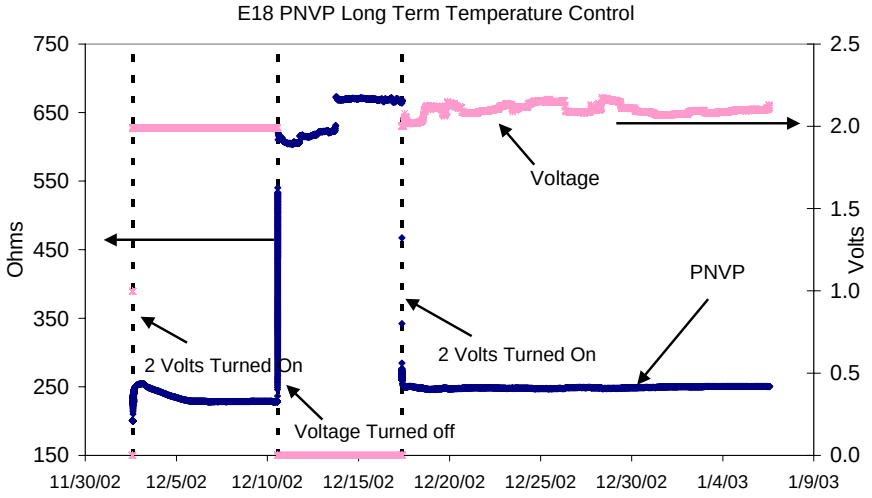

Figure 18. Response of PNVP with and without constant-voltage heating.

The remaining three polymers showed a similar response to the experiment. The resistances of all polymers were less erratic in 100% humidity conditions with a constant voltage being supplied to the heater bar.

For field use, a NTE956 adjustable voltage regulator was used to output a voltage from 1.2 volts to 37 volts depending on the potentiometer that is used. Adjusting the potentiometer can vary the voltage. The voltage can then be changed to yield the desired local temperature. The chemiresistor E28 was placed in a 500 mL Nalgene bottle filled with de-ionized water in order to simulate 100% humidity conditions. The voltage across the heater bar was increased using the voltage regulator to yield a RTD temperature of 25 °C. The sensor was left in the water for one month with constant voltage being supplied to it. Figure 19 shows the response to the RTD on the chemiresistor E28.

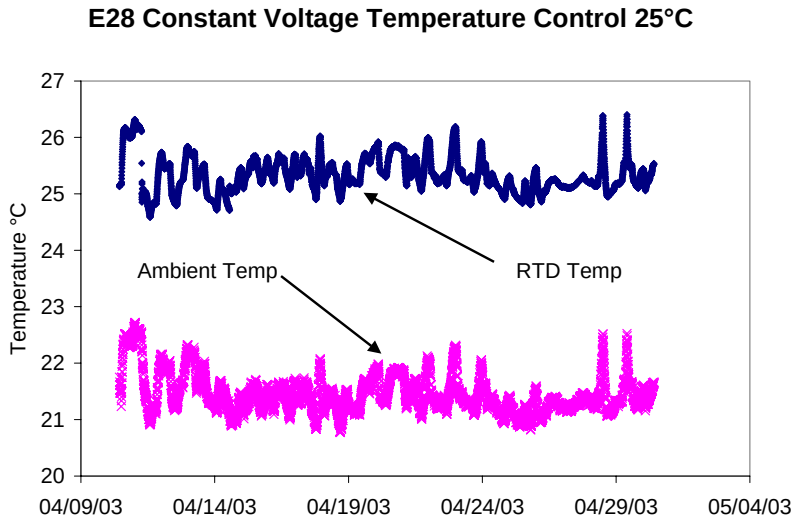

Figure 19. Local chip temperature (E28) and ambient temperature during a month-long test with constant voltage applied to the chemiresistor heater bar using an adjustable regulator.

The local temperature of the chip was maintained above the ambient with a range of 1.82°C and standard deviation of 0.32°C. The local temperature was correlated to the ambient temperature, which fluctuated with a range of 1.95°C and a standard deviation of 0.35°C. The response of the polymer sensors on the chemiresistor all appeared stable during the month long run in the water. Although the constant voltage method stabilized the resistances of the polymers and maintained the local temperature, this method responds to any change in the ambient environment. It is a viable and simple method in environments where small temperature fluctuations are acceptable. However, to address environments with large temperature fluctuations, a temperature compensation circuit was used that constantly adjusts the voltage supplied to the heater bar based on the temperature difference between the local and ambient environments.

4.3.1.3. Temperature Compensation Circuit

The Temperature Compensation Circuit was designed by Mark Jenkins (SNL), and it maintains the temperature of the chemiresistor by adjusting the voltage supplied to the heater bar based on the difference in local and ambient temperatures (see Figure 20). The Temperature Compensation Circuit reads the temperature by supplying a voltage across the RTD on the

chemiresistor. The voltage drop that occurs across the RTD corresponds to a temperature and can be recorded (see Figure 21 for calibration).

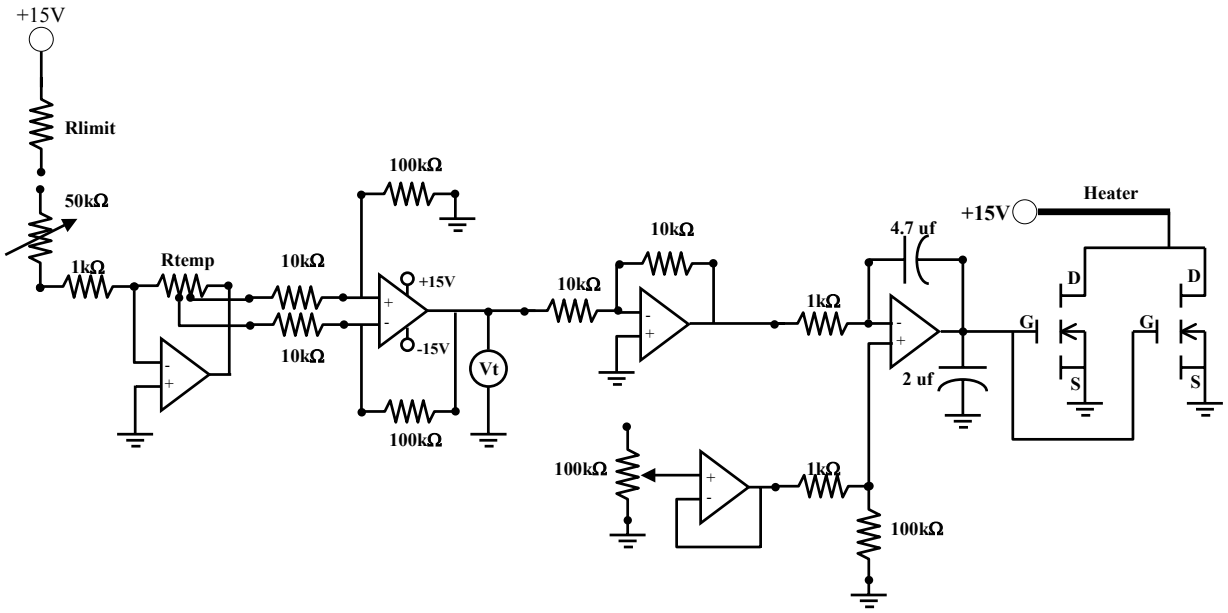

Figure 20. Temperature Compensation Circuit (designed by Mark Jenkins).

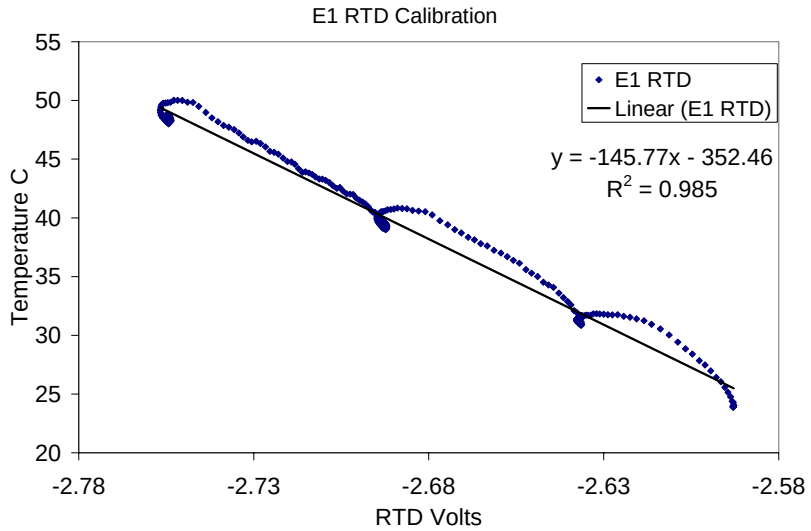

Figure 21. Results from the calibration of chemiresistor E1 RTD.

To evaluate how well the temperature of the chemiresistor sensor could be maintained using the Temperature Compensation Circuit, the chemiresistor was placed in a 250 mL Nalgene bottle filled with de-ionized water and exposed to variations in ambient temperatures. Figure 22 shows the response of the chemiresistor E26 to the experiment. The set point for the local chip temperature was 30ºC.

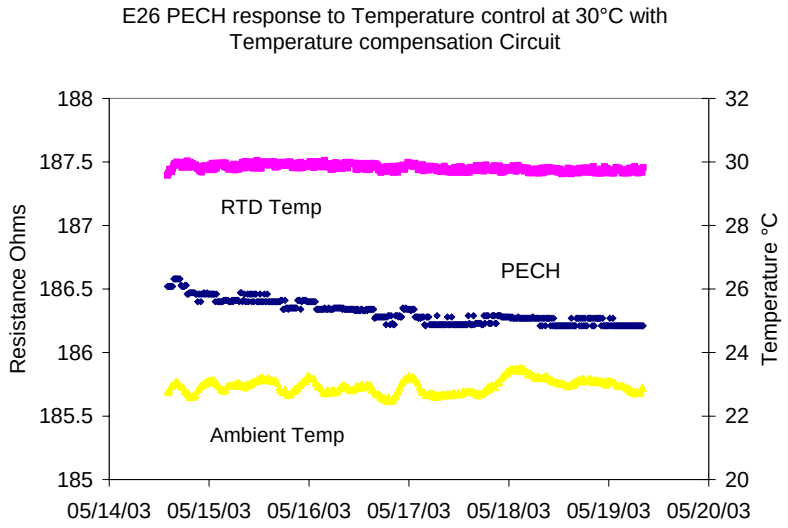

Figure 22. Chemiresistor E26 response to temperature control with the temperature compensation circuit.

The temperature was maintained at 30°C with a range of 0.5°C and a standard deviation of 0.1°C. Overall, the three temperature-control methods stabilized the resistances of the polymers and maintained the local temperature of the chip above ambient. The Temperature Compensation Circuit provided the best local temperature control. The programmable feedback loop utilized the data logger and did not require external circuits, but large voltage inputs caused larger swings in temperature. In environments where the temperature is fairly constant (e.g., the subsurface), a constant-voltage supply should be sufficient.

4.4. Carbon Analysis and Noise Comparison

In addition to fluctuations in temperature, the amount and type of carbon used in the polymer ink also impacts the sensitivity and stability (noise) of the chemiresistors. Various inks with different carbon percentages by mass of amorphous carbon black or graphitized carbon black from Columbian Chemicals were created to study the impacts of carbon concentration and type on the performance and stability of the chemiresistors. Four chips were assembled: two amorphous carbon black and two graphitized carbon black. The polymer used to evaluate the effects of carbon type and concentration was PEVA. The sensors were placed in a customized steel tube and then calibrated using a similar procedure found in 4.1.1. Figure 23 shows the results of the calibration run for the chemiresistor array E6, which had various carbon percentages by mass (relative to the total carbon/polymer mass) of amorphous carbon black, and Figure 24 show the response for chemiresistor array E8, which had different graphitized carbon black percentages.

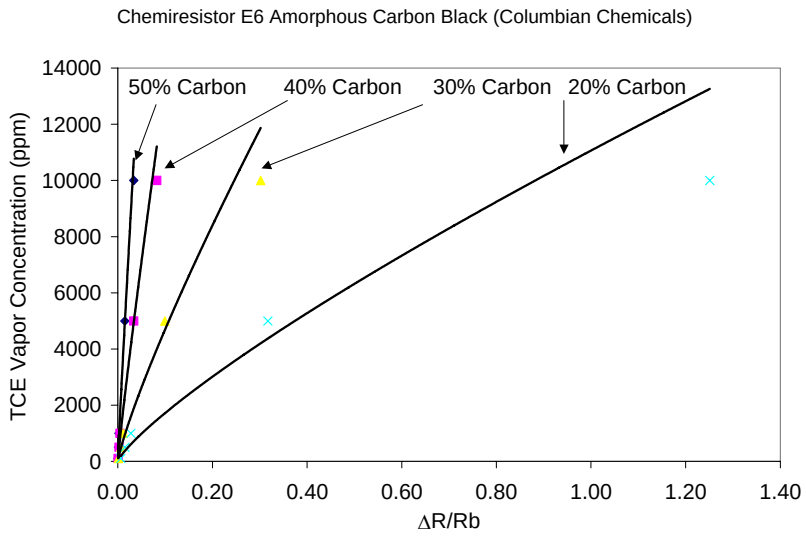

Figure 23. Chemiresistor E6 response to various TCE concentrations with different amorphous carbon black concentrations.

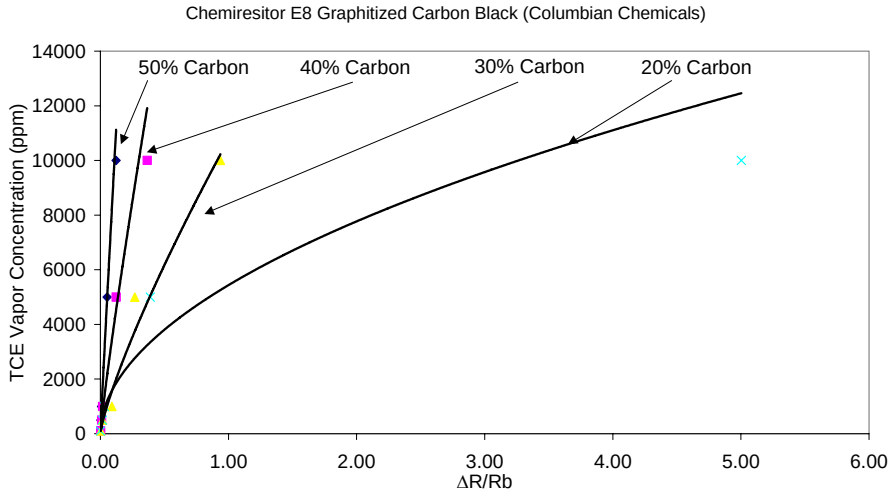

Figure 24. Chemiresistor E8 response to various TCE vapor concentrations with different graphitized carbon black concentrations.

In general the lower carbon concentrations yielded greater sensitivity to concentrations of TCE. With fewer electrically conductive pathways, the lower carbon-concentration polymers yielded greater changes in resistance when exposed to TCE.

The noise and stability of each sensor was also evaluated by the following experimental procedure. The sensors were connected to the Agilent 34970A datalogger and placed in customized six-inch steel tubes. The tubes were sealed to prevent the flow of air in and out of the system. The datalogger was programmed to take readings on a 0.01 second interval. Scans

were started and run until approximately 1600 scans had been taken. The standard deviations of each sensor were taken from sections of the data where the data appeared to be random without systematic increasing or decreasing trends.

The average standard deviation of the selected data for each chemiresistor can be found in Table 4. In general, the amorphous carbon black had a lower standard deviation than the graphitized carbon black for the same carbon percentage. The coefficient of variation, the standard deviation divided by the mean, is a normalized measure of the noise of a sensor. Table 4 also includes the coefficient of variation for the chemiresistors used in this evaluation.

Table 4. Standard deviation of the chemiresistors

	Carbon Percentage	Standard Deviation Ω	Coefficient of Variation
E5 (amorphous carbon black)	50%	4.06E-03	1.34E-05
	40%	1.15E-02	2.12E-05
	30%	4.64E-02	4.16E-05
	20%	3.54E+01	5.09E-04
E6 (amorphous carbon black)	50%	1.57E-03	7.75E-06
	40%	6.78E-03	1.71E-05
	30%	2.23E-02	3.88E-05
	20%	1.13E+01	5.70E-04
E7 (graphitized carbon black)	50%	3.90E-01	1.45E-04
	40%	5.30E-01	9.16E-05
	30%	1.68E+01	5.03E-04
	20%	3.54E+00	3.87E-04
E8 (graphitized carbon black)	50%	4.25E-02	4.39E-05
	40%	1.97E+00	2.04E-04
	30%	8.01E+01	6.11E-04
	20%	7.00E+02	8.33E-04

In general the amorphous carbon black had less noise then the equal carbon percentage of graphitized carbon black. Figure 25 shows a graphical representation of the coefficient of variation.

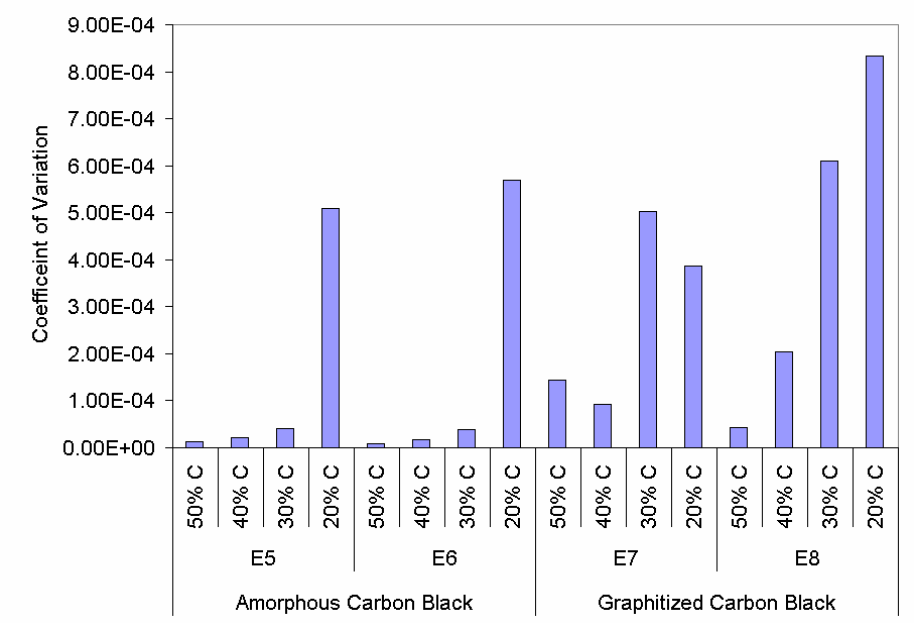

Figure 25. Coefficient of variation (noise) of the different chemiresistors with different carbon concentrations and carbon types.

4.5. Effective Resistivity Models

The previous section described the empirical impacts of carbon concentration and carbon type on the response and stability of the chemiresistor sensors. Several theoretical models can also be used to explain the relationship between the volumetric fraction of conductive and dielectric components and the resulting resistivity. Two such models include the generalized effective media (GEM) model and percolation theory. Each model predicts the resistivity of the composite as a function of the volumetric fraction of carbon. This section evaluates these models for different carbon concentrations, where the dielectric component is the polymer PEVA, and the conductive component is carbon black. Equation (2) shows the formula for resistivity where A is the cross-sectional area available for electrical conduction between the leads, L is the distance between the leads, and Ω is the resistance.

$$\rho = \frac{\Omega A}{L} \tag{2}$$

The distance, L, between the leads is known, and the cross-sectional area, A, was calculated by using a profilometer to measure the average thickness of the polymer deposition, which was multiplied by the length of the deposition (perpendicular to the L) as determined using a digital-camera-mounted microscope Figure 26 shows the results from the profilometer for one deposition. In this case the average thickness was 1.085 μm.

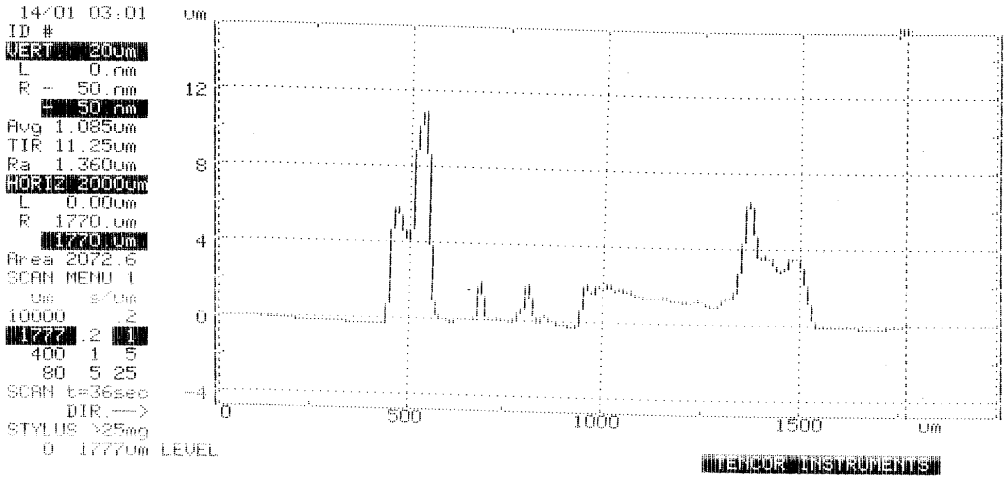

Figure 26. Polymer thickness along the width of a polymer deposition (image from L. Hua and W. Pitt at BYU).

The experimental resistances and the known geometry of the depositions were used to estimate the resistivity. Multiple depositions were performed for each volumetric fraction and carbon type. The length of each individual deposition and resistance was recorded. Then a resistivity was calculated for each deposition. These calculated resistivity values for each deposition were averaged for a given volume fraction. Table 5 includes the average resistivity values for each volumetric fraction. These measured values are compared to theoretical predictions using the generalized effective media model and the percolation model.

Table 5. Average calculated resistivity for different volume fraction of carbon blacks.

Graphitized Carbon Black	
Vc	Resistivity Ω cm
0.5	8.0
0.4	7.6
0.2	13
0.15	136
0.12	282286
0.11	829
0.09	OVLD
0.08	OVLD
0.07	OVLD

Amorphous Carbon Black	
Vc	Resistivity Ω cm
0.5	6.2
0.4	6.6
0.2	9.6
0.15	9.1
0.12	214
0.11	46
0.09	1350
0.08	932
0.07	38842

Vc = volumetric fraction of carbon
OVLD = over the resistance range of the Fluke multimeter.

The manufacturer of the carbon blacks, Columbian Chemicals, did not have resistivity data for the types of carbon used in this study. To estimate the resistivity of the carbon, an

approximation was made based on a linear regression to measured resistivities as a function of carbon concentration. This was done by plotting the last three resistivity values versus the corresponding volume fraction for each carbon type. A straight line was fit to the data and the resistivity value for a carbon volume fraction of one (pure carbon) was extrapolated, yielding a resistivity value of 0.092 Ω-cm for amorphous carbon black and 0.585 Ω-cm for graphitized carbon black. These values were used in the parameter estimation process for the percolation theory and GEM equations.

Unknown parameters in the equation are estimated using PEST software. PEST software accomplishes the estimation process by using a nonlinear estimation technique known as the Gauss-Marquardt-Levenberg method. PEST requires the user to generate the model program, and PEST changes the input variables for the program until it finds the optimal fit to the experimental data. The fixed parameters for both the GEM and percolation models were the resistivity of the polymer, resistivity of the carbon, and the volume fraction with it's corresponding resistivity value. The resistivity of the polymer PEVA has a range of 1E+12 Ω–cm to 1E+16 Ω–cm. For the parameter estimation process these values were kept constant at 1E+12 Ω–cm. The resistivity of the polymer does not have a large effect on the overall shape of the generated curves.

4.5.1. Percolation Model

The effective resistivity of a conductive and dielectric composite as a function of the volumetric fraction of the conductive component can be modeled by percolation theory (e.g., see Lundberg and Sundqvist, 1986). The percolation theory equation is given by:

$$\frac{(z-2)\rho_c\rho_m}{A+B+\left[(A+B)^2+2(z-2)\rho_c\rho_m\right]^{1/2}}=\rho \tag{3}$$

where

$$A=\rho_c\left[-1+(z/2)(1-(v_c/f))\right]$$

$$B=\rho_m\left[(zv_c/2f)-1\right]$$

and

ρ	Resistivity of the composite
ρ_m	Resistivity of the dielectric component
ρ_c	Resistivity of conductive component
v_c	Volume fraction of conductive component
z	Coordination number of conductive components
f	Total packing fraction

The parameters z and f were varied in order to closely match the observed resistivity for each carbon polymer composition. The values of ρ_m = 1E+12 Ω-cm, ρ_c = 0.092 Ω-cm for amorphous carbon black, and ρ_c = 0.585 Ω-cm for graphitized carbon black were used in the estimation process. Figure 27 shows the results from the PEST estimation process for graphitized carbon black. The optimized parameters for percolation theory with graphitized carbon black and PEVA were z = 18.1413, and f = 0.992425. The same procedure was followed to estimate the parameters for amorphous carbon black with PEVA (Figure 28). The optimized parameters for percolation theory with amorphous carbon black and PEVA were z = 16.2102, and f = 0.566794.

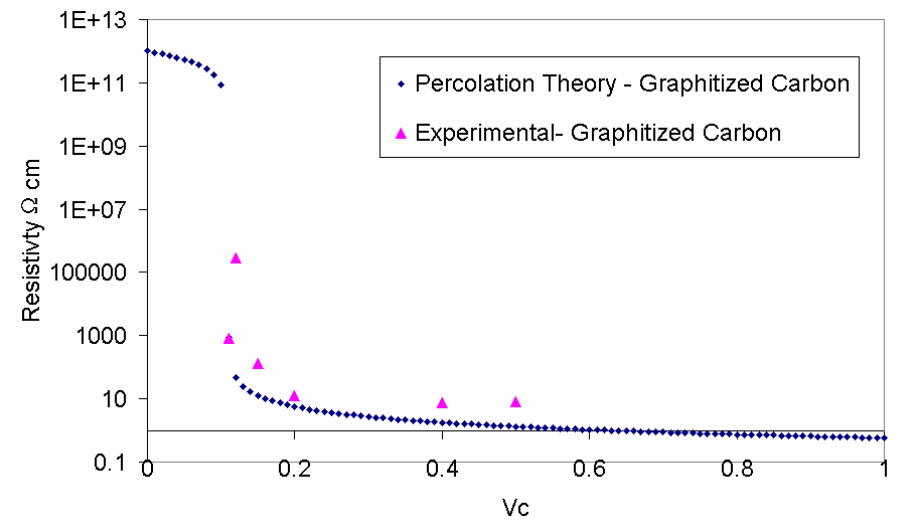

Figure 27. Predicted and measured resistivity values using percolation theory with graphitized carbon black and PEVA.

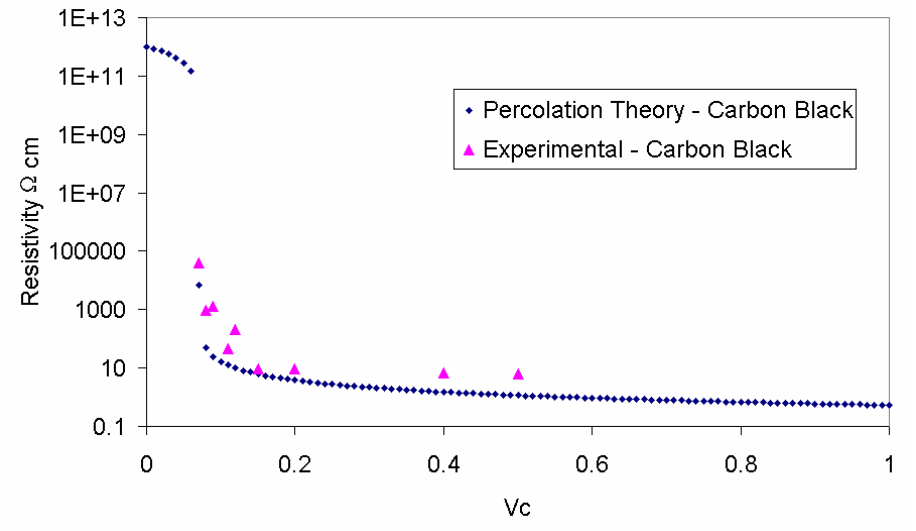

Figure 28. Predicted and measured resistivity values using percolation theory with amorphous carbon black and PEVA.

The packing fractions and coordination number of the two carbons in PEVA were different. This suggests some possible structural difference between the carbons. The process of creating the graphitized carbon black is done by subjecting amorphous carbon black to elevated temperature long enough to realign the molecular structure resulting in graphitized carbon. This change creates a highly ordered surface that appears to have effects on the packaging fraction and coordination number of the carbon in a polymer.

4.5.2. Generalized Effective Media Model

The generalized effective media (GEM) model proposed by McLachlan et al. (1990) describes the effective resistivity of a mixture of conductive and dielectric components as a function of volumetric fractions of conductive and dielectric components. The GEM equation is written as follows:

$$\frac{(1-f)(\rho_L{}^{-1/q} - \rho_M{}^{-1/q})}{\rho_L{}^{-1/q} + f_R\rho_M{}^{-1/q}} + \frac{f(\rho_H{}^{-1/q} + \rho_M{}^{-1/q})}{\rho_L{}^{-1/q} + f_R\rho_M{}^{-1/q}} = 0 \tag{4}$$

where

ρ_M	Resistivity of composite
ρ_H	Resistivity of dielectric component
ρ_L	Resistivity of conductive component
f	Conductive fraction
q	Experimental percolation exponent

f_R is given by the following equation:

$$f_R = \frac{1-f_C}{f_C} \tag{5}$$

where f_C is the critical volume fraction (percolation threshold) of the conductive component. The parameters of f_C and q were optimized in PEST for the GEM equation. The values of ρ_H = 1E+12 Ω-cm, ρ_L = 0.092 Ω-cm for amorphous carbon black, and ρ_L = 0.585 Ω-cm for graphitized carbon black were used in the estimation process. Figure 29 shows the results from the PEST estimation process of graphitized carbon black and PEVA. The optimized parameters for the generated theoretical curve for the graphitized carbon black are f_C = 0.083 and q = 2.053. The same fitting procedure was followed to optimize the parameters for amorphous carbon black with PEVA. The results of the estimation process are shown in Figure 30. The optimized parameters for the generated theoretical curve for the amorphous carbon black are f_C = .0666 and q = 2.309.

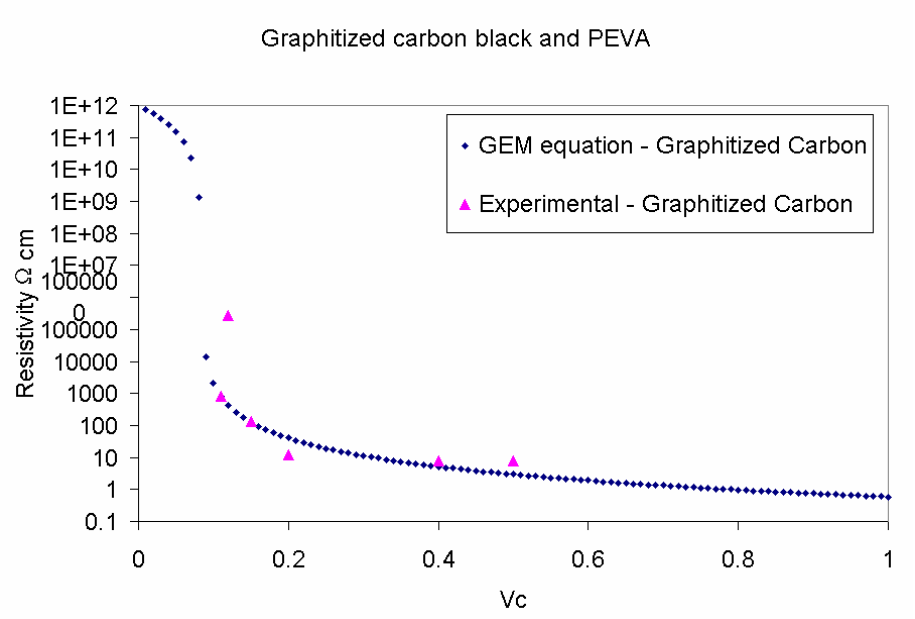

Figure 29. Predicted and measured resistivity values using the GEM model with graphitized carbon black and PEVA.

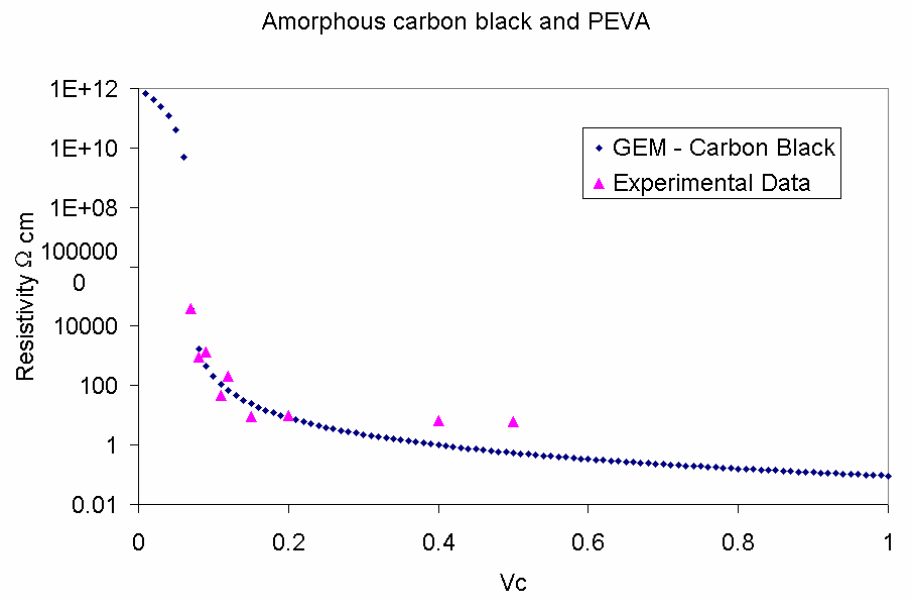

Figure 30. Predicted and measured resistivity values using the GEM model with amorphous carbon black and PEVA.

4.6. Limit of Detection Analyses

To calculate the theoretical limit of detection of the chemiresistor, the raw noise of the sensor was evaluated. This was done by finding the mean and standard deviation of the chemiresistor during a quiescent, non-exposed period. The limit of detection was defined as the minimum concentration that causes a change in resistance greater than three standard deviations above the mean of the noise. Therefore, any relative change in resistance that is above three standard deviations has a 99.7% chance that that value is not in the noise. The calculated standard deviation of each chemiresistor was multiplied by three and then divided by the mean in order to find the relative change in resistance ($\Delta R/R$) that corresponded to the theoretical limit of detection:

$$\frac{3\sigma}{Mean} = \text{minimum relative change} \tag{6}$$

The minimum relative change in resistance was then entered into the appropriate calibration curve. Table 6 shows the average theoretical limits of detection for seven chemiresistors with a 40% carbon percentage by weight. The theoretical detection limits for the non-polar polymers is on the order of 10 ppm of TCE in the aqueous phase, which corresponds to an aqueous concentration of ~100 ppb. However, interferences and environmental fluctuations in the field will increase these limits (see Section 7).

Table 6. Average theoretical limits of detection for different polymers on chemiresistors E34-E40.

	Average Limit of Detection to TCE (ppm)
PECH	16.9
PNVP	292.5
PIB	14.0
PEVA	23.6

4.7. Comparison to other Sensors and Designs

4.7.1. Linear vs. Spiral

Figure 31 shows a comparison between the traditional linear electrode design and a new concentric spiral design for chemiresistor sensors. The spiral design allows for a larger conductive contact area between the electrodes in a small circular footprint, which will accommodate deposition methods that produce small droplets. In addition, the concentric spiral design is expected to yield more consistent baseline resistances. Small aggregates of carbon particles that form in the ink are more likely to be evenly distributed between spiral electrodes

than linear electrodes. The next sections describe studies that compare the linear and spiral chemiresistor designs.

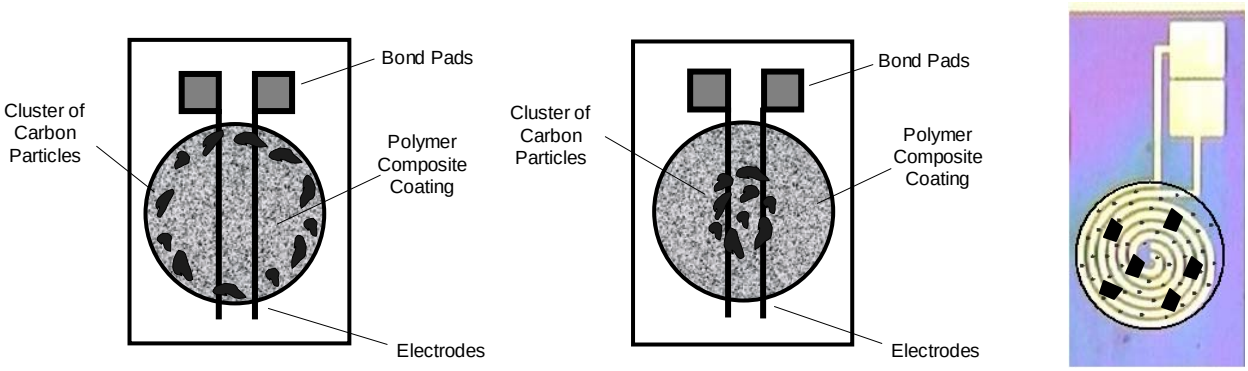

Figure 31. Illustration of impact of location of carbon aggregates on a linear electrode design (left and middle) and spiral electrode design (right). The spiral electrode is expected to be less sensitive to variations in carbon-aggregate size and location in the polymer deposition. The linear design is more sensitive because the aggregates may fall entirely around the electrodes rather than between them. In the spiral design, the aggregates will likely fall between electrodes, regardless of their location.

4.7.1.1. Experimental Approach.

Five linear and seven spiral chemiresistor chips were used to compare the performance and stability of the two designs. Figure 32 shows the prepackaged linear and spiral chemiresistors that were evaluated in this study. Inks comprised of 60% polymer and 40% (by mass) graphitized carbon black from Polysciences were deposited on the chemiresistor and packaged in a 16-pin DIP. Then the repeatability, noise, and the performance of these designs were evaluated and compared.

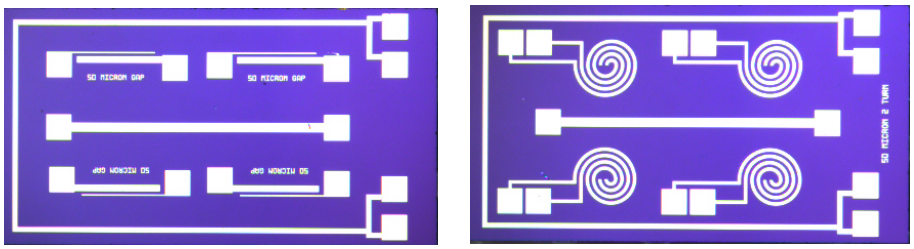

Figure 32. Linear and spiral design configurations on chemiresistor dies.

4.7.1.2. Repeatability and Noise Analysis

The noise and the repeatability of the linear and spiral chemiresistors were evaluated using the same procedure described in Section 4.4. In general the standard deviation of the measured resistance for the spiral chemiresistor was lower than that of the linear chemiresistor, and the

repeatability of the spiral chemiresistor was higher. Figure 33 shows the averaged standard deviation of the polymers for the linear and spiral chemiresistors evaluated.

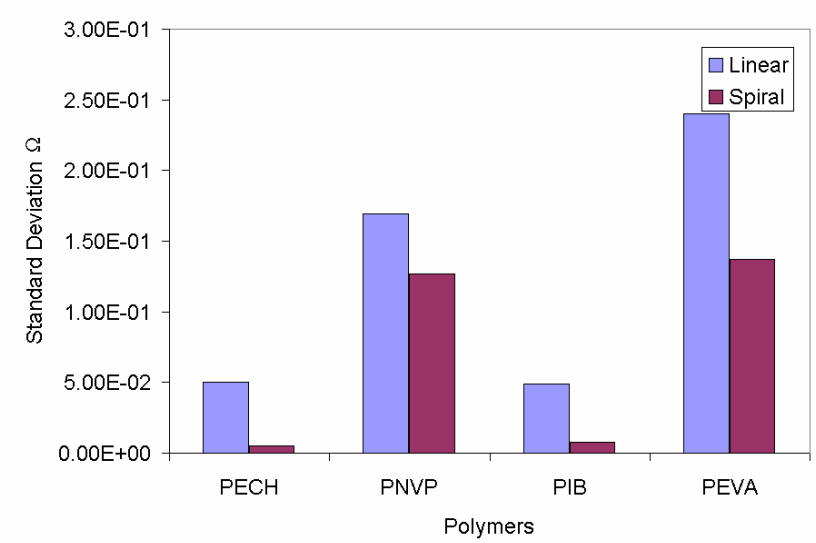

Figure 33. Averaged standard deviation of the spiral and linear chemiresistors.

Figure 34 shows the coefficient of variation for each polymer on the chemiresistors, which shows that there is not a clear difference in noise between the linear and spiral designs.

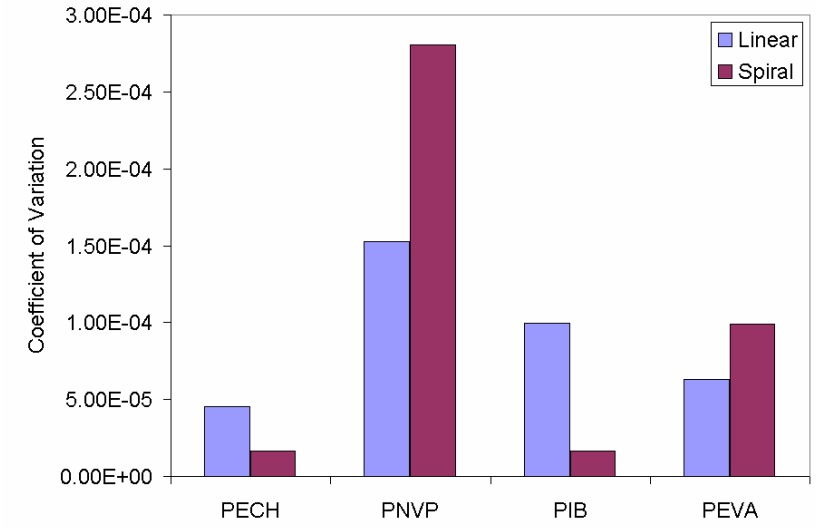

Figure 34. Averaged coefficient of variation of the spiral and linear chemiresistors.

4.7.1.3. Sensitivity/Performance Analysis

The sensitivity of the linear and spiral chemiresistors to TCE was evaluated. The sensors were placed in the modified Nalgene bottle and exposed to known concentration of TCE. TCE concentrations of 500, 1000, and 5000-ppm were added. The chemiresistors were allowed to stabilize in the TCE, which typically took 25-30 minutes due to the large volume of the Nalgene bottle. The effluent gas was monitored with an MTI M200 micro gas chromatograph. Figure 35 shows the response of the polymer PECH. In general the linear chemiresistors was more sensitive to TCE than the spiral (i.e., for the same concentration of TCE the linear chemiresistors had a greater change in resistance).

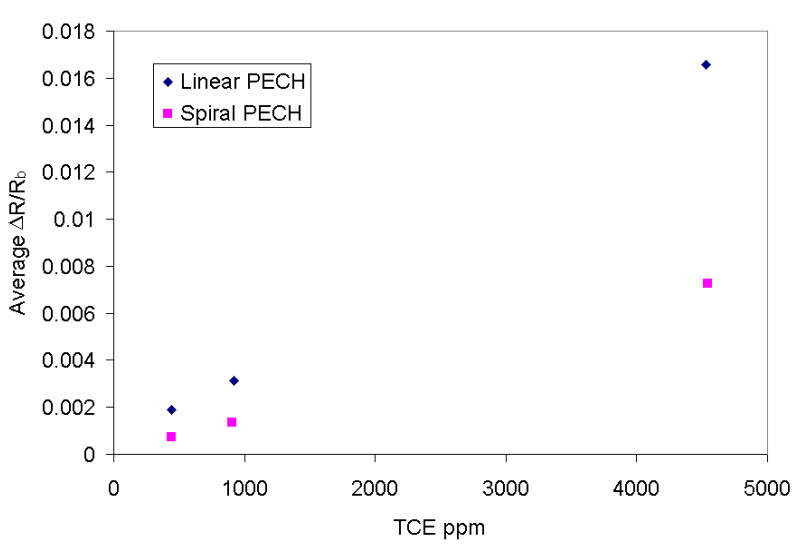

Figure 35. Average response of the polymer PECH to TCE using linear and spiral chemiresistor designs.

4.7.1.4. Theoretical Limits of Detection of Spiral and Linear Chemiresistors

The theoretical limits of detection were calculated using the same procedure found in Section 4.6. The theoretical limits of detection were averaged for the different designs and plotted in Figure 36 (outliers that passed the Q-Test were not included in calculation of the average limit of detection). The linear design shows a lower limit of detection for two of the polymers (PNVP and PEVA), and the spiral design shows a lower limit of detection for PIB. There is no clear trend that indicates one design has a lower limit of detection over the other.

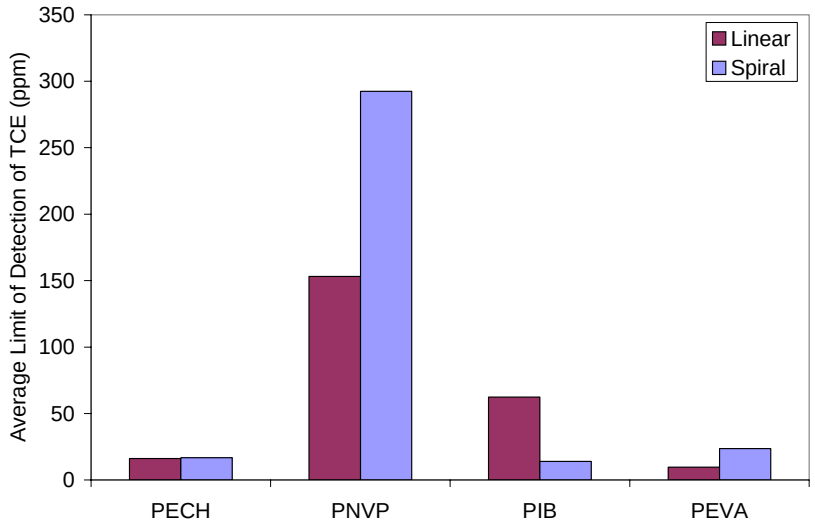

Figure 36. Theoretical limits of detection of linear and spiral chemiresistor designs.

4.7.2. SAW vs. Chemiresistor Evaluation

Surface-acoustic-wave (SAW) sensors are another category of microchemical sensors that are being studied for use in real-time chemical detection. This section summarizes a side-by-side comparison of these two sensors. A more detailed description of the evaluation can be found in Ho et al. (2003b).

The SAW sensor consists of an input transducer, a chemically adsorbent polymer film, and an output transducer on a piezoelectric substrate, which is typically quartz. The input transducer launches an acoustic wave that travels through the chemical film and is detected by the output transducer. The Sandia-made device runs at a very high frequency (approximately 525 MHz), and the velocity and attenuation of the signal are sensitive to the viscoelasticity and mass of the thin film. SAWs have been able to distinguish organophosphates, chlorinated hydrocarbons, ketones, alcohols, aromatic hydrocarbons, saturated hydrocarbons, and water.

The SAW array used in these tests has four channels—each channel consisting of a transmitter and a receiver, separated by a small distance. Three of the four channels have a polymer deposited on the substrate between the transmitter and receiver. The purpose of the polymers is to adsorb chemicals of interest, with different polymers having different affinities to various chemicals. When a chemical is absorbed, the mass of the polymer increases, causing a slight change in phase relative to the reference (fourth) channel, which does not contain a polymer.

4.7.2.1. Calibration

The chemiresistor and SAW sensors were calibrated using controlled concentrations of TCE. The sensors were both placed in customized six-inch steel tubes that allowed the sensors to be

exposed to a flowing stream of varying concentrations of TCE vapor. Data were logged using either a Campbell Scientific CR23X or an Agilent 34970A multiplexer.

Figure 37 shows the calibration results for chemiresistor array E2. Data for the SAW array P9 was analyzed and graphed in a similar manner. Figure 38 shows the results of the calibration run for SAW array P9, which contained the following polymers: polyisobutylene (PIB) and two channels with poly(vinyl tetradecanal) (PVTD).

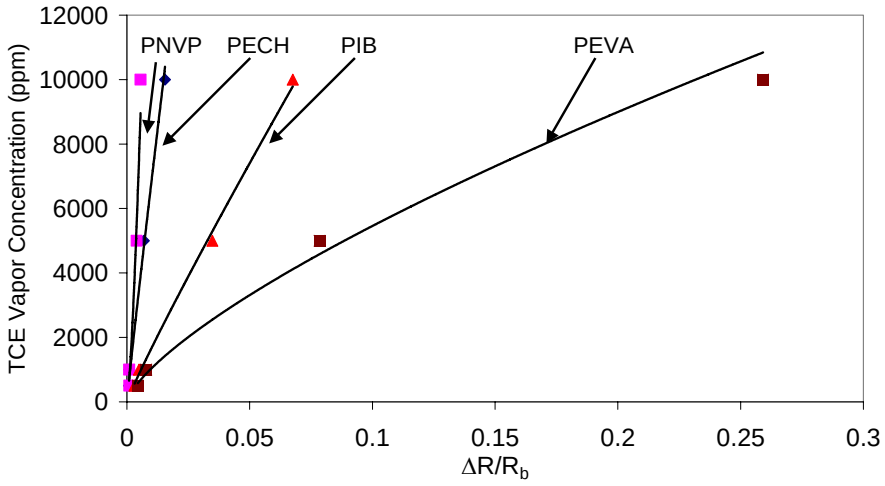

Figure 37. Chemiresistor response to TCE calibration

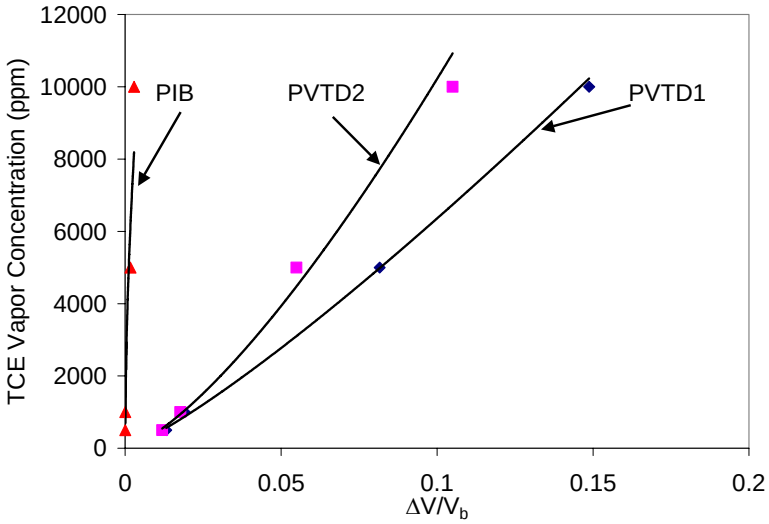

Figure 38. SAW array P9 response to TCE calibration.

4.7.2.2. Theoretical limits of detection

The theoretical limits of detection of the SAW and the chemiresistor sensors were evaluated following the same procedure found in Section 4.6. The standard deviations calculated during a quiescent (no exposure) period were plugged into the calibration equations determined from Figure Figure 37 and Figure 38. Figure 39 shows the resulting theoretical detection limits for chemiresistor array E2 and SAW array P9. Although different polymers were used, it appears that the chemiresistor and SAW sensors have similar limits of detection. The response of the PIB polymer on the chemiresistor array yielded a much lower limit of detection than the PIB polymer on the SAW array.

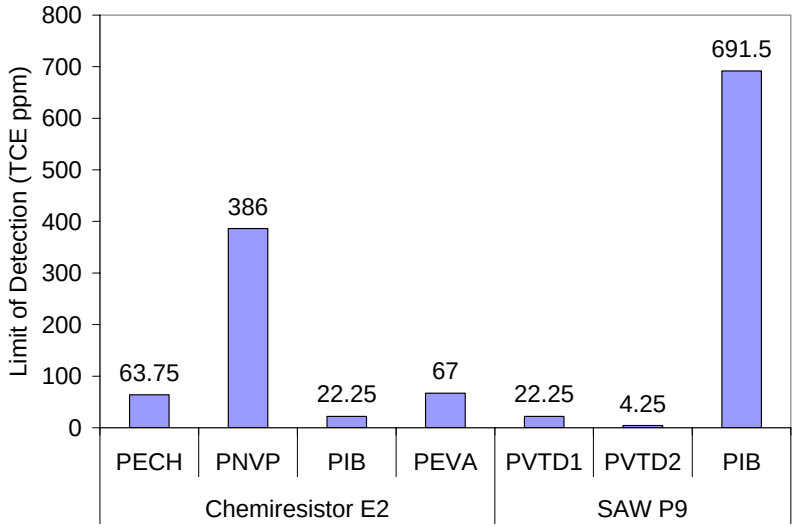

Figure 39. Theoretical limits of detection of TCE (ppm) for the chemiresistor array E2 and SAW array P9

4.7.3. Piezoresistive Microcantilever vs. Chemiresistor Evaluation

The piezoresistive microcantilever (PRM) sensor is based on a similar principle as the chemiresistor sensor for analyte detection. Polymers are used to absorb chemicals, but PRMs use microcantilevers to transduce the swelling or contraction of the polymer into a measurable resistance change in the microcantilever (Porter et al., 2003) (Figure 40).

The polymer is dissolved in a solvent and then deposited onto a piece of silicon. The PRM is pushed into the polymer, embedding the cantilever (Figure 41). The cantilever contains two channels of piezoresistive material. As chemical vapors come into contact with the polymer, the

polymer swells. This causes the cantilever to bend, which causes a change in resistance in the piezoresistive material.

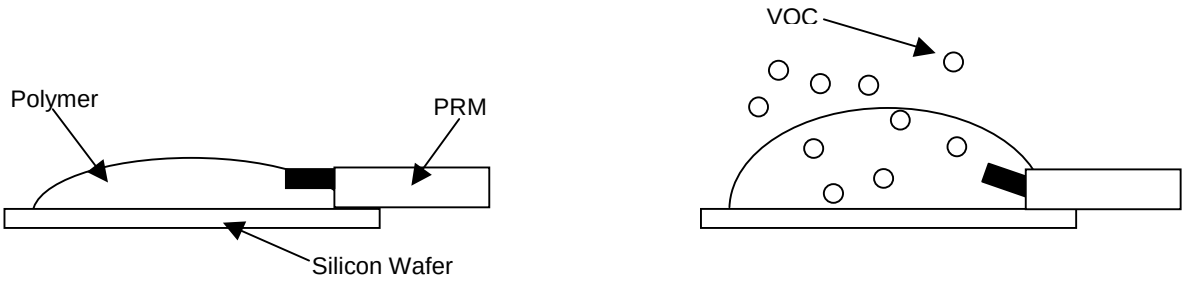

Figure 40. Inflection of the microcantilever caused by swelling of the polymer, which changes the resistance of the microcantilever.

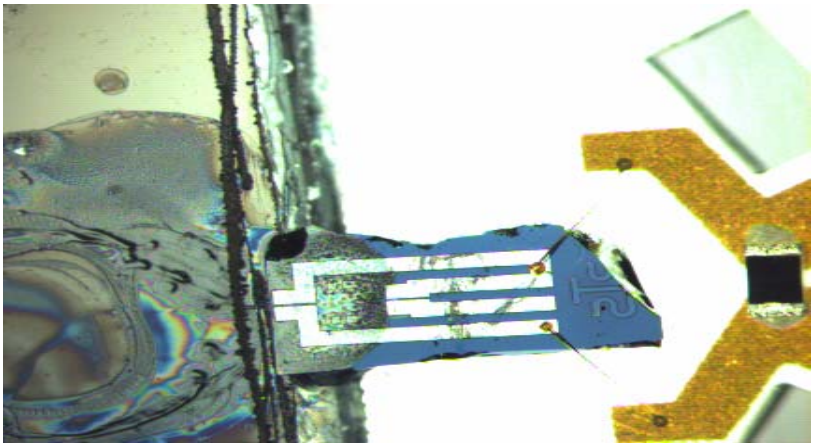

Figure 41. Shows a close up of the PRM cantilever and polymer on a silicon wafer

The PRM and chemiresistor sensors were compared side by side in a Nalgene bottle to evaluate the responses to chemical warfare simulants. Methyl Salicylate was used as the mustard gas simulant. The nerve gas simulant used was dimethyl methanephosphonate (DMMP). The PRM array was assembled with four cantilevers, a silicon wafer, and superglue. Four polymers were used for both sensors: PECH, PNVP, PIB, and PEVA.

PECH, PNVP, PIB, and PEVA loaded with carbon black were prepared, with 0.120g of polymer and 5 mL of solvent used for the chemiresistor polymers. The PRM polymers used were PVNP and PEVA. For these PRM sensors, 0.25000g of polymer was dissolved in 5.0 mL of solvent. Each polymer contained 40% carbon by weight except for the PRM polymers, which contained

no carbon black. 50uL pipettes were used to deposit the carbon-loaded ink onto the chemiresistor substrate. The polymer concentration for the PRM was increased so that a thicker layer of polymer could be deposited around the cantilever.

The experimental apparatus includes two flow meters, a 500 mL customized Nalgene bottle to allow gas flow, and one bubbler with the liquid analyte.

The sensors were allowed to run for 5 minutes before being exposed to dry air at 730mL/min. Once the sensor readings stabilized, the saturated analyte vapor was bubbled into the bottle. When equilibrium was reached, the run was continued for several minutes. At the end of the run, dry air was turned on and data is collected for another minute or two. The first experiment was to determine the stability of the chemiresistor and the PRM when exposed to nerve gas and chemical warfare simulants. The response of the chemiresistor and the PRM were recorded for concentrations of 28, 80, and 141 ppm methyl salicylate and 93, 208, and 468 ppm DMMP. All the polymers responded to the simulants. However halfway through the experiment half the PRM array failed. The cantilevers embedded in the water sensitive polymer sheared off and no longer functioned.

The first experiment for evaluating the chemiresistor and PRM was to determine the limits of detection for each sensor using chemical warfare and nerve gas simulants. Methyl Salicylate and DMMP were chosen as the simulants because they exhibit many of the same chemical properties as the real agents. Methyl salicylate is used to represent mustard gas and DMMP is used for simulating Sarin. Limits of detection of the chemiresistor and the PRM were calculated using three standard deviations above the baseline noise as a metric, together with the calibration curves. The limits of detection were necessary to determine if the sensors were capable of detecting amounts below the lethal dose.

The first simulant tested was methyl salicylate. The PRM array had two functioning polymers on it: PECH and PNVP. The theoretical detection limit was 23.67 ppm for PECH and 2.46 ppm PNVP. The effects of mustard gas can start at 12 CT (1 CT = 1 mg-min/m^3) for eyes, 33 CT for inhalation, and 15 CT vapor contact with skin. The LCT_{50} for inhalation is 900 and the ICT_{50} is 150. LCT_{50} is the CT required to kill 50% of the population and the ICT_{50} is the required amount to incapacitate 50% of the population. The PRM array is able to detect methyl salicylate under both the LCT_{50} and the ICT_{50} ppm limit. The chemiresistor contained four polymers PECH, PNVP, PIB, and PEVA. PNVP showed no response to the simulant so the data was not included. The limits of detection for the other polymers were: 0.066 ppm, 1.6 ppm, and 0.41 ppm, respectively, for PECH, PIB, and PEVA. The chemiresistor was able to detect the simulant under the LCT_{50} and ICT_{50} ppm values.

The second simulant test used DMMP. Sarin gas has an LCT_{50} of 42-74 and ICT_{50} 30-60 for Rhesus Monkeys with 2 minute and 10 minute exposures. The limit of detection for the two PRM array was 54.15 ppm and 190.21 ppm for PECH and PNVP, respectively. The PECH polymer is borderline for detecting the simulant under the LCT_{50} value and the PNVP does not detect the simulant within the required range. The limits of detection for the chemiresistor polymers were: 0.1 ppb, 0.78 ppb, and 0.78 ppb, respectively, for PECH, PIB, and PEVA. The chemiresistor was able to detect the simulant under the LCT_{50} and ICT_{50} value.

The second evaluation was to determine the stability of the chemiresistor and PRM in the presence of different chemical vapors. The stability of each sensor was measured by calculating the coefficient of variation. At the 28, 80, and 141 ppm concentration of methyl salicylate, the chemiresistor had a higher coefficient of variation by an order of magnitude compared to the PRM. On exposure to different concentrations of DMMP the chemiresistor had a higher coefficient of variation by up to two orders of magnitude. The standard deviation of the sensors was taken before chemical vapor exposure to determine the noise of the sensor. In each case the standard deviation and the coefficient of variation of the PRM was less then the chemiresistor. In summary, the PRM appeared to be more stable than the chemiresistor, but the chemiresistor was more sensitive (and more rugged) than the PRM.

5. Preconcentrator Testing and Development

5.1. Overview of Preconcentrators

Preconcentrators have been used for many years in analytical chemistry applications for collecting molecules (called analytes) that are present in very low concentrations, often in air or water. The analytical instruments, like gas chromatography, are not able to detect these low concentrations directly, so specialized materials called adsorbent resins were developed to act as room temperature adsorbers of many molecules. These materials are usually high surface area powders and have absorption properties that are catalogued [http://www.sisweb.com/index/referenc/resins.htm]. The most important property is the ability to absorb almost all the analyte from a stream of air passing through a packed column and then release all the analyte molecules when the column is heated to a specified high temperature, often a few hundred degrees Celsius. There are no perfect absorbers for all analyte molecules. The adsorption characteristics of a given resin will depend on the specific analyte. Even at room temperature, most analytes that have been loaded onto the resin will desorb at a low rate when the analyte concentration is zero above the absorber.

Because of these less-than-perfect features of currently available adsorbent resins, portable systems for doing quantitative analysis of multianalyte, low concentration air samples (in industrial hygiene for example), are fairly complicated. The Zellers' group at the University of Michigan has been active in the design, fabrication and testing of such portable systems (Tian et al., 2003). To get quantitative analysis over wide ranges of concentrations in mixtures of analytes with variable relative humidity, they find they need pumps with well defined pumping volumes through the packed preconcentrator column, chromatographic separation columns which need to be heated, scrubbers and detector arrays, along with the associated plumbing.

We are investigating a much simpler system in which a micromachined, hot plate preconcentrator is coupled to a chemiresistor array. There are no pumps and valves, so preconcentration occurs by analyte diffusion and convection to the resin (or phase) on the microhotplate (Hughes et al., 2000). This simple, low-power system will probably never be able to achieve the kind of quantitative analysis of analyte mixtures of more complex portable instruments, but we feel there are many applications where the information gathered by a hybrid

preconcentrator/chemiresistor array can be valuable. One example is the "smoke alarm" mode where the hybrid is deployed and is monitored in almost real time for a leak or breakthrough of analyte (often a VOC) into a well or chemical processing facility. Operators are then alerted without the need for quantitative information about exact concentrations (which may be changing rapidly in any case).

Our hybrid concept is closer to Solid Phase Microextraction (SPME) where preconcentration of analyte occurs on a thin fiber coated with adsorbent resin, often a polymer (Zhang et al., 1984). The loading of the SPME fiber occurs by diffusion and convection, which can be in air, water, soil or headspace of a sample bottle. Quantitation of the concentration of analyte is not achieved by complete stripping of the analyte from a measured volume as in the tube preconcentrators discussed above, but by equilibration of the adsorbent phase (resin) with sample volume. The sample volume is kept large enough so that the extraction does not lower the concentration by much. The fiber is then withdrawn into a pencil like holder and transported to a commercial instrument like a GC. The injection port of the GC is specially designed to accommodate the fiber and heat it quickly to a specified high temperature (a few hundred degrees C is common). A carrier gas flows the desorbed analyte molecules into the GC. In this way the collection step can be separated from the expensive commercial analytical instrument. Our microhotplate combines the heater and the adsorbent resin into one tiny device that can be heated much faster and with much less power than other types of preconcentrator. The small size means that it must be located very near the chemiresistor array for efficient sensing to occur.

5.1.1. Model of adsorption and desorption from adsorbent layers on the microhotplate

The simplest model that captures the main features observed with these adsorbent resins is the famous Langmuir adsorption isotherm. It gives a concentration dependent loading of the layer, along with temperature dependent desorption and saturation of layer at high loading concentrations. It was derived for physical adsorption on surfaces, but has been often applied to more complex cases such as the resins where the analyte molecules are adsorbed into bulk phases like the polymer support and pores of the high surface area resin. The Langmuir model can be expressed in the form of a differential equation for the rate of loading (or occupation) of the sites on the layer. Let Θ be the fraction of loading sites filled, with $\Theta = 1$ the maximum loading of the layer at high loading concentration and low temperature. The expression becomes $d\Theta/dt = kf(1-\Theta) - kr\Theta$, with kf the rate of loading, proportional to the concentration of analyte in the vapor contacting the layer. The kr is the desorption rate which increases exponentially with temperature (with an activation energy which depends strongly on which material and analyte is used). From this equation it can be seen that there will be a steady state at some level of Θ that depends on the concentration. The kf goes to zero when the hotplate is removed from the loading area and the concentration of analyte goes to zero and then only the kr term is operative and the analyte slowly desorbs from the layer depending on the temperature.

The rate equation can be integrated to give the loading as a function of the time of exposure to a given concentration of analyte: $\Theta = a/b - (1/b)\exp[\ln(a) - bt]$, b is the sum (kf +kr), and a= kf. The

values of kf and kr can be extracted from a set of data that compares the transient chemiresistor signal with a variety of loading times and loading concentrations.

The same microhotplates with similar phases on them are being developed for the Sandia MicroChemLab (Manginell et al., 2000). In that system, there is a pump that draws air samples across the microhotplate preconcentrator and then uses a heat pulse to desorb whatever has been adsorbed into a micromachined chromatograpic column. The column elutes onto an array of chemical sensors, which could be chemiresistors, but are usually SAW devices with polymer coatings. The MicroChemLab is smaller and lower power consuming than the systems with tube preconcentrators, but may be less quantitative in analysis of certain mixtures of analytes. The following sections will describe our efforts to integrate the micro-hotplate preconcentrator with the chemiresistor sensor in a passive mode that does not require any pumps or valves.

5.2. Fabrication of Preconcentrators

The fabrication of the micro-hotplate preconcentrator (Manginell et al., 2000) utilized a KOH-etched 4 inch wafer (yield ~200 hot-plates) with a silicon nitride coating. The KOH-etching produces a 1-micron thick silicon nitride membrane, which has a very low thermal mass. A binding agent was created by mixing .5% Polyisobutylene (0.92 g/ml PIB) in 1 ml of TCE (1.4642 g/ml TCE) by mass. This binding agent was then deposited onto the hot-plate with 65m x 510m x ~5' of High Pressure PEEK tubing (Upchurch, P/N 1543) in combination with 10-32 female-female LUER, Teezel (Upchurch, P/N P-659) and BD 10ml Syringe, LUER-LOK™ Latex Free (Upchurch, P/N B-310). Two different applications were used. In some cases the binding agent was spread over the total surface of the silicon nitride membrane and in others one dot of binding agent was applied to the surface of the silicon nitride membrane (Figure 42).

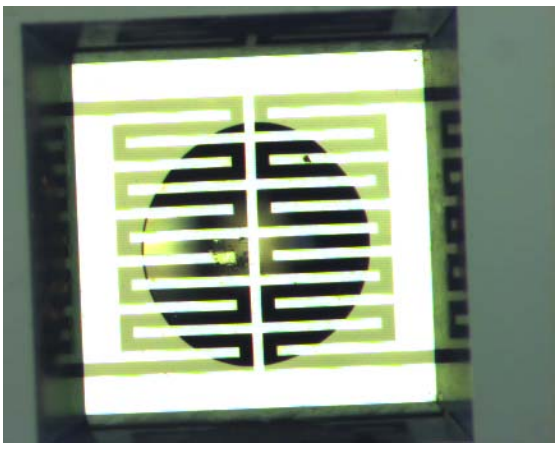

Figure 42. Polymer deposition onto silicon-nitride membrane of preconcentrator (see www.sandia.gov/sensor/PC_deposition_7-1-03.mpg (4.2 MB) for a video of the deposition).

Carboxen 1003 40/60 mesh (Supelco, P/N 10471) was ball milled to ≤325 mesh and was deposited on top of the binding agent. The preconcentrators were then placed in an oven at

~100ºC for 1-2 hours to allow for the adhesion of Carboxen 1003 to the polymer binding agent. (Figure 43).

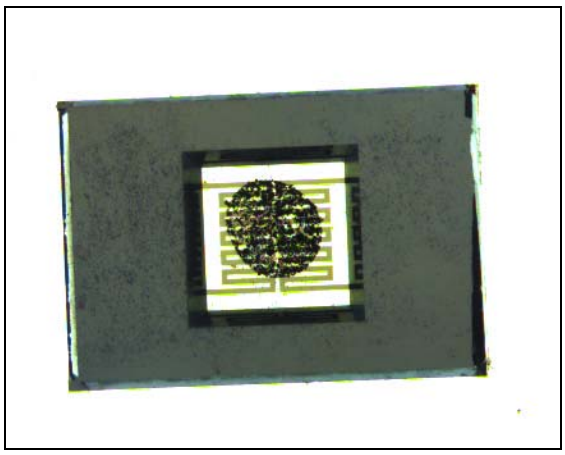

Figure 43. Preconcentrator with Polymer and Carboxen 1003.

Wires were then soldered to the preconcentrator utilizing a solder (62% Tin, 36% Lead, 2% Silver) with a melting point of 179ºC (350ºF). This solder allows for a smooth and consistent flow of solder onto the platinum pads. A smooth and consistent solder flow is very important to avoid a weak/cold solder joint which could lead to erratic and inconsistent readings, or a lack of heating voltage being applied.

5.3. Preconcentrator Heating

Tests were conducted on the preconcentrator to identify the temperature response, linearity, and stability, as well as to identify the actual temperature achieved when 5 volts was applied for a prescribed duration. Four preconcentrators and a T-Type thermocouple were placed in an oven. The oven was set to ~110ºC and allowed to stabilize. The oven was then turned off and permitted to drop to room temperature (~23ºC). During this process the resistance of the preconcentrator and the thermocouple was monitored using the Agilent 34970A datalogger. The associated data was collected and plotted using Microsoft® Excel 2000. The resistance was plotted as a function of temperature recorded by the T-Type thermocouple to establish a calibration curve. As can be seen in Figure 44 the preconcentrator responds to temperature in a linear manner.

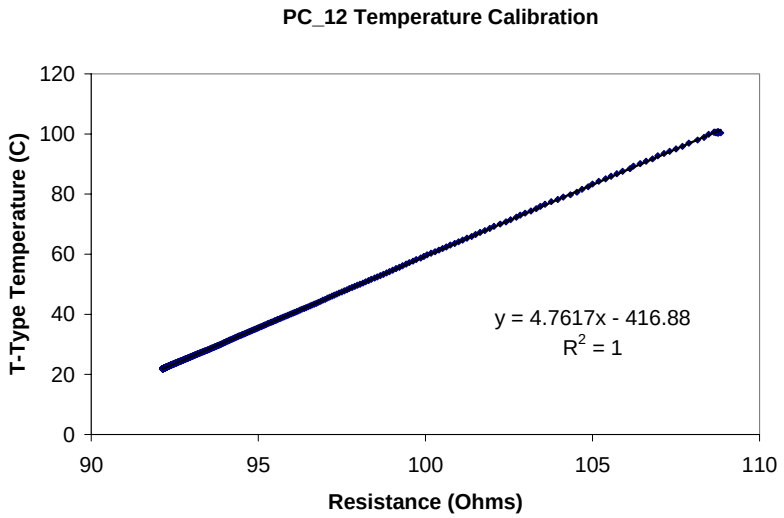

Figure 44. Temperature vs. preconcentrator resistance.

The preconcentrators were then connected to a power supply that was adjusted to supply 5 volts for 10 seconds. The resistance value was calculated from the measured current and voltage utilizing Ohms Law and then plugged into the temperature-calibration curve fit to calculate the temperature of the preconcentrator under energized conditions. Figure 45 shows all four preconcentrator temperatures as a function of time before, during, and after the heating. All four reach a temperature of ~300ºC very rapidly and are fairly steady. After the power supply was turned off, the preconcentrator temperature dropped back down to ambient temperatures very quickly.

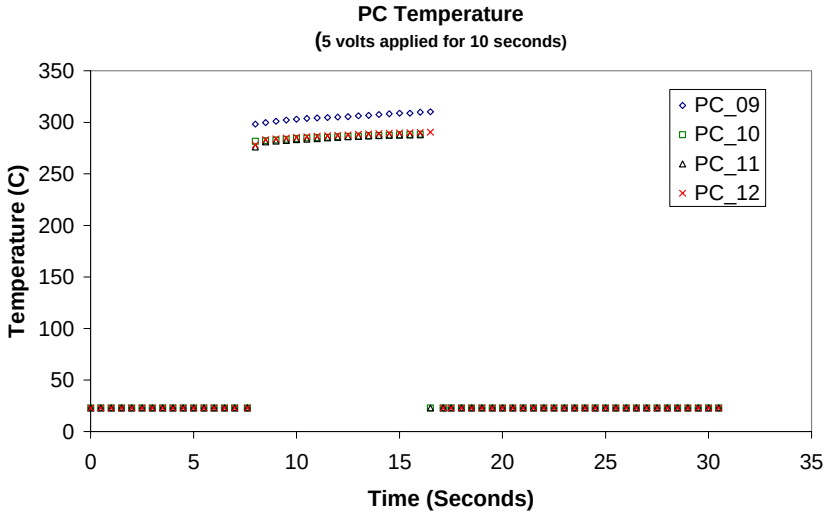

Figure 45. Preconcentrator temperature as a function of time before, during, and after heating.

5.4. Two-Piece Preconcentrator/Chemiresistor Testing

Tests were conducted at the IMRL facility to determine the response of a chemiresistor sensor to m-xylene with and without preconcentration. Results showed that by adding a microfabricated preconcentrator to a chemiresistor sensor, detection limits of m-xylene were decreased by more than two orders of magnitude, from 13.5 ppm to 61.8 ppb, without significantly increasing the complexity of the sensing system.

Controlled chemical exposures were performed through the use of custom gas cylinders of m-xylene with analytically verified concentrations or gas-washing bottles filled with liquid m-xylene. A range of concentrations are generated by diluting and controlling gas flows through a series of valves (SMC solenoid valve NVZ110 and Nupro/Swagelok stainless bellows valve SS-4BK-1C) and mass flow controllers (Brooks Instrument 5850E mass flow controllers) operated through a LabVIEW interface on a Macintosh computer. Analyte concentration levels were confirmed through the use of a RAE Systems ToxiRAE or ppbRAE photo-ionization detector.

The chemiresistor sensor (A64) used in this study consisted of a four-chemiresistor array on a single silicon substrate with integrated on-chip platinum-wire temperature sensor and resistive heater bars for temperature control. Arrays are packaged in a 16-pin DIP for ease of electrical connections. Chemiresistor polymer solution preparation involves dissolving the polymer in a solvent and adding 40% by weight of 20-30 nm graphitized carbon particles. The polymer solution is subjected to sonication from a point ultrasonic source to enhance ink uniformity, using 15 half-second pulses separated by one-second rest periods. Solution deposition on the sensor silicon substrate is performed with an Asymtek Century Series C-708 automated fluid dispensing system.

Preconcentrator devices are fabricated on a Bosch-etched silicon wafer, with platinum-wire heating elements supported by a thin silicon nitride membrane. A solid analyte-absorbent phase is dispersed in a thin dissolved polymer film used strictly for phase adhesion to the substrate. Individual preconcentrator substrates are also packaged in a 16-pin DIP for ease of electrical connections. Voltage pulses that are applied to heat the preconcentrator are controlled through manual triggering of a Systron Donner Model PLS 50-1 precision power supply.

The use of two 16-pin DIPs to separately package the chemiresistor and the preconcentrator is a departure from previous work, where both devices were packaged within a single 32-pin DIP (Hughes et al., 2000). Results from this work clearly showed the feasibility and the advantages of using the devices together in a small sensor system. However, as effectiveness of the sensor is directly impacted by the proximity of the analyte source to the sensor itself, we hypothesized that detection limits could be additionally lowered by reducing the distance from the preconcentrator to the sensor. Rather than working with a lateral diffusion distance from the two planar devices, we placed the two 16-pin DIPs in a face-to-face orientation to allow only a short vertical distance between the chemiresistor and the preconcentrator. Figure 46 shows a photograph of the custom housing designed for mating the two 16-pin DIPs in the lab.

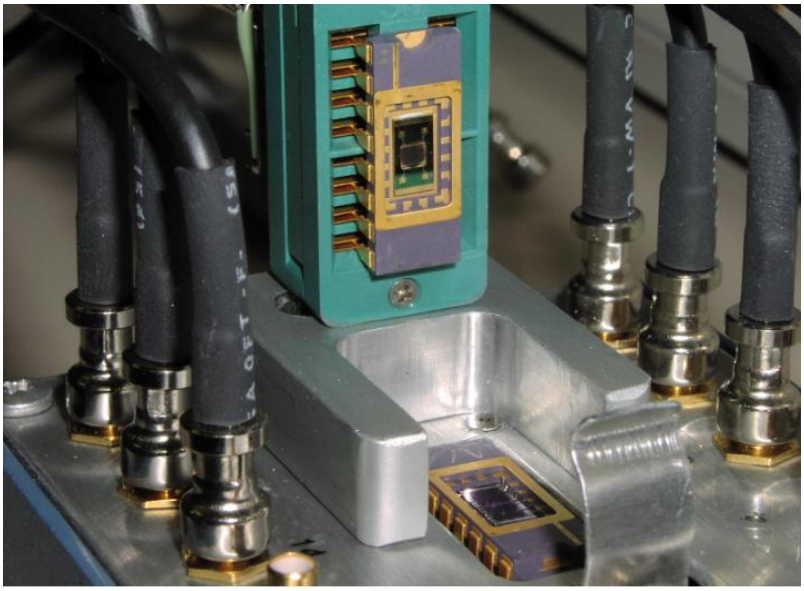

Figure 46. Chemiresistor and preconcentrator dies with custom housing for face-to-face mating. Both the chemiresistor die and preconcentrator die are packaged individually in 16-pin DIPs.

5.4.1. Results and Discussion

Our work to date using the two-piece preconcentrator/chemiresistor configuration has focused on the detection of m-xylene (an aromatic hydrocarbon found in gasoline) as a representative environmental contaminant of interest. We selected poly(ethylene-vinyl acetate) (PEVA) as our chemiresistor polymer, due to past experience with the responsive qualities of PEVA to m-xylene exposures. Commercially available preconcentrator phases were then considered for use in the study based on temperatures of absorption and desorption that would be consistent with environmental monitoring scenarios for analyte loading (~30°C under elevated temperature conditions to prevent moisture condensation on the sensor) and the typical temperature attained by the preconcentrator for analyte thermal desorption (300°C in less than 1 millisecond, due to the small thermal mass of the silicon nitride membrane on the hotplate).

5.4.1.1. Selection of Preconcentrator Phases

From our initial screening, five preconcentrator phases were identified for further study: Carbosieve, Carbotrap, Carboxen 569, Carboxen 1000, and Tenax GR. Each phase was prepared on an individual preconcentrator device and exposed to a flowing stream of 0.2% saturated vapor pressure of m-xylene (~21 ppm) for a five-minute period. Subsequent to loading the preconcentrator phase with m-xylene, the devices were mated face-to-face with the chemiresistor using the custom housing, and pulsed with five volts for five seconds. The magnitude of response of the chemiresistor sensor to all five phases, represented as an increase in chemiresistor resistance relative to the initial baseline resistance ($\Delta R/R_b$, %), is shown in Figure 47. As clearly shown, the Carboxen 1000 phase outperforms all other preconcentrator phases for

preconcentration of m-xylene, with an average $\Delta R/R_b$ of 143%, more than five-times the signal provided by any other preconcentration phase. Carboxen 1000 was therefore selected for continued performance assessment.

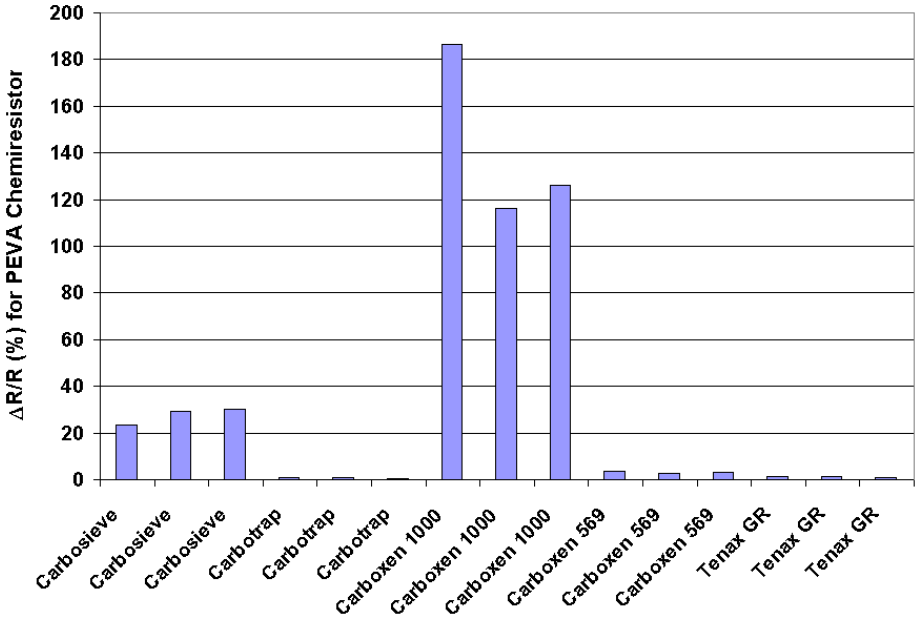

Figure 47. Preconcentrator screening data for PEVA chemiresistor response to m-xylene vapor.

5.4.1.2. Preconcentrator Enhancement of Chemiresistor Detection Limits

In order to assess the performance improvement provided by a preconcentrator, a study of the detection limit for the unaided chemiresistor sensor was performed. As mentioned previously, we had predicted the capability of chemiresistors to detect an analyte to be as low as 0.1% of the saturated vapor pressure. The noise threshold of the sensor was estimated to be equal to three times the standard deviation (σ_{Rb}) of the sensor response during quiescent, unexposed (no chemical), ambient conditions. This value was then divided by the average baseline resistance ($R_{b,avg}$) during the quiescent period to yield the relative change in resistance ($3\sigma_{Rb}/R_{b,avg}$) that corresponds to a minimum detection limit above the noise threshold. For the PEVA chemiresistor used in these experiments, $3\sigma_{Rb}/R_{b,avg} = 0.249\%$. The polynomial fit to calibration data (Figure 48) allows determination of a limit of detection of 13.5 ppm. This detection limit of 13.5 ppm corresponds to slightly less than 0.12% of the saturated vapor pressure of m-xylene (11,600 ppm under our typical laboratory conditions).

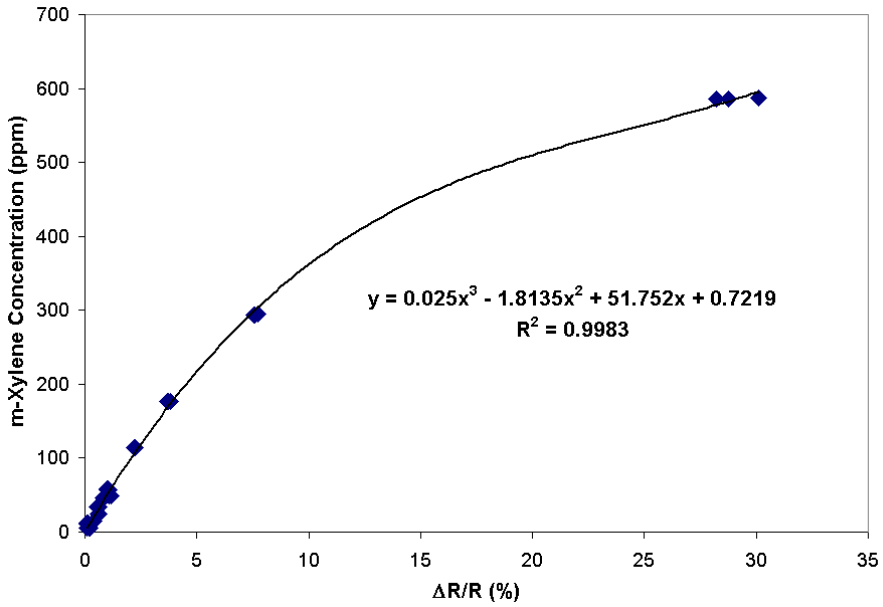

Figure 48. Calibration curve for the unaided (no preconcentrator used) PEVA chemiresistor A64 in response to m-xylene vapor.

To assess the improvement in detection limits provided by preconcentration, the Carboxen 1000 preconcentrator was exposed to a series of low concentration m-xylene streams, with preconcentration capability measured by the response of the PEVA chemiresistor. When using the chemiresistor to detect extremely low concentrations of m-xylene through the assistance of a preconcentrator, as in this case, the thermal expansion of the PEVA polymer due to the heating of the preconcentrator device must be taken into consideration to avoid confusion with swelling caused by the presence of the analyte. At the very low concentrations involved in a detection limit study, this is especially important, as the temperature response of the chemiresistor begins to be on the order of the analyte response of the chemiresistor. The necessary correction is accomplished by subtracting the response of the chemiresistor to an average blank heat pulse (no absorbed analyte) from the response of the chemiresistor to a corresponding analyte-loaded pulse. Both the analyte-loaded pulse and the blank heat pulse are calculated as individual $\Delta R/R_b$ values, each with its respective baseline resistance value (to keep consistent with changes in ambient conditions that can impact the baseline), and simple subtraction of one value from the other correctly accounts for the temperature rise associated with the heat pulse.

Applying similar logic to that previously used on the unaided chemiresistor, a detection limit was conceptually defined as a sensor signal that can be differentiated above the signal noise, quantitatively seen as a signal greater than or equal to three standard deviations above the mean noise level. However, in this instance, the sensor signal, an analyte-loaded pulse, must be differentiated from the blank heat pulses, so the mean and standard deviation for the limit of detection are in reference to the set of blank heat pulse $\Delta R/R_b$ values, and not to simple resistance values. As temperature correction must still be applied to remove the influence of the

heat pulse, the sensor response corresponding to the limit of detection is calculated as the three standard deviations above the mean blank heat pulse, corrected by the mean blank heat pulse. The equation can be written as follows:

$$\left[\left(\frac{\Delta R}{R_b}\right)_{\text{avg heat pulse}} + 3\sigma_{\text{avg heat pulse}}\right] - \left(\frac{\Delta R}{R_b}\right)_{\text{avg heat pulse}} = 3\sigma_{\text{avg heat pulse}} \quad (7)$$

For the combination of the Carboxen 1000 preconcentrator and the PEVA-40-C chemiresistor, $3\sigma_{\text{avg heat pulse}} = 0.153\%$. Using the polynomial fit to data for preconcentrator exposures over a range of 0 to 2500 ppb (with an R-squared value of 0.9946) (Figure 49), the limit of detection at three standard deviations above the mean is 61.8 ppb. Comparing both detection limits at three standard deviations above the mean, preconcentration of m-xylene therefore decreased the detection limit to less than 1/200th of the limit without preconcentration, an improvement of more than two orders of magnitude.

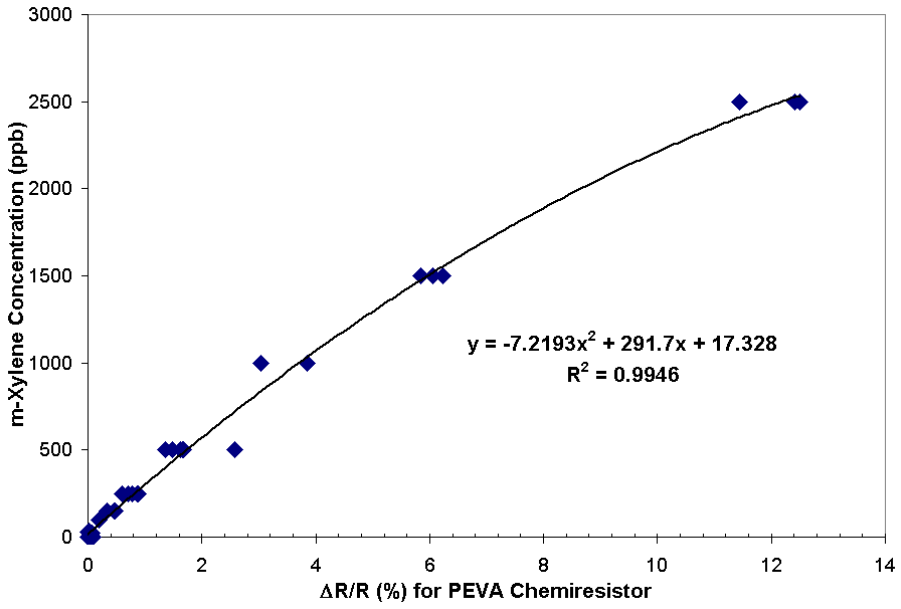

Figure 49. m-Xylene calibration curve for a PEVA chemiresistor coupled with a Carboxen 1000 preconcentrator. Each m-xylene exposure was for five minutes, followed by a five second, five volt pulse to the preconcentrator.

Ongoing tests have shown that the Carboxen 1000 preconcentrator is similarly capable of enhancing the chemiresistors' detection limits to other volatile organic compounds such as trichloroethylene and isooctane. Work is currently underway to integrate the preconcentrator and chemiresistor into the same probe described in Section 3.3. The next section describes these efforts.

5.5. Integrated Chemiresistor/Preconcentrator Probe

In the previous section, the preconcentrator was packaged in a 16-pin DIP separate from the chemiresistor. For field applications, an integrated housing containing both the chemiresistor and preconcentrator is desired so that a single field-deployable probe can be used. The following sections describe the construction, calibration, and testing methods that were used for the integrated probe.

5.5.1. Construction of Field-Deployable Integrated Preconcentrator/Chemiresistor Probe

A manifold was designed to mate the preconcentrator against the chemiresistor in a face-to-face configuration. The manifold was designed and manufactured utilizing PEEK™ polymer (Polyetheretherketone). The PEEK™ polymer was chosen because of its superior strength, ability to withstand high temperatures (up to 300ºC), and resistance to chemical solvents. The preconcentrator was epoxied in the PEEK™ manifold to create an assembly that can be easily fitted with the chemiresistor (Figure 50). The preconcentrator/PEEK manifold assembly was then mated to the 16-pin DIP with epoxy. The chemiresistor/preconcentrator package was then placed into the stainless-steel waterproof package and the PC wires were connected to two of the unused wires within the sensor cable (Figure 51).

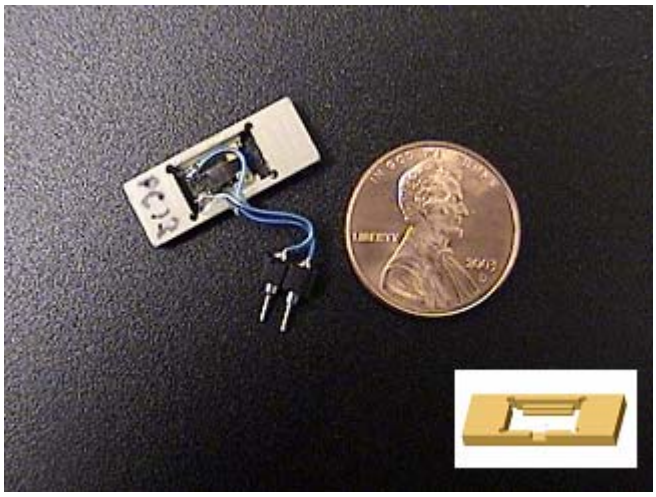

Figure 50. Manifold assembly for integration of the preconcentrator with the chemiresistor waterproof package (see Figure 7).

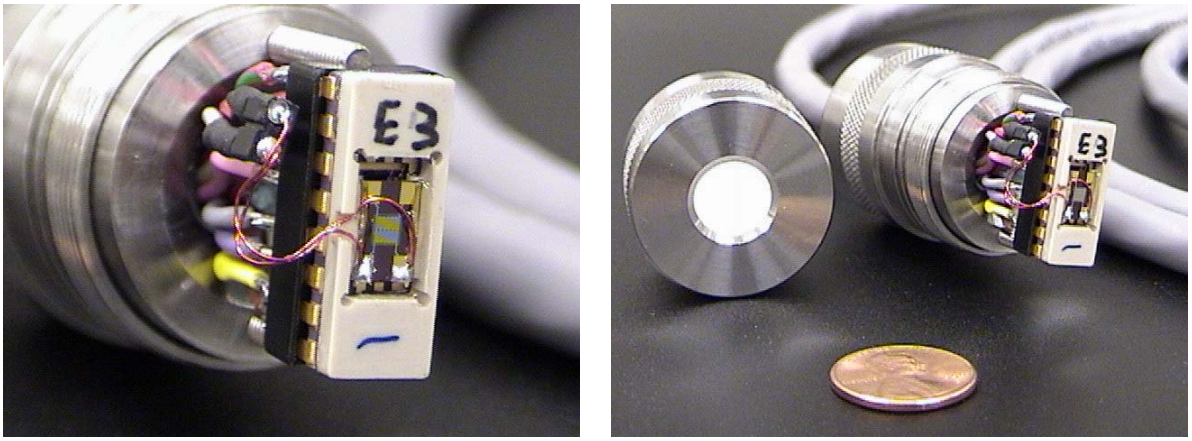

Figure 51. Preconcentrator manifold assembly integrated with the chemiresistor.

5.5.2. Calibration and Testing

This integrated preconcentrator/chemiresistor probe was then calibrated and tested. Figure 52 shows the setup used to test the preconcentrator/chemiresistor assembly. Two gas cylinders, one with dry air and one containing a chemical of interest (e.g., TCE, m-Xylene), were used in conjunction with flow meters on each output to allow for multiple concentrations by controlling the output of each bottle (e.g., TCE (50ppm bottle) and dry air mixed at equal amounts on each flow meter would generate a concentration of 25ppm. The concentration is then monitored by an MTI M200 Micro Gas Chromatograph. The flow is then divided into three different flow streams. To assure equal flow through each apparatus, adjustable flow control valves were placed before each apparatus in conjunction with three flow meters down stream from the apparatus. Each sensor is placed into an apparatus and monitored by a Campbell Scientific, CR5000 Measurement and control system. The CR5000 also controls the 5volts applied to the preconcentrator by turning on and off the CR5000 switched 12volt output. The switched 12volt output ran through a 3 terminal positive voltage regulator(P/N:NTE960, Specs: V_o:5V, I_o:1A , P_D:15W, V_{in}:35V Max). When the switched 12 volts, from the CR5000, is applied to the input of the regulator, the voltage regulator generates an output of 5 volts, which is applied to the preconcentrator.

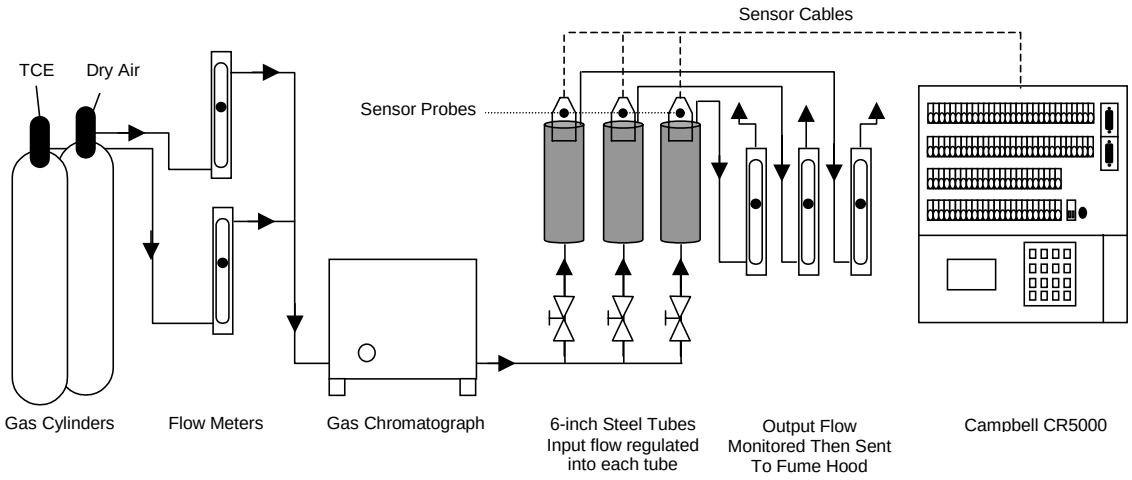

Figure 52. Calibration and testing setup for the preconcentrator/chemiresistor assembly.

A series of purge (pre-fire) pulses were needed to clear the preconcentrator of any previously accumulated chemicals. All pulses are 5 seconds in duration (for exact timing and processes see Section 12.1) As shown in Figure 53, the process starts with a series of five pre-fire pulses to purge the preconcentrator. Data is collected during the pre-fire period. After the fifth pre-fire pulse a 15-minute load time is started. One minute prior to the "Subtraction or Concentration" pulse, data collection is initiated at a rate of 1 data point every second for 60 seconds. Prior to the last pre-fire (<20msec) pulse the sample rate is stepped up to a rate of 1 data point every 20 millisecond (50/sec) for 10 seconds for 500 data points. The sample rate is stepped back down to a rate of 1 data point every second for 200 seconds for a total of 760 data points over a 4 minute and 30 second period. Varying the data collection rate allows us to insure that we catch the pulse peek while voltage is being applied to the preconcentrator. Additionally, it also enables us to keep the total number of data points to a minimum for processing purposes.

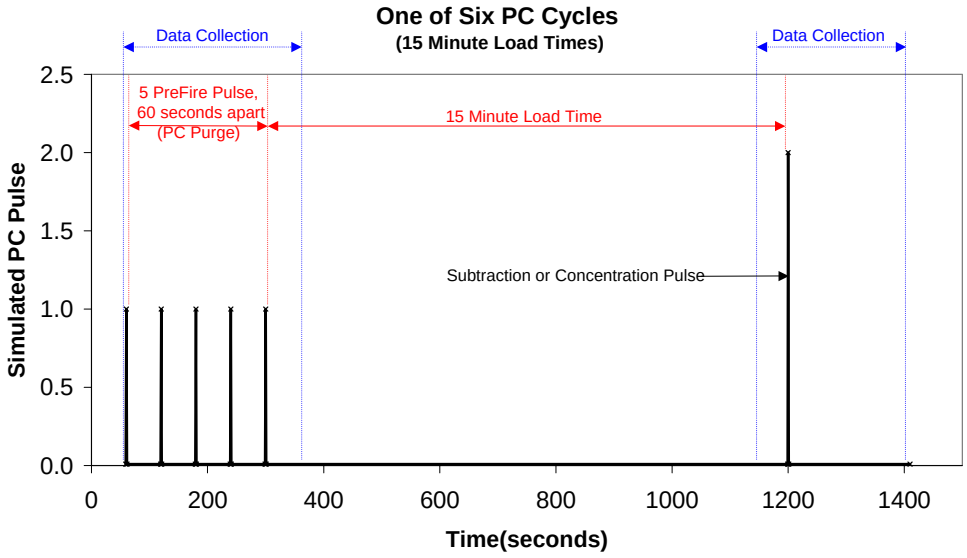

Figure 53. One of six total cycles used during calibration of the preconcentrator.

Figure 54 shows all six cycles of the experiment. The first cycle consists of five pre-fire pulses followed by a 15-minute load at which time a subtraction pulse is initiated. The subtraction pulse is a resistance measurement, with 5 volts applied, taken over a period of time while exposing the PC to dry air. This subtraction pulse is then stored into memory for future use. As soon as the subtraction pulse is complete (5 volt supply turned off), the chemical gas flow is started, which exposes the preconcentrator to the chemical of interest. The chemical gas continues to flow through the apparatus for the duration of the experiment. After the subtraction pulse is complete, the chemiresistor is allowed to stabilize for ~5 minutes. Following this stabilization period, five pre-fire pulses are initiated and a 15-minute exposure to the chemical gas begins. At the conclusion of the 15-minute load time, an exposure pulse is initiated. The exposure pulse is a resistance measurement, with 5 volts applied, taken over a period of time while exposing the preconcentrator to a chemical of interest. This exposure pulse is then subtracted from the subtraction pulse and the difference is the influence of the chemical of interest on the preconcentrator and chemiresistor. With that in mind, the preconcentrator can be exposed to multiple concentrations and a calibration curve can be generated.

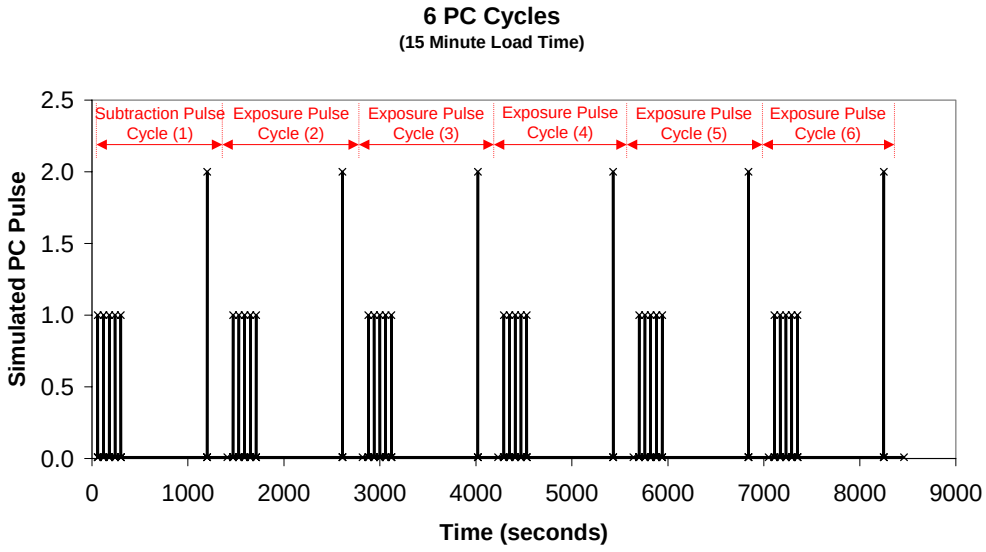

Figure 54. All six cycles with one subtraction pulse and five exposure pulses.

5.5.3. Calculation of Confidence Level

The determination of confidence was calculated by taking the standard deviation of a population of 50 data points while dry air was supplied. The 1σ value (1 Standard Deviation) was multiplied by two to create a 2σ value and by three to create a 3σ value. These values were used to calculate the limit of detection at a specific confidence level where 1σ: 68%, 2σ: 95%, 3σ: 99.7%. As seen in figure 1 only four of the fifty data points fell outside the mean ±1σ value. In addition, all fifty values fell within the within the Mean ±2σ and the Mean ±3σ values. Figure 55 (lower left) shows the actual σ value and its associated tolerance span for each Mean ±(1,2,3)σ.

One of our concerns was that the individual pulses prior to the TCE pulses might be outside of the established 3σ values. Figure 55 (lower right) shows that only one of our individual subtraction pulses was outside the 3σ values that were established during the 50-noise/detection limit pulses. We also wanted to identify if there was a normal distribution of Max ΔR/Rb values during the 50-noise/detection limit pulses. As seen on the graph, it appears that within 1σ there is a normal distribution of values across the range.

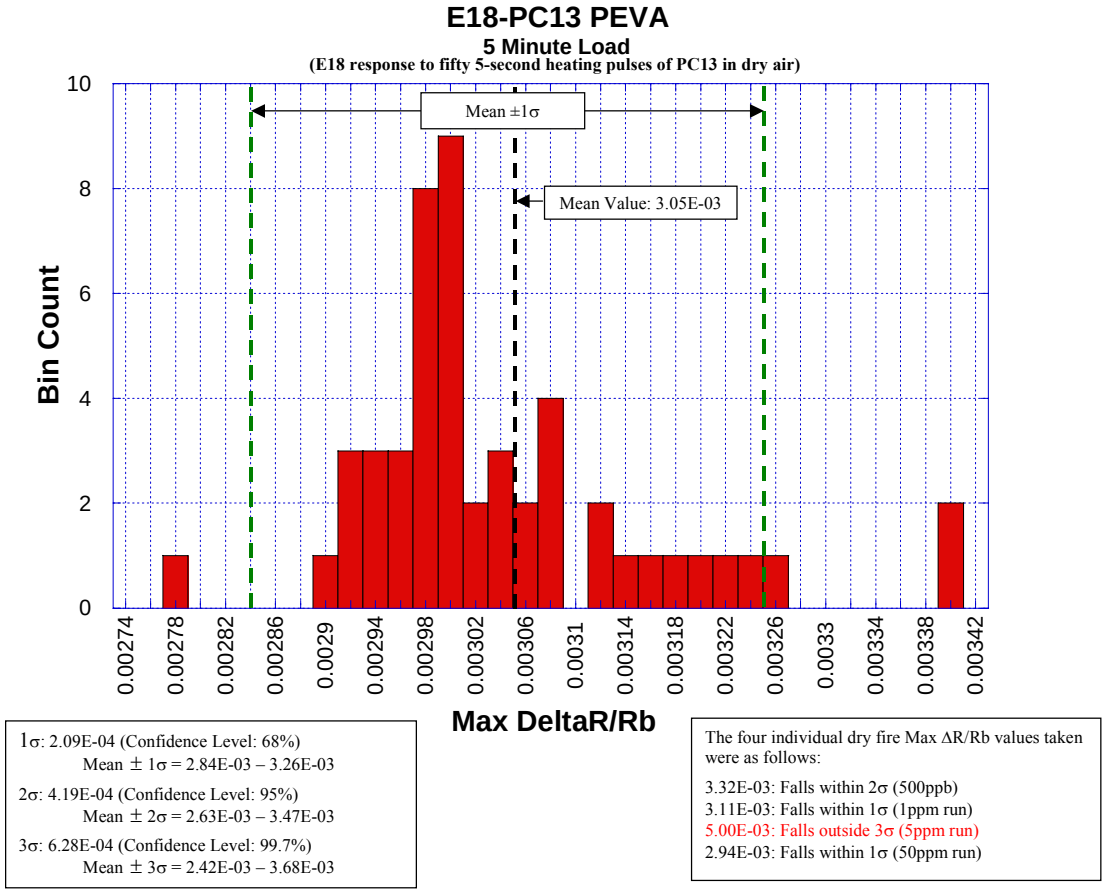

Figure 55. E18-PC13 PEVA histogram of 50 data points with dry air supplied during periodic heating of the preconcentrator.

5.5.4. Calibration Results.

Calibration of the Chemireisistor/Preconcentrator sensor package consisted of exposing the sensor package to 50ppm, 5ppm, 100ppb, and 50ppb concentrations of TCE over a given amount of time. The data was graphed in TCE concentration as a function of ΔR/Rb. A power trend line ($y=cx^b$, *where c and b are constants)* was applied to the data points. The 3σ value was then applied (x) to the power curve line fit. As seen in Figure 56, the limit of detection for E18-PC13 is 2.2 ppm with a power-law fit.

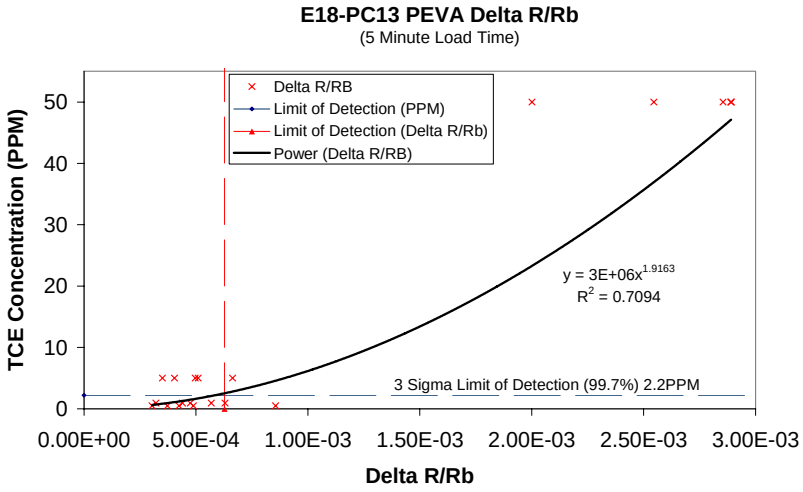

Figure 56. E18-PC13 PEVA calibration to TCE.

5.5.5. Hypothesis/Methods of Testing

These tests were conducted with the intention of identifying the different responses between two testing methods. The testing methods were conducted to identify the reabsorption behavior of the analyte gas onto the preconcentrator following single and multiple pre-fire pulses and to determine whether or not a preconcentrator completely covered with sorbent responds the same as a preconcentrator with only a dot of sorbent. The testing methods were conduced with method #1: initial pre-fire pulse only, and method #2: 5 pre-fire pulses to allow the preconcentrator to purge any residual TCE to disperse through the Gore-Tex membrane. Both methods consisted of the following: ~5ppm TCE in the gas phase, 15-minute load time, and 5-second pulse at 5-volts.

Method #1:

1. Dry air applied
2. Five (5) pre-pulse
3. 15-minute load time
4. 10 baseline readings
5. 5 second pulse at 5-volts (Dry-Heating pulse)
6. TCE (~5ppm) started
7. 15 minute load time
8. 10 baseline readings
9. 5-second pulse at 5-volt (TCE-Heating pulse)
10. Repeat steps 6,7 four more times for a total of 5 TCE-Heating pulses.

Method #2

1. Dry air applied
2. Five (5) pre-pulse
3. 15-minute load time
4. 10 baseline readings
5. 5 second pulse at 5-volts (Dry-Heating pulse)
6. TCE (~5ppm) started
7. Five (5) pre-pulses
8. 15 minute load time
9. 10 baseline readings
10. 5-second pulse at 5-volt (TCE-Heating pulse)
11. Repeat steps 6-8 four more times for a total of 5 TCE-Heating pulses.

5.5.5.1. Results of Method #1

This method utilized only one pre-fire pulse to purge the preconcentrator sorbent prior to the baseline pulse. As can be seen in Figure 57 one there is apparent drift after the Concentration pulse.

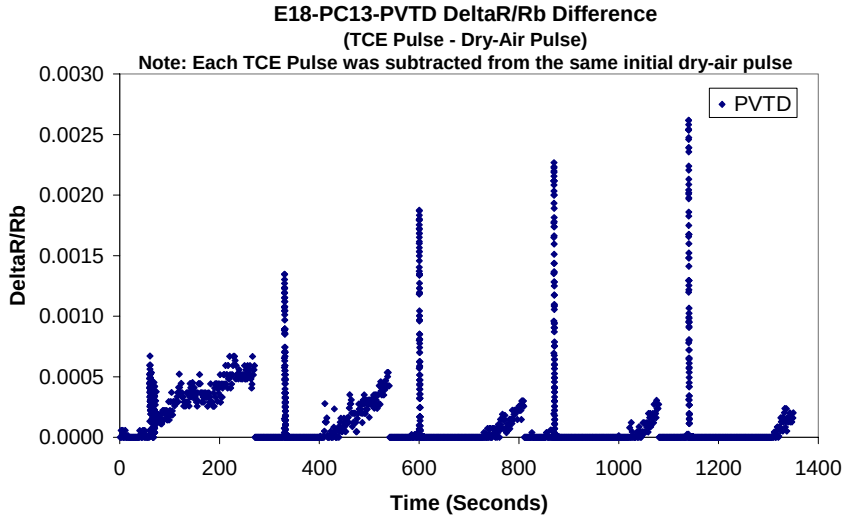

Figure 57. E18-PC13-PVTD response to Method #1.

5.5.5.2. Results of Method #2

This method utilizes five pre-fire pulses to purge the PC sorbent prior to the dry fire pulse. As seen in Figure 58 a purging pulse appears to create a much more stable and clean pulse.

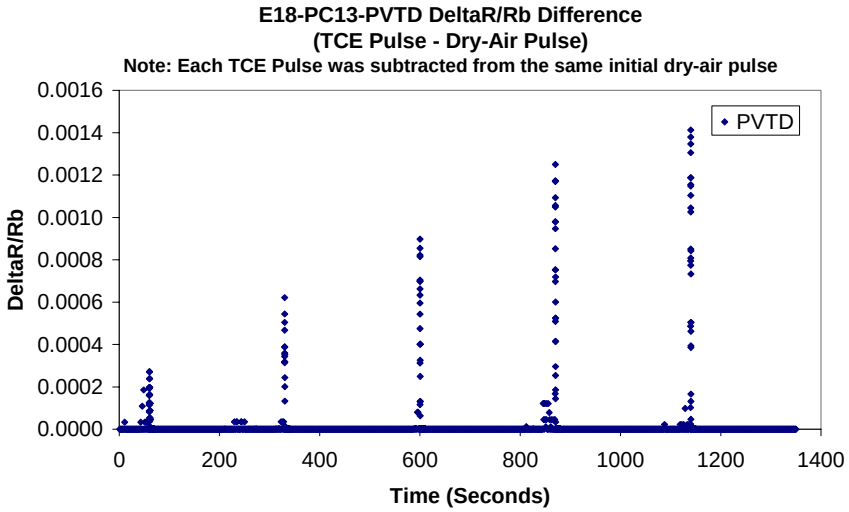

Figure 58. E18-PC13-PVTD response to Method #2

The results of the ΔR/Rb Max values can be noted in Figure 59. The response is greater without pre-fire pulses than with. This could be due to resorbtion of material onto the Preconcentrator. Also noticed was that the polymer reached equilibrium more rapidly during method 2. With these issues in mind it was decided that the five pre-fire pulses, prior to the subtraction pulse, would be the best method for future testing. It was also noted that the preconcentrator that was completely covered with Carboxen 1003 provide erratic results compared to the dot deposition method of sorbent onto the preconcentrator.

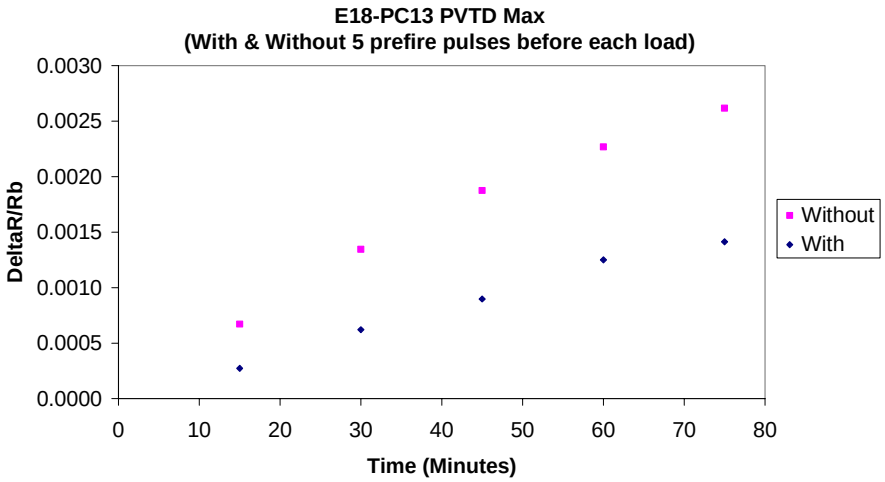

Figure 59. E18-PC13-PVTD maximum changes in relative resistance.

5.5.6. Data Processing

The data was gathered by collecting the resistance readings (*R*) from the chemiresistor and subtracting the average of ten (10) baseline values taken just prior to the pre-fire pulse. This baseline average (*Rb*) is then used to calculate $\Delta R/Rb$, where $\Delta R = R–Rb$.

$$\Delta R / R_b Diff = \left(TCEPulse\left[\Delta R / Rb = \frac{R - Rb}{Rb} \right] \right) - \left(DryAirPulse\left[\Delta R / Rb = \frac{R - Rb}{Rb} \right] \right) \quad (8)$$

This process is done for both the subtraction and the concentration pulses. Only one subtraction pulse is taken under dry air conditions. The subtraction is followed by a 15-minute load time, and then the concentration pulse is initiated. Four more concentration pulses are completed and subtracted from the initial subtraction and a new ***ΔR/RbDiff*** values is calculated

5.5.7. Stabilization Testing

The initial stabilization testing was performed after the preconcentrator was allowed to sit for more than 24 hours in ambient conditions. The preconcentrator was pulsed with 5 volts for 5 seconds and 15 minutes apart. This test was conducted to identify the point at which the preconcentrator produced consistent pulse heights. PC13 mounted on chemiresistor E18 produced expected results. With each recurrent pulse, the preconcentrator ΔR/Rb dropped until the Preconcentrator was purged and reached a stable and consistent reading. PC14 mounted on chemiresistor E22 produced erratic results. PC14 showed results that were not expected; with each recurrent pulse the preconcentrator did not drop and reach a stable and consistent reading (Figure 60). From the plot, we determined that at the sixth pulse, the preconcentrator had reached a fairly stable condition. At this point the preconcentrator would be considered purged and further loading could be performed.

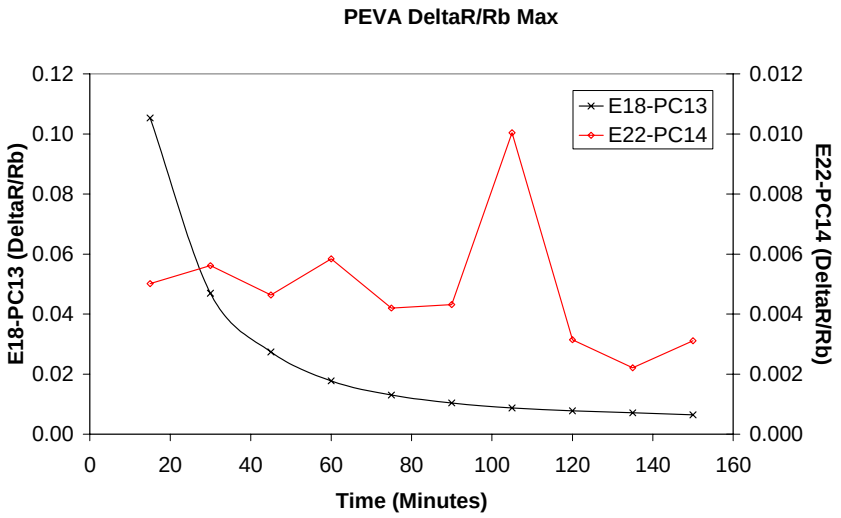

Figure 60. Stabilization test to determine number of purges required to clean the preconcentrator.

5.5.8. Different Load-Time Testing

The different load time testing was conducted to identify if different load times would affect the pulse height. The test was conducted starting with a pre-fire process to ensure the preconcentrator was purged of any unknown airborne contaminants. The preconcentrator was then allowed to load for a 60-minute duration and then pulsed. This process continued in the follow order 30, 15, 5, 5, 15, 30, 60-minute load time. Figure 61 shows the results of the test.

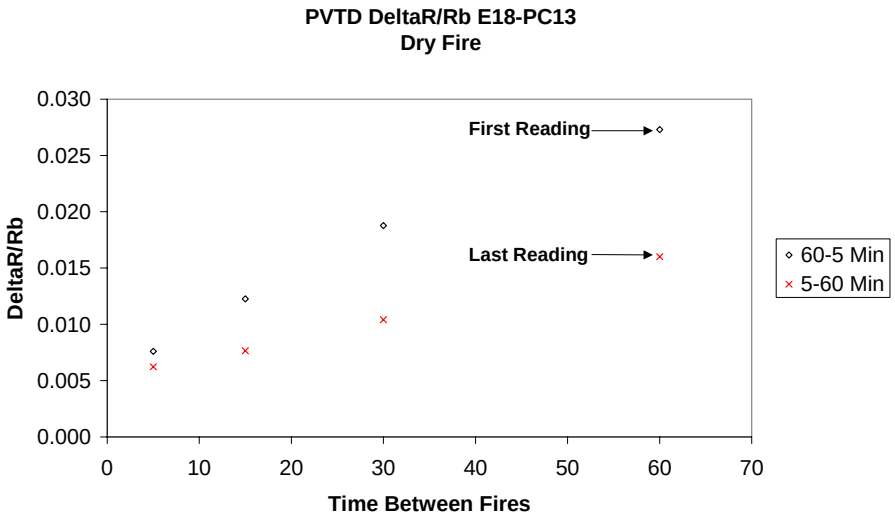

Figure 61. Sensitivity to different load times.

PC13 mounted on chemiresistor E18 again produced expected results; with each pulse the preconcentrator ΔR/Rb increased as the load time increase. PC14 (with the carbon spread over the entire membrane) mounted on chemiresistor E22 produced erratic results.

The difference in the responses for the same load times may be attributed to the previous load time in the sequence. For example, the response of the E18-PC13 60-minute load time shows a difference of ~.01 ΔR/Rb. The load time prior to the first reading was 60 minute and the load time prior to the last reading was 30 minutes.

The erratic reading of PC E22-PC14 could be attributed to the increased thermal mass of the preconcentrator at its outer edges. The preconcentrator has very little thermal mass on the membrane itself, but at the outer edges of the preconcentrator the thermal mass increases due to the increased amount of silicon. This could cause inconsistent heating of the preconcentrator, which would cause inconsistent purging of the TCE from the Carboxen and erratic readings by the chemiresistor.

6. Data Analysis and Discrimination

6.1. Discrimination Analysis using VERI

Analysis of experimental data from an array of chemiresistors requires examination of multiple signals simultaneously – one from each of the polymeric films in the array. Some early work in the analysis for chemiresistors focused on the use of three-dimensional plots, where each axis on the graph can represent the response of a single polymer film. Through simple mathematical transformation of the individual and combined sensor response signals, each sensor detection event can be spatially represented for visual convenience on the surface of one-eighth of a unit sphere, as illustrated in Figure 62.

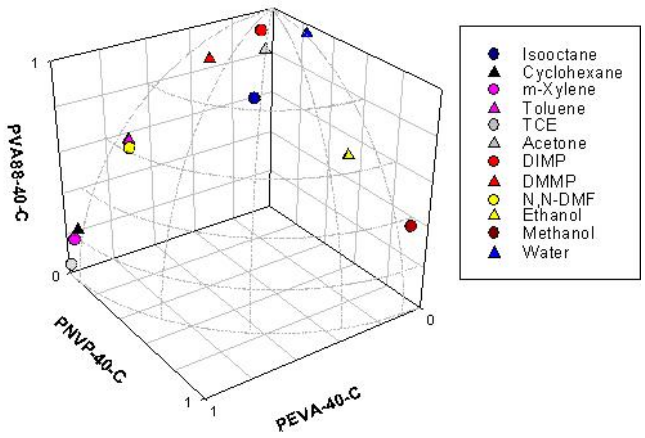

Figure 62. Example of a three-dimensional plot showing combined response data from three chemiresistors in a particular sensor array to 12 different analytes.

Obviously, however, this type of analysis is limited to three polymer films at a single time. To address this issue, the Visual-Empirical Region of Influence (VERI) pattern recognition algorithm was used (http://www.sandia.gov/imrl/XVisionScience/Xusers.htm). The VERI algorithm, developed at Sandia, allows determination of grouping for n-dimensional data in a manner consistent with human perception of data clusters through application of an established region of influence shape on a two-dimensional projection of the n-dimensional data. With each chemical detection signal as a combination of responses from all n sensors, any subset of three detections can be placed on a hyperplane for analysis with the region of influence shape, shown in Figure 63.

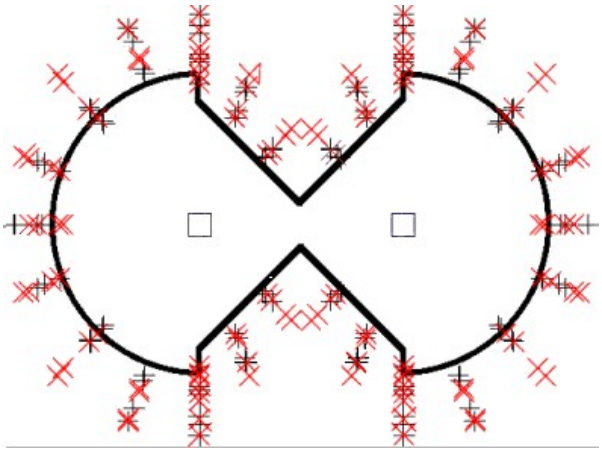

Figure 63. The region of influence shape used in Sandia's VERI algorithm for pattern recognition.

The two particular detections being analyzed for placement in a single group are placed in the center boxes of the VERI shape, with the size of the fixed shape scaled to correspond to the distance between the two points. Every other detection is then individually examined for grouping with one of the other two points. As shown in Figure 64, grouping of the two detections is dependent upon finding no other detection points that fall within the boundary of the VERI shape. The algorithm can therefore be used to determine grouping of unknown sensor detection data by analyte or class of analyte, or to evaluate successful discrimination of a known set of analytes based on a particular subset of sensors. Our use of the VERI algorithm specifically focused on the latter application, with the evaluation of an array to correctly identify different analytes. We also used the VERI algorithm to determine optimum array size based on a particular data set. In one particular study, we determined that an optimized array of four chemiresistors was able to correctly identify six different analytes more than 82% of the time. Complete details of these studies can be found in Davis et al. (2002).

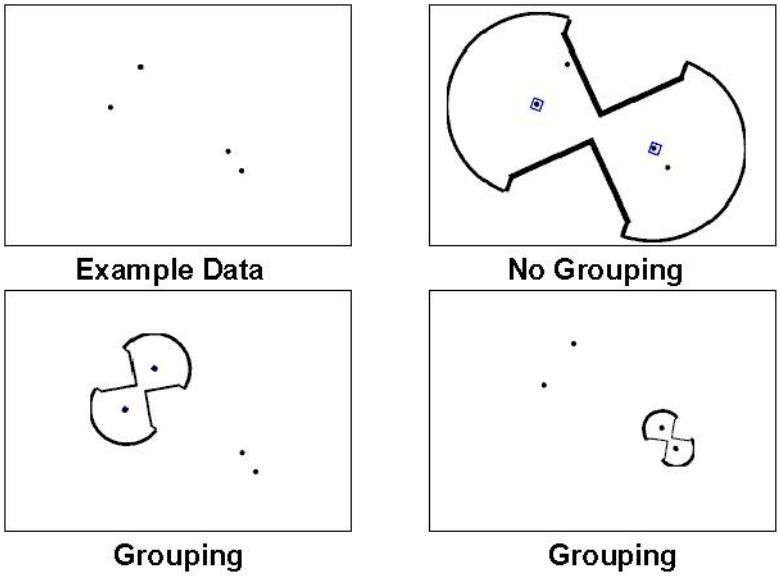

Figure 64. Example of application of the VERI shape to four points of two-dimensional data for grouping determination.

6.2. Partial-Least-Squares Data Analysis

Analysis was also performed on the data obtained from chemiresistor array calibration. Customary calibration methods typically involved a process of repeated exposures of a particular analyte at a given concentration within a sequence of increasing concentrations, at a fixed temperature and relative humidity (see Figure 65 for an example). Our analysis worked to determine the applicability of the calibration data obtained in a carefully controlled laboratory environment to the uncontrolled environment typically found in the field. For this work, partial least squares (PLS) was used as a multivariate data analysis method, allowing simultaneous

examination of all sensor data from the chemiresistor sensors and associated temperature sensor. A key observation was that the customarily used systematic calibration sequence allowed for sensor drift or hysteresis to be included in the sensor analyte detection signal. To try to minimize these effects, a randomized sequence of exposure concentrations was proposed for comparison to the systematic calibration sequence (see Figure 66 for example). Using a cross-validative approach, the PLS calibration model determined from either the systematic or the randomized calibration sequence was used to try to predict concentrations from the other calibration sequence. In every case, the PLS calibration model based on randomized calibration data was superior in predicting concentrations, both in different temperature and humidity conditions, as well as for short or long term durations between collection of calibration data and predictive data. The customary process for calibration was therefore revised to include randomized concentration sequences, to take advantage of this predictive robustness. Details of this work can be found in Rivera et al. (2003).

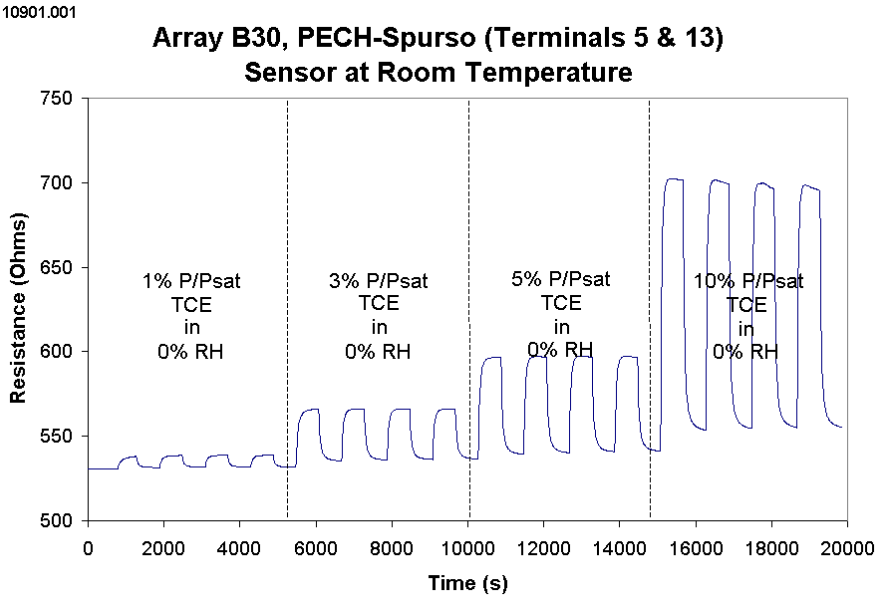

Figure 65. Example of raw resistance plot from a single chemiresistor under the systematic calibration sequence.

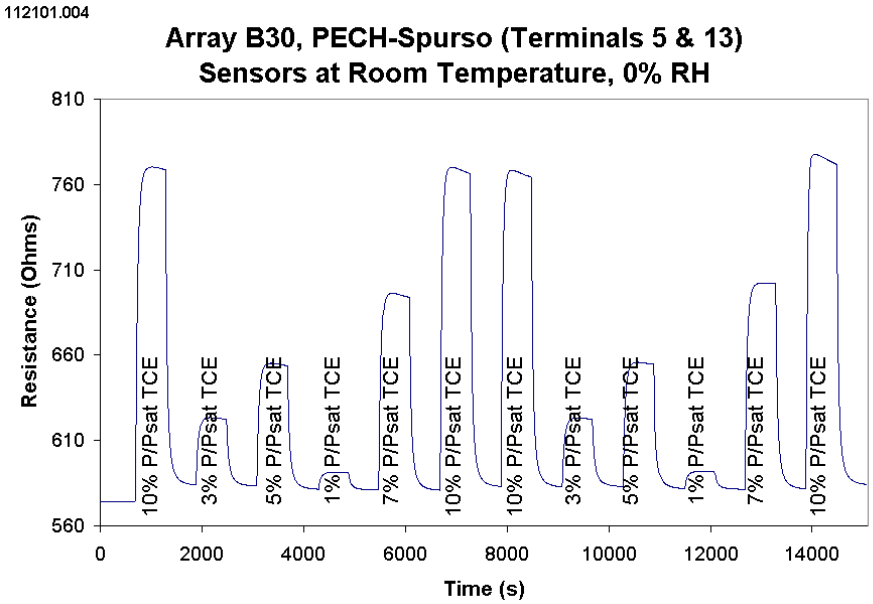

Figure 66. Example of raw resistance plot from a single chemiresistor under the randomized calibration sequence. Note the reduction in drift and hysteresis.

6.3. Multivariate Data Analysis using Statistica™

Section 4.1.1.3 provides a detailed discussion of the calibration process for the development of a multivariate regression model using Statistica™. This section presents a demonstration of a chemiresistor that was calibrated and deployed with a multivariate factor-analysis model.

The chemiresistor E4 was calibrated to water and acetone separately. The results were analyzed using Statistica™ and the resulting model was programmed into a Campbell CR10X data logger (see Section 12.2 for a listing of the program). A Real Time Data and Monitoring (RTDM) file was created to give a visual of the programs functions for demonstration purposes. Figure 67 shows a screen image of the created RTDM file.

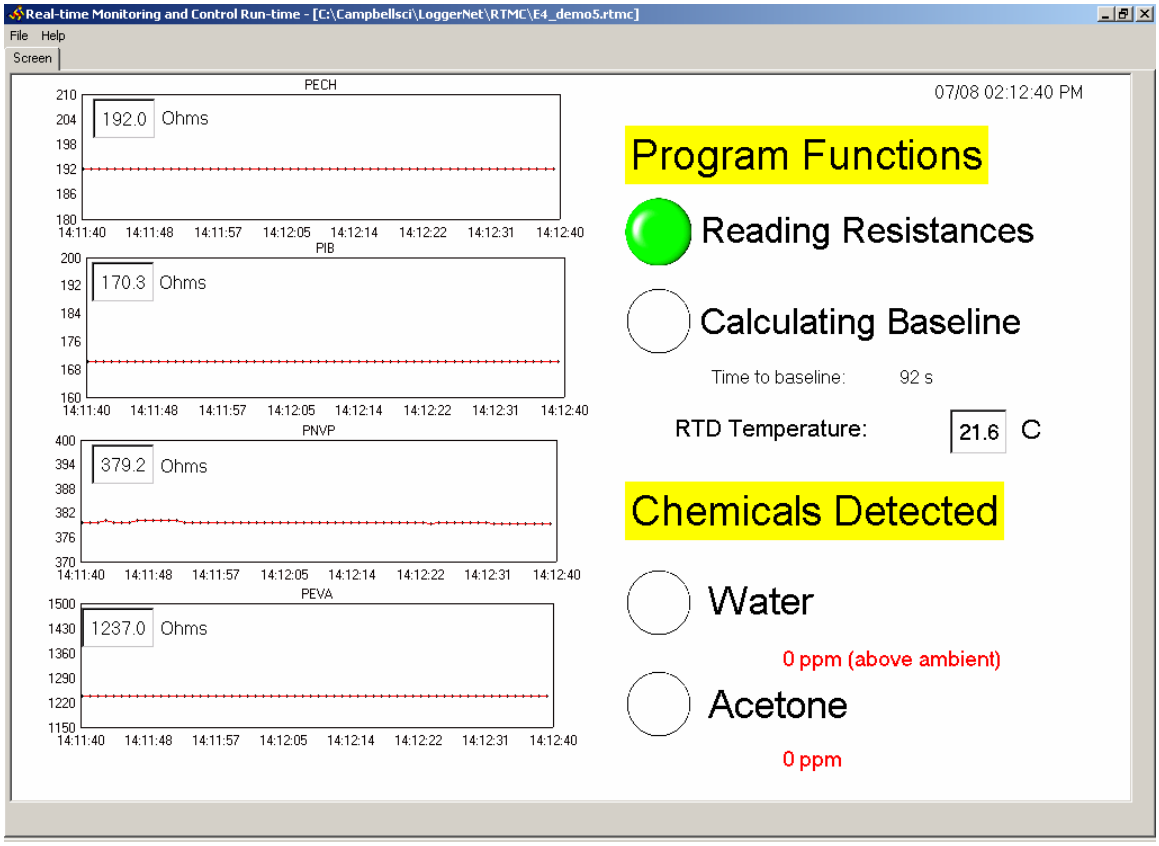

Figure 67. Screen image of the RTDM file.

The resistances of each of the four chemiresistors in the array are shown on the left of the screen, and the rapid response of the chemiresistors upon exposures to various chemicals can be observed. The right side of the screen allows the user to see the program functions. Also located on the right side are alarms that will turn on once the sensor is exposed to water and/or acetone. Figure 68 shows the response of the chemiresistor to an exposure of nail polish remover, which contains both acetone and water.

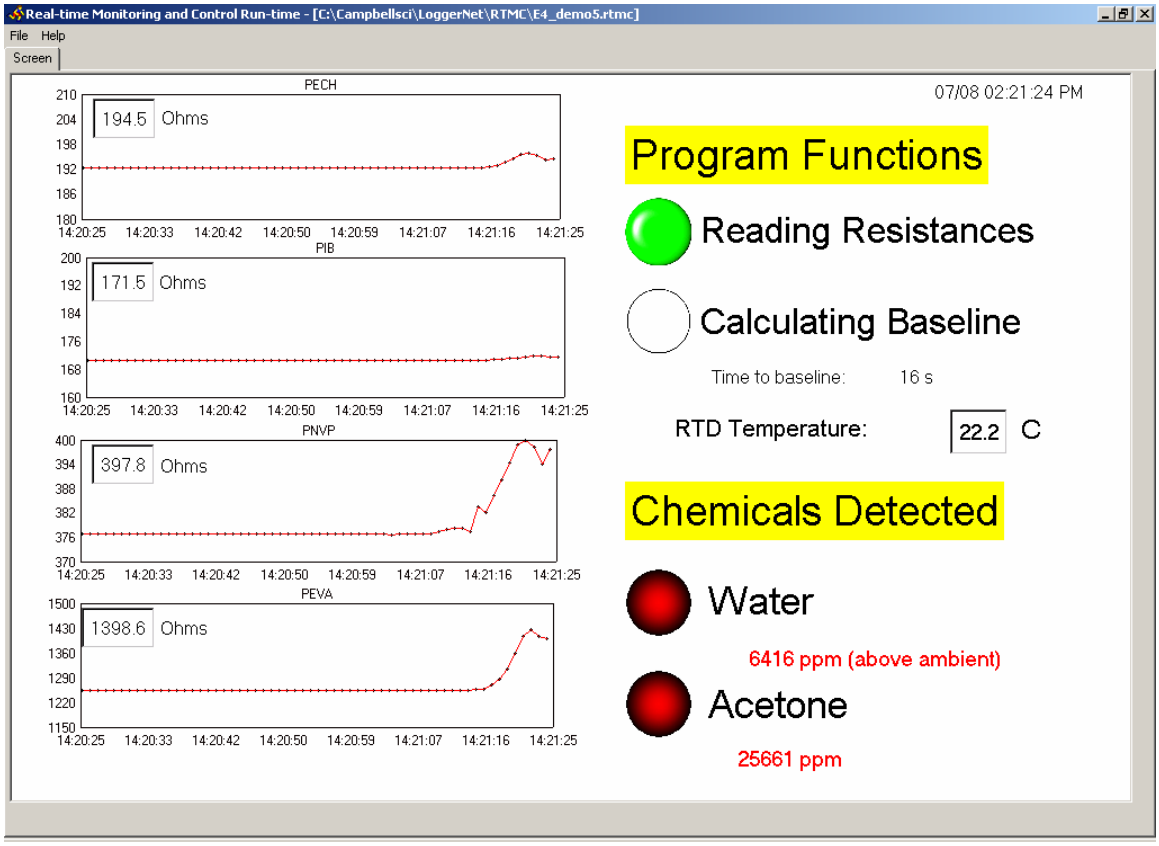

Figure 68. Screen image of the RTDM file upon exposure to nail polish remover.

If acetone or water alone is exposed to the chemiresistor the appropriate indicator will light up, and the calculated concentration will be displayed. The buttons are linked to flags in the program that are triggered "high" once a threshold concentration has been exceeded. The threshold concentrations are set relatively high for demonstration purposes. This demonstration shows the chemiresistor's ability to discriminate between analytes, quantify the concentrations, and provide a rapid response. A video of the E4 chemiresistor demonstration can be viewed online at www.sandia.gov/sensor/E4_chemiresistor_demo.mpg.

7. Field Studies

Three field studies were conducted to evaluate engineering requirements, long-term performance, and other issues associated with the operation of the chemiresistor in actual environmental conditions. The three sites include Edwards Air Force Base, CA, the Nevada Test Site, and the Chemical Waste Landfill, NM. Results of the Edwards Air Force Base and Nevada Tests Site field tests have been recently documented (Ho et al., 2002; Ho et al., 2003b), so the focus of this section will be on the field tests at the Chemical Waste Landfill.

7.1. Edwards Air Force Base

In FY02, field tests were conducted at Edwards Air Force Base to test the ruggedness, operation, and performance of the in-situ chemiresistor probe developed at Sandia. In the first phase of testing, the housing was submerged beneath the water table at well 18-MW37. The housing was lowered deeper and deeper beneath the water table until leaking was observed. In the second and third phases of testing, a chemiresistor sensor was placed in the housing and connected via cable to a data logging station that operated continuously using solar power (Figure 69). The sensor was lowered down the well and operated for a period of time in both the unsaturated and saturated zones. Major findings and recommendations regarding these tests include the following.

- The 304 stainless-steel housing showed signs of corrosion over the course of the tests. The operation of the chemiresistor sensor was not adversely impacted, but the use of plastic housings (e.g., PEEK) may decrease the corrosion of the housing in oxidizing aqueous environments.

- The Gore-Tex® polymer membrane prevented liquid water from entering the housing up to depths of ~30 ft.

- The chemiresistor sensor operated continuously over a four-month period in well 18-MW37 using a Campbell Scientific data logger powered by a 12 amp-hour battery and 20-Watt solar panel. Data were logged from the station manually using a laptop and serial connection; we recommend implementing a cell phone modem (or other wireless communications device) for the capability to log data remotely and automatically.

- The measured concentrations (using off-site laboratory analysis of grab samples) near the surface of the water table at well 18-MW37 were too low for detection by the chemiresistor, so direct comparisons could not be made. The use of an integrated preconcentrator assembly to increase the detection limits of the chemiresistor is currently being investigated. Additional tests in wells with higher concentrations (> 1000 ppmv) are desired.

- The results of all four polymers on the chemiresistor sensor chip showed instability during the field tests, even though the temperature and relative humidity were nearly constant (~21ºC, 100% RH). Estimated concentrations using the chemiresistor readings were anomalously high. We speculate that the large water-vapor concentrations (100% relative-humidity environments) may have caused condensation and spurious readings (continual sorption and creep of the polymers). The use of automated temperature control (or continuous heating) to keep the chip temperature above the local ambient may prevent condensation and improve the stability.

A complete description of these tests and the results are provided in Ho et al. (2002). The report can be viewed online at www.sandia.gov/sensor/SAND2002-4135.pdf.

Figure 69. Left: Lowering sensors down well 18-MW37. Middle: View of cables from top of well casing. Right: Downloading data from the data logger. (from Ho et al., 2002)

7.2. Nevada Test Site

Microchemical sensors developed at Sandia National Laboratories were tested at the Nevada Test Site as part of the Advanced Monitoring Systems Initiative program. Two sensors, the chemiresistor sensor and the surface-acoustic-wave (SAW) sensor, were evaluated in the tests (Figure 70). Both sensors rely on sorption of chemicals onto polymer films to produce a change in an electrical signal that can be recorded and calibrated, but different transduction mechanisms are used. The primary purpose of the tests was to evaluate the feasibility of using these devices in potentially long-term, unattended applications such as long-term monitoring of subsurface contaminants.

A complete monitoring system was developed that provided real-time monitoring of the sensors via the internet. Engineering issues such as sensor packaging, data acquisition, power requirements, and telemetry were addressed during the development and testing of the sensor systems. In addition, issues such as data processing, noise, and interferences from fluctuating environmental variables were also encountered and evaluated during the field tests. Results showed that both sensors could be operated remotely and continuously for long-term monitoring applications using commercial data-acquisition systems and custom-designed packaging. Both the chemiresistor and SAW sensors experienced drift in the signal and were impacted by fluctuations in temperature and humidity. However, results from the chemiresistor showed that exposure to large concentrations of contaminants (e.g., trichloroethylene) overwhelmed the fluctuations caused by temperature and humidity variations. Results also showed that the chemiresistor sensor exhibited better stability and sensitivity than the SAW sensor for the conditions and analytes that were tested, which was contrary to initial theoretical predictions.

A complete description of these tests and the results can be found in Ho et al. (2003a,b) and Ho and Lohrstorfer (2002). The final SAND report detailing the tests at the Nevada Test Site can be viewed online at www.sandia.gov/sensor/SAND2003-0799.pdf.

Figure 70. Sandbox Test. Left: Placement of tubes for contaminant (center tube) and sensors. Right: Sandbox with data-logging station in background. (from Ho et al., 2002)

7.3. Chemical Waste Landfill

7.3.1. Introduction

A number of improvements that were recommended in the previous field tests were incorporated into a real-time in-situ chemiresistor monitoring system deployed at the Chemical Waste Landfill. The suggested improvements include the use of multivariate data analysis to provide real-time processing and interpretation of the chemiresistor-array data. In addition, localized heating was added to the chemiresistor chip to maintain the local temperature above the dew point in water-saturated environments.

The monitoring system at the Chemical Waste Landfill includes two chemiresistors to detect trichloroethylene (TCE): one is deployed 60 feet below the ground surface in the unsaturated zone, and the other chemiresistor is deployed near the water table approximately 500 feet below the surface. A relative humidity sensor, thermocouple, and pressure transducer are also deployed in the unsaturated zone well to monitor changing environmental conditions. In the saturated-zone well, localized heating is implemented on the chemiresistor chip to prevent condensation. A thermocouple and a pressure transducer are also deployed in the saturated-zone well to monitor groundwater temperature and water level. A multivariate regression model was developed through rigorous calibrations of the chemiresistor sensors to different concentrations of TCE under varying environmental conditions. This model was programmed directly into the data logger so that data could be processed in real time (see Section 12.3 for the Campbell 23X program). This system has been operating continuously since March of 2003. A cost analysis of this field test indicated that the annual cost of remotely operating the in-situ chemiresistor sensor system is less than the costs associated with manually sampling two wells (with off-site laboratory analysis).

7.3.2. Data Logging and Processing

To collect the sensor information at the Chemical Waste Landfill (CWL) the Campbell Datalogger CR23X was used. Since the CWL is a remote site without convenient access to electrical outlets, a battery was used to power the CR23X. An 80-amp hour battery manufactured by Interstate was used to power the CR23X. The CR23X datalogger will operate accurately on a range of 11 to 16VDC. To ensure that the battery voltage of the datalogger remains above 11VDC, a 20-watt solar panel is used to recharge the battery. The datalogger has constant power and collects data at preset intervals. Once the data is collected the program turns on a cell phone that is housed inside the datalogger. The CR23X interfaces with web posting software via the cell phone. The CR23X, cell phone, and modem are all in a Campbell Scientific enclosure that is mounted on a tripod. The solar panel and a Yagi antenna are also mounted on the tripod (Figure 71).

Figure 71. Solar-powered remote data-logging stations next to well D3 at the Chemical Waste Landfill.

Two wells at the CWL were monitored for TCE concentration. The first well monitored was D3 with the chemiresistor E19. The chemiresistor E19 had been calibrated for different temperatures, humidity, and TCE concentrations following a multivariate calibration procedure found in Section 4.1.1.3. The results were analyzed using Statistica™ and a multivariate model was entered into the program for the CR23X:

$$TCE\ (ppm) = 2.26E+03 - 2.19E+02*TempC + 3.82E+05*\Delta R/R_{b\ PNVP}*\Delta R/R_{b\ PEVA} + 2.40E+03*\Delta R/R_{b\ PVTD}*TempC + 1.43E+03*\Delta R/R_{b\ PEVA}*TempC + 2.99E+01*\Delta R/R_{b\ PVTD}*Vp - 4.75E+04*\Delta R/R_{b\ PIB}*\Delta R/R_{b\ PNVP}*TempC + 8.07E+03*\Delta R/R_{b\ PIB}*\Delta R/R_{b\ PVTD}*\Delta R/R_{b\ PEVA}*TempC$$

Where:

TempC = Temperature of sensor in degrees Celsius
Vp = Water vapor pressure of water in pascals

We also monitor the temperature, humidity, and atmospheric pressure of the well D3 for use in the model. The physical parameters were monitored with an Omega Engineering T-type

thermocouple, HX92 humidity probe, and a PX215 pressure transducer. The parameters were used to report the in-situ conditions of the well and to correct for temperature and water vapor in the multivariate model. The model generated by Statistica™ relies on a baseline value that was established at 9 ºC in dry conditions (0% relative humidity). To compensate for the presence of water vapor, an additional calibration to water vapor alone was performed. This was done by exposing chemiresistor E19 to known concentrations of water vapor and plotting the response. Table 7 shows the power functions for the water calibration of the chemiresistor E19.

Table 7. Vapor pressure calibration for chemiresistor E19.

	Polymer	Calibration Equation
E19	PIB	$y = 3E\text{-}06x^{0.9584}$
	PNVP	$y = 6E\text{-}07x^{1.7798}$
	PVTD	$y = 3E\text{-}06x^{1.1034}$
	PEVA	$y = 4E\text{-}07x^{1.3308}$

x = Water vapor pressure (Pa)
y = $(\Delta R/R_b)$

The vapor pressure of the system at the time that the baseline is recorded is plugged into the water vapor calibration for each polymer. The result is plugged into the following equation to generate a vapor-pressure-corrected baseline.

$$\text{Vapor-pressure-corrected baseline } \Omega = \frac{\Omega_R}{\left(\frac{\Delta R}{R_b}\right) VPCalibration + 1} \tag{9}$$

Where:
Ω_R = Baseline resistance of polymer, not corrected.

The program then takes the vapor pressure corrected baseline and corrects for the temperature. To compensate for the effects of temperature the response of the chemiresistor was calibrated for temperature. This was done by placing the calibration apparatus in the oven and flowing dry air across the sensors. The dry air passes through a 50ft of copper tubing prior to the sensor to insure that the temperature of the air is equal to that of the oven. Table 8 shows the temperature calibrations for each polymer on the chemiresistor E19.

Table 8. Temperature calibration equations for the chemiresistor E19

	Polymer	Calibration Equation
E19	PIB	y = 0.2279x + 125.53
	PNVP	y = 0.167x + 97.305
	PVTD	y = 0.3871x + 222.32
	PEVA	y = 0.624x + 147.02

x = Temperature ºC
y = Resistance (Ohms)

The program uses the slope of the temperature calibration equations for each sensor to compensate for the temperature of the ambient environment:

$$\text{Temperature \& Vapor Corrected Baseline} = \text{VPCorrected} - \text{Slope}*(\text{Ambient Temp} - 9\ ^{\circ}\text{C}) \quad (10)$$

The temperature and vapor corrected baseline is then recorded by the datalogger and used in the Statistica™ model to predict the chemical concentration in the well. The chemiresistor E19 operated successfully and without incident for the duration of the field demonstration. Two commercial sensors malfunctioned in the well D3. They were the PX215 pressure transducer and the temperature/humidity probe. These sensors were replaced with functional ones.

The second well monitored was MW2BL. The well was monitored with a submersible pressure transducer, thermocouple, and a chemiresistor. The pressure and temperature were monitored with a CS400 submersible pressure transducer from Campbell Scientific and a submersible T-type thermocouple, respectively. A total of three chemiresistors were deployed to monitor the chemical concentration of this well (two malfunctioned because of water leaking into the probe). The following equation shows the model generated by Statistica™ for chemiresistor E25, which is currently operating in the well.

$$\text{TCE (ppm)} = -3.45\text{E+00} + 1.56\text{E+05}*\Delta R/R_{b\ PECH} - 3.82\text{E+07}*\Delta R/R_{b\ PECH}*\Delta R/R_{b\ PIB} - 1.88\text{E+06}*\Delta R/R_{b\ PECH}*\Delta R/R_{b\ PEVA} + 5.79\text{E+05}**\Delta R/R_{b\ PNVP}\ **\Delta R/R_{b\ PEVA} + 4.62\text{E+07}*\Delta R/R_{b\ PIB}*\Delta R/R_{b\ PEVA}$$

Sensors were calibrated with the heater bar activated to yield ~25ºC locally on the chip in 100% humidity conditions. All calibration techniques were chosen to represent the in-situ environment of MW2BL. This eliminated the need to mathematically correct the baseline for temperature and humidity. Chemiresistor E25 was deployed after E20 and E21 failed due to water breaching the probe. This sensor was placed approximately 10 ft above the water level and has been operating since March 2003. A constant 3 volts is applied to the heater bar to maintain the temperature at ~25ºC, slightly above the ambient groundwater temperature of ~20ºC. A chronology of deployment events is listed in Section 12.4.

The multiple sensors used in the field demonstration occupied all of the differential channels on the CR23X. Additional channels were made available through the use of a Campbell Scientific AM16/32 relay mutliplexer. The CR23X is programmed using the Edlog program found with the LogerNet software offered by Campbell Scientific. The program has a prescribed threshold of 5000-ppm TCE. This is done to avoid false positives that can be caused by rapid fluctuations of water vapor or temperature. The multivariate calibrations rely on a $\Delta R/R_b$ values. The baseline value, R_b, is calculated once a week at midnight by taking a two-minute average of the resistances of each polymer/carbon composite. The predicted chemical concentration is calculated using this baseline value for one week. The baseline is recalculated every week to compensate for any drift that may occur. As a result, this system is designed to monitor significant changes that may occur in concentration over short durations.

7.3.3. Web Posting

A web site was created to post the data collected from the Chemical Waste Landfill in near-real-time (Figure 72). The website displays many different aspects of the monitoring station located at the Chemical Waste Landfill (CWL), such as current subsurface sensor readings, maps of the location and wells, live video of the site (SNL internal use only), and photos of the sensors.

.

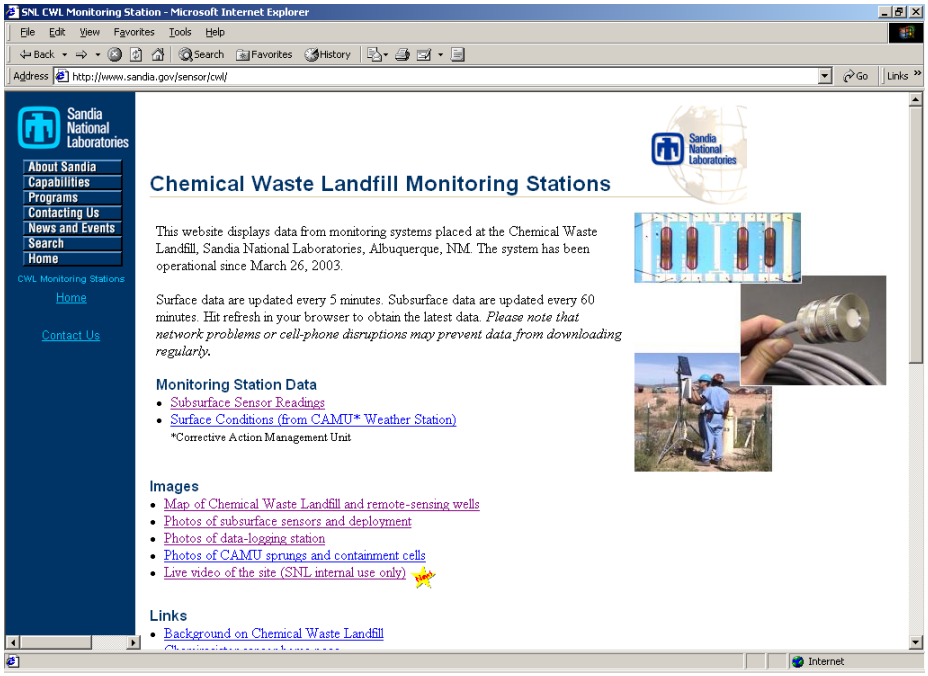

Figure 72. Web site containing near-real-time data collected from the Chemical Waste Landfill (www.sandia.gov/sensor/cwl).

A unique aspect of the web site is the ability to display near-real-time data from a remote location. This is accomplished by utilizing two Campbell Scientific, Inc. software packages (LoggerNet Version 2.1, Real Time Data Monitor (RTDM) Version 1.6) and a cellular transceiver with an external RJ11C telephone interface. A computer with LoggerNet software, RTDM software, and a Hayes-compatible phone modem is connected to a standard phone line and used to call the cellular equipped data-logging station every hour. The LoggerNet software application allows the user to set-up, configure, and retrieve data, locally and remotely, from multiple data-loggers. The Edlog feature of LoggerNet allows the user to create unique programs that can collect, process, and store data for future retrieval. The Setup and Connect feature of LoggerNet allows the user to connect to the logger on a specified schedule allowing the user to collect data without human initiation.

RTDM is a software application that allows the user to create a unique data display. Through the use of RTDM Designer (Figure 73), the user can create an object-oriented form, which can display data from a data (*.dat) file. Items such as numeric and text displays, charts/graphs, alarms, and diagnostic data can be display and manipulated based on the creators needs.

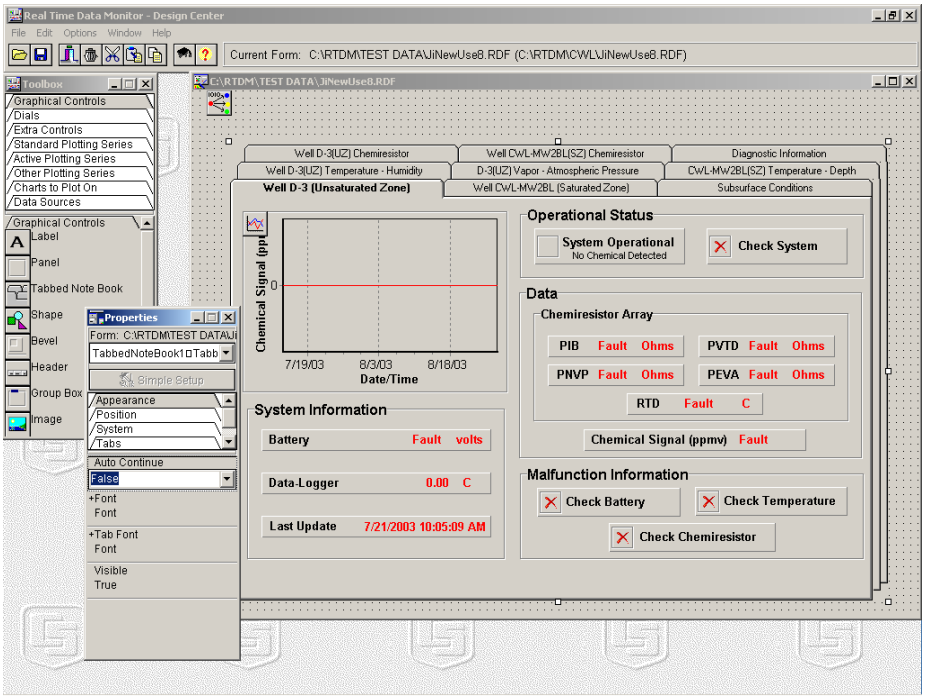

Figure 73. Screen image of RTDM Design Center.

RTDM monitors the source data file and when the source data file is updated, RTDM updates the information contained within a currently running form. Once the data is updated, RTDM initiates a Timed Output Image, which creates a Graphics Interchange Format (GIF) or Joint Photographic Experts Group (JPG) file and posts it to a specified path. These GIF or JPG files can then displayed via the web (Figure 74).

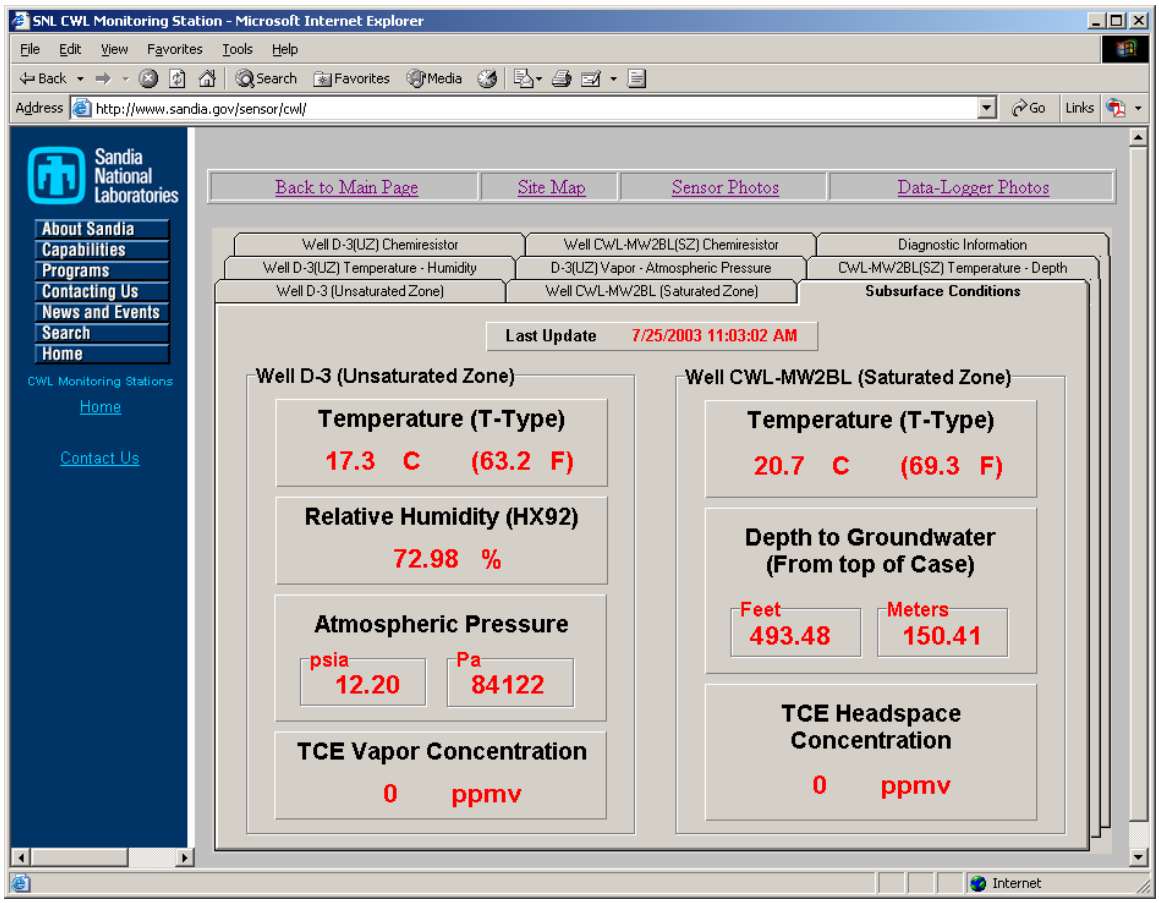

Figure 74. Screen image of subsurface data posted to www.sandia.gov/sensor/cwl.

8. Alternative Chemiresistor Designs and Applications

8.1. Chemicouples™

The Chemicouple™ is an alternative chemiresistor design that relies on the capillary action of the ink to distribute the carbon/polymer composite onto the electrodes. The major benefit of this design is that it does not rely on a manual topical deposition technique that tends to yield large variations in the deposited polymer. A crude Chemicouple™ was constructed by cutting equal lengths of 30-gauge wire and then stripping both ends. The shielded part of the wire was then super-glued together. One side of the exposed wires was trimmed to 5 mm. The trimmed end is then fully submerged in the polymer/carbon ink and let dry (Figure 75).

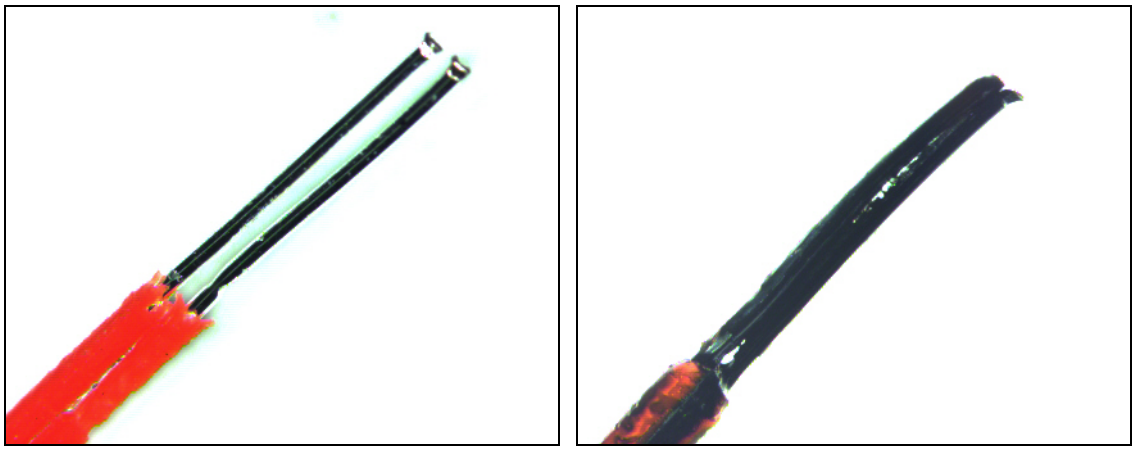

Figure 75. (Left) Chemicouple™ prior to the polymer/carbon coating. (Right) Chemicouple™ after dipping in polymer/carbon ink.

A set of 4 Chemicouples™ were soldered into a 16-pin socket. The sensitivity of the Chemicouples™ was tested by placing the socket in a modified Nalgene bottle and exposing them first to dry air and then to 1000-ppm TCE. All of the Chemicouples™ in the socket responded in a similar manner during the introduction of TCE. Figure 76 shows the response of two of the Chemicouples™ on the socket. A notable increase in the Chemicouple™ resistance is recorded, and the response is quite stable. A significant advantage of the Chemicouples™ is that they are extremely easy and cheap to manufacture.

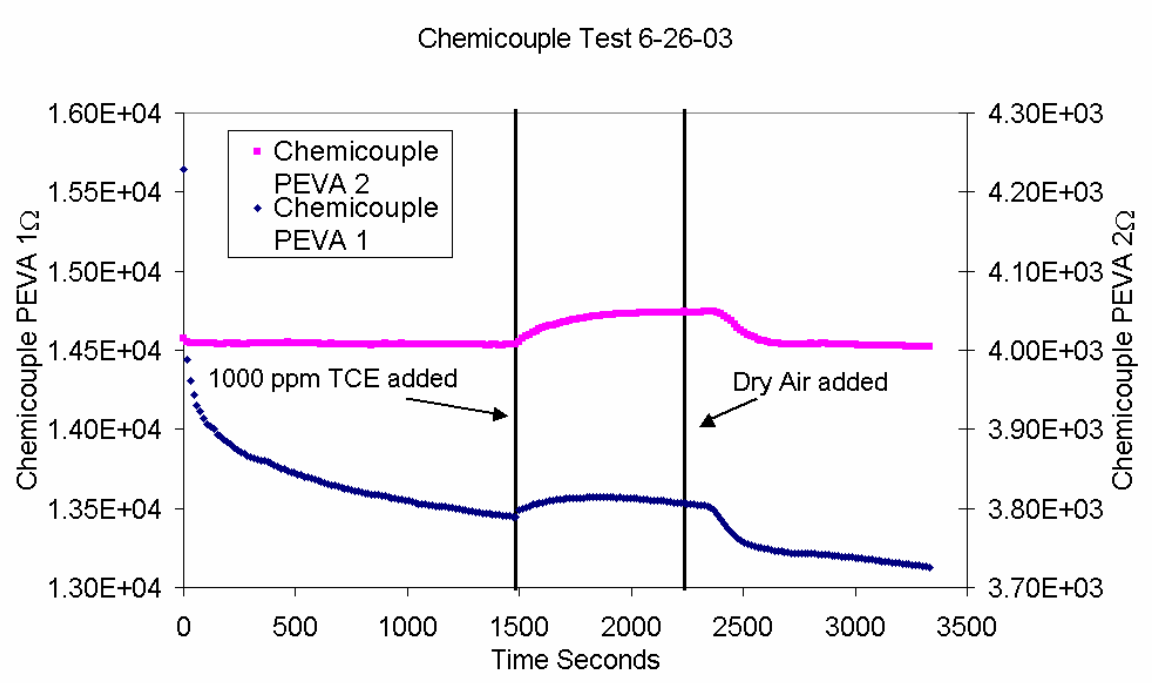

Figure 76. Chemicouple™ response to 1000-ppm TCE.

8.2. ChemSticks™

ChemSticks™ are similar in design to the Chemicouples™, except that the leads are fabricated on a solid surface. The solid is envisioned to be a thin object, such as a glass or ceramic rod. The ChemSticks™ could be dipped directly into the carbon/polymer ink for more uniform distribution and better repeatability. Figure 77 shows some conceptual sketches of the ChemStick™ design (SNL Technical Advance SD-7373). A cooperative research and development agreement (CRADA) is currently investigating the manufacture and performance of these devices.

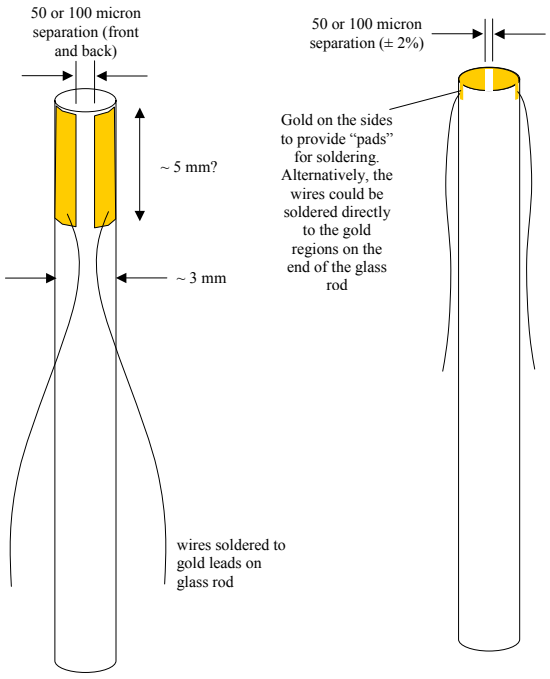

Figure 77. ChemStick™ designs.

8.3. Bioresistors™

An increasing demand for real-time, rugged, inexpensive, and easy-to-use biological sensors has arisen in recent years. There is a national security concern over detecting both airborne and aqueous biological warfare agents, and there is a strong desire in the environmental safety and health arena to develop quick and simple methods for detecting biological contaminants such as *Cryptosporidium* and *Giardia* in the nation's water supply. However, existing methods for detecting biological warfare and water contaminants can be costly and time consuming. Some of the methods include manual sampling and lab analysis, SAW sensors, fluorimetry, and cantilever-based sensors. These methods have several shortcomings. The manual method

requires significant time and labor costs, SAWs require delicate high-frequency electronics, and microcantilevers are not currently field deployable.

Our recent activities have produced an alternative approach to developing biological sensors using molecular imprinting with polymer-based conductometric sensors (chemiresistors). Although molecular imprinting methods (Jenkins et al., 2003) and the use of polymer-based chemiresistor sensors (Ho and Hughes, 2002 and U.S. Patent 6,017,440) have been studied previously, the combination of molecular imprinting with polymer-based chemiresistor sensors has not been widely investigated. We believe this approach has significant potential that will provide new avenues for the development of biological sensors, and a Technical Advance that describes the proposed processes and methods has been submitted (Kooser et al., 2003).

We have recently developed methods to build and test a molecular imprinted polymer-based chemiresistor. This involves using thin-filmed polymer layers with molecular imprinting that will allow the biomolecules to absorb into the polymer. Another approach is based on biofunctionalization of the metal resist and silicon surface. This involves direct binding of the sensing layer onto the chemiresistor and monitoring the change in resistance as the antigen binds to the sensing layer. The biomolecules of interest for this study are avidin-biotin, BSA-aBSA, and, time permitting, a viral simulant.

The imprinted polymer-based sensors were assembled by taking two monomers of a polymer and then polymerizing the monomers around the target molecule. Once the polymer was formed the target molecule was removed from the polymer via dissolution using a flushing solution. This leaves an imprint of the molecule in the polymer (Figure 78). In effect this creates a plastic antibody or binding site that is unique for the target molecule. The conductive medium used in the polymer was lithium ions. Lithium ions are biologically more compatible than the carbon particles that are currently used in the chemiresistors.

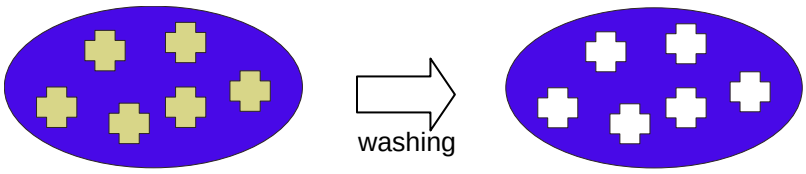

Figure 78. Illustration of molecular imprinting by polymerizing monomers around a target biomolecule (e.g., bovine serum albumin). The left images show the target biomolecules mixed with the polymer matrix. The right image shows the polymer structure after the biomolecules have been washed out, leaving behind an imprint (or hollow regions) in the polymer. These imprints provide a geometrically specific site for the target biomolecule to rebind into.

A preliminary experiment was conducted to determine the feasibility of using a polymer-based sensor for detecting biological agents. A thin-film molecular imprinted biochemiresistor was made using a 50-micron gap chemiresistor with polyvinyl acetate (PVAc) polymer mixed with lithium perchlorate (Figure 2). Bovine serum albumin (BSA) was added to the polymer mixture.

This polymer was deposited along the length of the chemiresistor wire. The BSA was washed out of the polymer with water, leaving behind an imprint. The preliminary results (Figure 79) show that molecular-imprinted polymer-based sensing methods hold promise in providing unique detection of biological agents in water. Experiments are continuing to investigate methods of molecular imprinting and biofunctionalization.

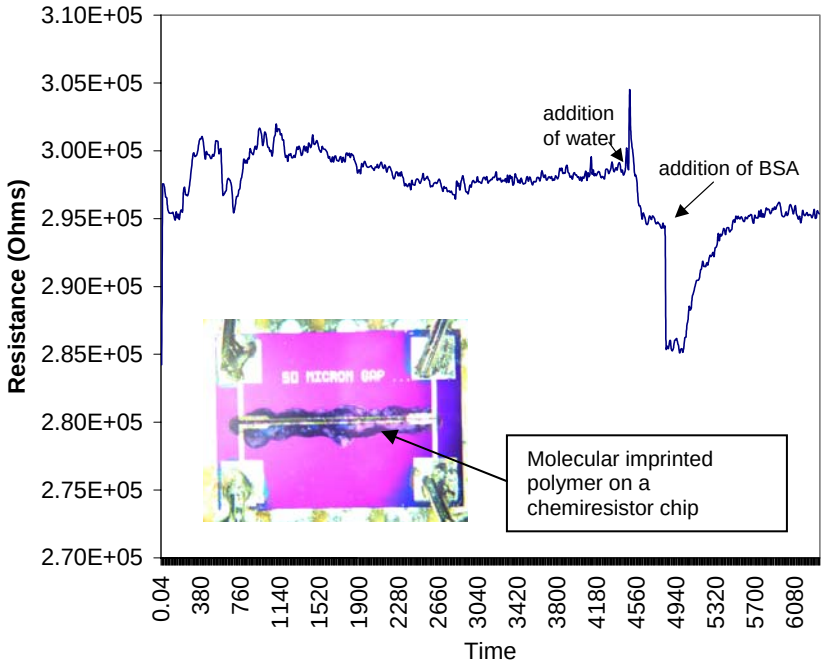

Figure 79. Response of the imprinted polymer to water and bovine serum albumin. The polymer was deposited on the chemiresistor chip and then submerged in water. 100 µL of clean water was added to the existing water to determine any impacts, and then the bovine serum albumin was added to the water. The response for the bovine serum albumin was significantly different in both magnitude and direction then that of the clean water.

8.4. Characterization of Contaminant Source Location

A desirable feature during in-situ monitoring is the capability to not only detect the presence of contaminants, but to also characterize the contaminant in terms of its composition and location in situ. A benefit of in-situ, real-time monitoring is the ability to exploit the transient nature of contaminant transport in the subsurface to provide estimations of the source location of a contaminant spill or leak. Time-dependent concentrations recorded by the in-situ sensor can be used to inversely determine the location of the contaminant release through comparisons with theoretical predictions of contaminant transport in porous media. Predictions of contaminant "breakthrough curves" are derived from the diffusion equation, and the distance between the sensor and the contaminant source is optimized to yield the best fit between the predicted and

observed breakthrough curve. Details of this analysis are provided in Ho and Hughes (2002), and only the results are summarized here.

An experiment was performed to test this concept. The experiment consisted of a one-dimensional sand-filled tube with the contaminant source on one end and the sensor on the other end. Figure 79 shows the experimental apparatus. At time zero, the contaminant was added to the reservoir on one end and the concentrations were recorded by the sensor. The breakthrough curve of the contaminant vapor concentration was recorded as a function of time and compared to predicted values assuming different distances between the contaminant source and the sensor.

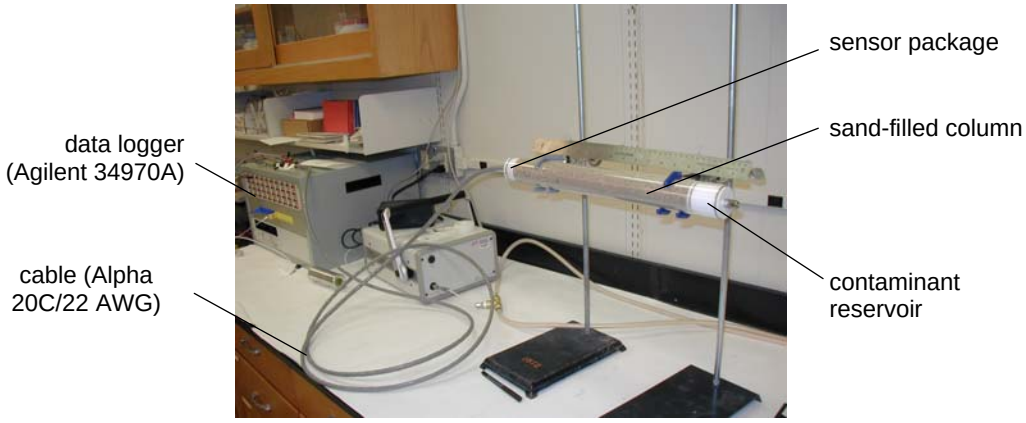

Figure 80. One-dimensional column experiment used to test chemiresistor sensor package in porous media (from Ho and Hughes, 2002).

Results indicate that the measured time-varying concentrations for the 20 cm experiment align most closely with the predicted results that assume a distance of 20 cm. Similarly, the measured concentrations for the 36 cm experiment most closely match the predicted results that assume a distance of 40 cm (Figure 81). Slight deviations in the experimental breakthrough curves may be due to additional factors not considered in the model such as adsorption of the vapors onto the sand, which would tend to flatten the breakthrough curves. Nevertheless, a simple visual inspection of the experimental and theoretical breakthrough curves appears to be sufficient to estimate the distance to the source-term location. More rigorous parameter-estimation methods can be used to better quantify the location based on the analytical predictions. In addition, triangulation methods can be used to determine the contaminant-source location in multiple dimensions.

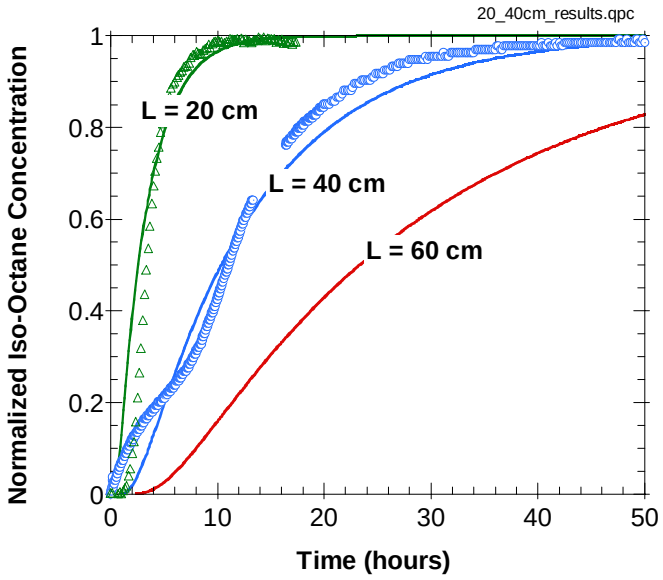

Figure 81. Plot of normalized concentration as a function of time for the 1-D column experiment. The data points are shown as symbols, and the results of the analytical solution are shown as solid lines for three assumed distances (from Ho and Hughes, 2002).

9. Return on Investment

One of the metrics that can be used to gauge the success of a project is the "return on investment." The return on investment includes not only direct revenue from external sources, but also scientific publications, presentations, intellectual property, partnerships, and media coverage, all of which position Sandia as a recognized leader in this field and may ultimately yield additional revenue through continued research, proposals, and/or licenses. This section summarizes the intellectual property, scientific publications, presentations, collaborations, and additional revenue that have been generated from this LDRD project.

9.1. Patent Applications and Technical Advances

- SD-6976, Ho, C.K., M.W. Jenkins, R.C. Hughes, Waterproof microsensor for in-situ monitoring of volatile compounds, Sandia National Laboratories Patent Application filed 5/2002.
- SD-6894, Ho, C.K., Method for characterizing subsurface volatile contaminants, Sandia National Laboratories Patent Application filed 10/24/02.
- SD-7097, Ho, C.K., Automated monitoring and remediation system for volatile subsurface contaminants using in-situ sensors, Sandia National Laboratories Patent Application filed 10/24/02.

- SD-7307, Ho, C.K., Portable vapor diffusion coefficient meter, Sandia National Laboratories Patent Application filed 10/24/02.
- SD-7095, Ho, C.K., Circular chemiresistors for microchemical sensors, Sandia National Laboratories Patent Application filed 1/23/03.
- SD-7372, Ho, C.K., Confined cavity chemiresistors for microchemical sensors, Sandia National Laboratories Patent Application filed 1/23/03.
- SD-7373, Ho, C.K., Multi-pin chemiresistors for microchemical sensors, Sandia National Laboratories Patent Application filed 1/23/03.
- SD-7542, Kooser, A.S., C.K. Ho, and L.K. McGrath, Molecular-imprinted chemiresistor sensors for chemical and biological detection, Sandia National Laboratories Technical Advance filed 8/19/03.

9.2. Publications and Presentations

9.2.1. Publications

- Davis, C.E., C.K. Ho, R.C. Hughes, and M.L. Thomas, 2003 (in review), Enhanced Detection of m-Xylene Using a Preconcentrator with a Chemiresistor Sensor, *submitted to Sensors and Actuators B: Chemical*.
- Hua, L. W.G. Pitt, L.K. McGrath, and C.K. Ho, 2003 (in preparation with BYU), Resistivity measurements of carbon-polymer composites in chemical sensors: impact of carbon concentration and geometry, will be submitted to *Sensors and Actuators B: Chemical*.
- Ho, C.K. and C.F. Lohrstorfer, 2003, Subsurface Monitoring of TCE Using an In-Situ Chemiresistor Sensor, accepted for publication in *Groundwater Monitoring and Remediation*, 3/03.
- Rivera, D., M.K. Alam, C.E. Davis, and C.K. Ho, 2003, Characterization of the ability of polymeric chemiresistor arrays to quantitate trichloroethylene using partial least squares (PLS): effects of experimental design, humidity, and temperature, *Sensors and Actuators B: Chemical*, v. 92, no. 1-2, 110-120.
- Ho, C.K., E.R. Lindgren, K.S. Rawlinson, L.K. McGrath, and J.L. Wright, 2003, Development of a surface acoustic wave sensor for in-situ monitoring of volatile organic compounds, *Sensors*, 3, 236-247.
- Ho, C.K., J. Wright, L.K. McGrath, E.R. Lindgren, K.S. Rawlinson, and C.F. Lohrstorfer, 2003, Field Demonstrations of Chemiresistor and Surface Acoustic Wave Microchemical Sensors at the Nevada Test Site, SAND2003-0799, Albuquerque, NM.
- Ho, C.K., and R.C. Hughes, 2002, *In-Situ* Chemiresistor Sensor Package for Real-Time Detection of Volatile Organic Compounds in Soil and Groundwater, 2002, *Sensors*, 2, 23-34.
- Ho, C.K. and C.F. Lohrstorfer, 2002, Demonstration of Chemiresistor Microsensors for Subsurface Monitoring of Volatile Organic Compounds, SAND2002-1968C, In Proceedings of the Spectrum 2002 Conference, Reno, NV, August 4-8, 2002, ISBN: 0-89448-664-0.

- Ho, C.K., L.K. McGrath, and J. May, 2002, FY02 Field Evaluations of an In-Situ Chemiresistor at Edwards Air Force Base, CA, SAND2002-4135, Albuquerque, NM.
- Davis, C.E. R.C. Hughes, M.L. Thomas, C.K. Ho, Data Analysis Methods for Real-Time VOC Chemiresistor Sensor, SAND2002-0591C, in proceedings of the Sensors Expo Conference, San Jose, CA, May 20-23, 2002, 179-191.
- Ho, C.K., R.C. Hughes, M.W. Jenkins, D.A. Lucero, M.T. Itamura, M. Kelley, and P. Reynolds, 2001, Microchemical Sensors for In Situ Monitoring and Characterization of Volatile Contaminants, SAND2001-1093C, In Proceedings of the 2001 Containment and Remediation Conference, Orlando, FL, June 10-13, 2001.
- Ho, C.K., M.T. Itamura, M. Kelley, R.C. Hughes, 2001, Review of Chemical Sensors for In-Situ Monitoring of Volatile Contaminants, SAND2001-0643, Sandia National Laboratories, Albuquerque, NM.

9.2.2. Presentations

- Ho, C.K., 2004, Continuous Monitoring of Volatile Organic Compounds in the Subsurface Using an In-Situ Chemiresistor Sensor, **invited presentation** to be made at the 2004 North American Environmental Field Conference, Tampa Bay, FL, January 13-16, 2004.
- Ho, C.K., 2003, Development of an In-Situ Chemiresistor Sensor for Continuous Monitoring of Volatile Organic Compounds in Air, Soil, and Water, SAND2003-1709A, abstract presented at FAME (Frontiers in Assessment Methods for the Environment) Symposium, Minneapolis, MN, August 10-13, 2003.
- Ho, C.K., 2003, From Chemiresistor Sensors to Real-Time Subsurface Hydrocarbon Monitoring Systems: Lessons Learned, SAND2002-4095A, **invited presentation** at the National American Chemical Society Meeting, New Orleans, LA, March 23-27, 2003.
- Ho, C.K., L.K. McGrath, and J. May, 2003, In-Situ Chemiresistor Sensors for Monitoring Subsurface Contaminants, **invited presentation** at the 2003 CUPA Conference, Anaheim, CA, 2/5/03.
- Hughes, R.C., C.K. Ho, and C.E. Davis, 2003, Chemiresistor Microsensor Arrays for Detecting Volatile Organic Chemicals, **invited presentation** at Seventeenth International Forum on Process Analytical Chemistry, Phoenix, AZ, January 21-24, 2003.
- Rivera, D.A., M.K. Alam, C.K. Ho, C.E. Davis, R.J. Simonson, and W.G. Yelton, 2003, Augmented Least Squares Techniques and Hybrid Least Squares Techniques for Calibration Maintenance of Chemiresistor and Surface Acoustic Wave Sensors, SAND2003-0784A, Pittsburg Analytical Conference, Orlando, FL, March 10-13, 2003.
- Ho, C.K., L.K. McGrath, and J. Wright, 2003, Field Tests of a Chemiresistor Sensor for In-Situ Monitoring of Vapor-Phase Contaminants, SAND2003-0328A, presented at the 2003 EGS-AGU-EGU Joint Assembly, Nice, France, April 6-11, 2003, Albuquerque, NM.
- McGrath, L.K. and C.K. Ho, 2002, Automated Temperature Control for the Chemiresistor Sensor, 7th Annual Sandia Student Internship Program Symposium, Albuquerque, NM, 8/1/02.

- Ma, I.T. and C.K. Ho, 2002, Factors that Impact the Response of the Chemiresistor Sensor, 7th Annual Sandia Student Internship Program Symposium, Albuquerque, NM, 8/1/02.
- Ho, C.K., L.K. McGrath, and J. May, 2002, Deployment of a real-time microchemical sensor for groundwater quality monitoring at Edwards Air Force Base, SAND2002-2069P, poster and presentation at the New Mexico Water Research Symposium, 8/13/2002, Socorro, NM.
- Rivera, D.A., M.K. Alam, C.K. Ho, and C.E. Davis, 2002, Application of Multivariate Calibration Methods to Chemiresistor Array Data, SAND2002-2971A, abstract presented at the Federation of Applied Chemistry and Spectroscopy Society Meeting, October 13-17, 2002, Providence, RI.
- Ho, C.K., 2002, Invited presentation to Sandia Leadership Council on microsensors for real-time soil- and water-quality monitoring, Albuquerque (4/02).
- Ho, C.K., 2001, Invited presentation to Senator Bingaman on microsensors for real-time water-quality monitoring, Cooperative Monitoring Center, Albuquerque (2/19/01).
- Ho, C.K., 2001, Invited to discuss long-term research needs with the National Academy of Sciences Committee on Long-Term Research Needs for Managing Transuranic and Mixed Waste at DOE Sites. Presented chemiresistor sensor and need for long-term monitoring.
- Ho, C.K., 2001, Presented prototype in-situ chemiresistor sensor to WIPP audience (Westinghouse, LANL, DOE, SNL staff and managers) to evaluate use of sensors to monitor VOC concentrations in repository environments, Carlsbad, NM, 7/18/01.
- McLain, A.A and C.K. Ho, 2001, Evaluation Of Diffusion In Porous Media Using A Novel Detection Method, abstract/presentation at Geological Society of America Annual Meeting, Boston, MA, Nov. 5-8, 2001, SAND2002-2203A, Vol. 33, No. 6.
- McLain, A.A and C.K. Ho, 2001, Impact of Moisture Content and Grain Size on Hydrocarbon Diffusion in Porous Media, SAND2001-3081A, abstract/poster presented at the AGU 2001 Fall Meeting, San Francisco, CA, December 10-14, 2001.

9.3. Media Coverage

During the course of this LDRD project, we have contributed writing, illustrations, images, and/or interviews (through SNL media relations) to over 30 articles in ABQ Tribune, Sandia Lab News, Geotimes Magazine, ASCE Civil Engineering Magazine, Chemical Engineering Magazine, Sensors Magazine, Science Daily Magazine, Poptronics Magazine, Red Herring Magazine, Technology Review, Weapons Complex Monitor, US Water News, Environmental Laboratory Washington Report, Scientific American, Information Week Magazine, and more. The publicity resulting from these articles has generated numerous commercial contacts and has positioned Sandia as a recognized leader in the field of microchemical sensors for environmental monitoring.

9.4. Technology Transfer and Revenue

- Explored collaboration opportunities with numerous companies to potentially commercialize microchemical sensor. Gave presentations and hosted visits to Shell

International, Hogentogler, Lighthouse Worldwide Solutions, Coca-Cola, Ardesta, Hach Co, Veeder-Root, RAE Systems, Team Specialty Products, MesoSystems, L&M Technologies, Semorex, Inc., and other companies.

- Awarded DOE EMSP (Environmental Management and Science Program) that was jointly proposed with INEEL to use our in-situ chemiresistor sensors in INEEL's mesoscale experiments to detect biological degradation of TCE. (FY04~$50K, FY05~$40K, FY06~$140K)

- A CRADA (Cooperative Research and Development Agreement) was initiated with a company in FY03 to investigate manufacturing and design methods that would improve the stability and performance of the chemiresistor sensors. (~$50K)

- A Work for Others contract was awarded to Sandia from Edwards Air Force Base from FY02 to FY04 to deploy and test our in-situ chemiresistors at their contaminated sites. (~$80K)

- A DOE contract was awarded to Sandia as part of DOE/Nevada's Advanced Monitoring Systems Initiative in FY02 and FY03 to test our in-situ chemiresistor and surface-acoustic-wave sensors at the Nevada Test Site. (~$300K)

- We were asked by Sandia's Environmental Restoration department to deploy our in-situ chemiresistor sensor system at the Chemical Waste Landfill and produce a web site for real-time monitoring of the site (www.sandia.gov/sensor/cwl). (~$30K)

- Received funding from Brigham Young University and INEEL in FY02 and FY03 to provide in-situ detection of TCE in their research experiments using our chemiresistor sensors ($5K).

- Awarded funding from New Mexico Small Business Assistance Program in 2001 for proposal developed with Voss Scientific to develop remote in-situ sensing system for DOE SBIR/STTR grant. ($5K)

10. Summary

This report documents the activities conducted as part of a three-year Sandia LDRD project to develop microchemical sensors for real-time monitoring of subsurface contaminants. Many aspects of the chemiresistor sensor development, from design and fabrication to field testing, have been described in detail in this report and other cited publications produced as part of this project.

A significant aspect of this project has been the laboratory testing and evaluation of the chemiresistor to understand and improve the performance of the chemiresistor sensors. Numerous experiments were performed at both the In-Situ Sensing Lab and at the IMRL Chemiresistor Lab. Polymers were optimized and selected for our particular applications and analytes of interest. Temperature control of the chemiresistor chip was developed to improve the

accuracy and stability of the chemiresistor sensors. An analysis of the carbon concentration and carbon type on the sensitivity and noise of the chemiresistor was also performed to determine the optimal combinations. Theoretical models for polymer/carbon composites were employed to predict the resistivity of our chemiresistors. Analysis of the limit of detection of our chemiresistors showed that without preconcentration, the limit of detection to TCE was ~10 ppmv. With preconcentration, the limits of detection for m-xylene were found to be lowered by over two orders of magnitude.

The design and testing of preconcentrators to enhance the apparent sensitivity of the chemiresistors was also a significant part of this LDRD. The fabrication of the preconcentrators was described in detail, along with tests that evaluated the heating and response of the preconcentrators. An integrated preconcentrator/chemiresistor probe was also designed and tested for field use.

Data analysis methods were evaluated to determine approaches that could be used to provide both discrimination and quantification of target analytes with multiple input variables. The Visual Empirical Region of Influence method was investigated along with partial-least squares. Multivariate regression models generated by Statistica™ were also developed and deployed.

Three field studies were also conducted to test the performance of the in-situ chemiresistor sensor in actual environmental field conditions. Tests at Edwards Air Force Base, CA, the Nevada Test Site, and the Chemical Waste Landfill, NM were performed to determine engineering requirements for sensor deployment, data acquisition, power requirements, telemetry, data processing, and information dissemination. These tests culminated in a web site that posts near-real-time data from chemiresistors and other sensors deployed at the Chemical Waste Landfill (www.sandia.gov/sensor/cwl).

Alternative designs and applications were investigated that produced some novel alternatives to the chemiresistor. These included the Chemicouple,™ the ChemStick,™ and the Bioresistor.™ In addition, a new method of characterizing subsurface contaminant locations was also demonstrated using analytical predictions of contaminant mass diffusion through the subsurface combined with measured in-situ contaminant vapor concentrations.

Finally, a “return on investment” was presented that listed the significant accomplishments from this LDRD project. These included seven patent applications and eight technical advances, a dozen scientific publications, nearly 20 invited and contributed presentations, media coverage in over 30 magazines and news publications, a CRADA, Work for Others contracts, and collaborations with academic universities and other national laboratories.

11. References

Davis, C.E. R.C. Hughes, M.L. Thomas, C.K. Ho, Data Analysis Methods for Real-Time VOC Chemiresistor Sensor, SAND2002-0591C, in proceedings of the Sensors Expo Conference, San Jose, CA, May 20-23, 2002, 179-191.

Ho, C.K., M.T. Itamura, M. Kelley, R.C. Hughes, 2001, Review of Chemical Sensors for In-Situ Monitoring of Volatile Contaminants, SAND2001-0643, Sandia National Laboratories, Albuquerque, NM.

Ho, C.K., and R.C. Hughes, 2002, *In-Situ* Chemiresistor Sensor Package for Real-Time Detection of Volatile Organic Compounds in Soil and Groundwater, 2002, *Sensors*, 2, 23-34.

Ho, C.K. and C.F. Lohrstorfer, 2002, Demonstration of Chemiresistor Microsensors for Subsurface Monitoring of Volatile Organic Compounds, SAND2002-1968C, In Proceedings of the Spectrum 2002 Conference, Reno, NV, August 4-8, 2002, ISBN: 0-89448-664-0.

Ho, C.K., L.K. McGrath, and J. May, 2002, FY02 Field Evaluations of an In-Situ Chemiresistor at Edwards Air Force Base, CA, SAND2002-4135, Albuquerque, NM.

Ho, C.K., E.R. Lindgren, K.S. Rawlinson, L.K. McGrath, and J.L. Wright, 2003a, Development of a surface acoustic wave sensor for in-situ monitoring of volatile organic compounds, *Sensors*, 3, 236-247.

Ho, C.K., J. Wright, L.K. McGrath, E.R. Lindgren, K.S. Rawlinson, and C.F. Lohrstorfer, 2003b, Field Demonstrations of Chemiresistor and Surface Acoustic Wave Microchemical Sensors at the Nevada Test Site, SAND2003-0799, Albuquerque, NM.

Hughes, R.C., S.V. Patel, and R.P. Manginell, 2000, A MEMs based Hybrid Preconcentrator/chemiresistor Chemical Sensor, Proceedings of the V Symposium on Microfabricated Systems and MEMS vol. 2000-19, pg. 142-150.

Hughes, R.C.; Casalnuovo, S.A.; Wessendorf, K.O.; Savignon, D.J.; Hietala, S; Patel, S.V.; and Heller, E.J., 2000, Integrated Chemiresistor Array for Small Sensor Platforms, SPIE Proceedings Paper 4038-62, p. 519, AeroSense 2000, April 24-28, 2000, Orlando, Florida.

Jenkins, A.L., R. Yin, and J.L. Jensen, 2001, Molecularly imprinted polymer sensors for pesticide and insecticide detection in water, Analyst 126, 798–802.

Kooser, A.S., C.K. Ho, and L.K. McGrath, 2003, Molecular-imprinted chemiresistor sensors for chemical and biological detection, Sandia National Laboratories Technical Advance SD-7542 filed 8/19/03.

Looney, B.B. and R.W. Falta (eds.), 2000, Vadose Zone Science and Technology Solutions, Battelle Press, Columbus, OH, 1540 pp.

Lundberg, B. and B. Sundqvist, 1986, Resistivity of a composite conducting polymer as a function of temperature, pressure, and environment: applications as a pressure and gas concentration transducer, J. Appl. Phys., 60(3), 1074-1079.

Manginell, R.P., G.C. Frye-Mason, R.J. Kottenstette, P.R. Lewis, and C.C. Wong, 2000, Microfabricated Planar Preconcentrator, Digest of the State Sensor and Actuator Workshop, Hilton Head, SC, June 2000, pg 179, Transducers Research Foundation, Cleveland.

McLachlan, D.S., M. Blaszkiewicz, and R.E. Newnham, 1990, Electrical Resistivity of Composites, *J. Am. Ceram. Soc.,* 73(8), 2187-2203.

Porter, T., M. Eastman, C. Macomber, W. Delinger, and R. Zhine, R., 2003, An embedded polymer piezoresistive microcantilever sensor, *Ultramicroscopy,* **97** 365-369.

Rivera, D., M.K. Alam, C.E. Davis, and C.K. Ho, 2003, Characterization of the ability of polymeric chemiresistor arrays to quantitate trichloroethylene using partial least squares (PLS): effects of experimental design, humidity, and temperature, *Sensors and Actuators B: Chemical*, v. 92, no. 1-2, 110-120.

Tian, WC, SW Pang, CJ Lu, CJ, Zellers, 2003, Microfabricated preconcentrator-focuser for a microscale gas chromatograph, Et Journal Of Microelectromechanical Systems;v.12, no.3, p.264-272.

U.S. Environmental Protection Agency (EPA), 1992, Measurement and Analysis of Adsistor and Figaro Gas Sensors Used for Underground Storage Tank Leak Detection, Report #EPA/600/R-92/219.

United States Patent 6,017,440; Lewis, et al; January 25, 2000; Sensor arrays for detecting microorganisms.

Wilson, LG., L.G. Everett, and S.J. Cullen (eds.), 1995, Handbook of Vadose Zone Characterization & Monitoring, CRC Press, Boca Raton, FL.

Zhang, Z., M. J. Yang, and J. Pawliszyn, 1994, Solid Phase Microextraction (SPME), Anal Chem. 66, 847A.

12. Appendices

12.1. CR5000 Program for Integrated Preconcentrator/Chemiresistor Data Collection

```
'*******************************
'* PCProgram_Ver6_030314m1.CR5        *
'* PC Testing Program
*
'* Written By: Jerome L. Wright       *
'* {CR5000}                           *
'* Date: 3/14/03                      *
'* CR5000 Data logger          *
'*******************************
'Constance
Const SixtyScans=60
Const Five00Scans=500
Const Two50Scans=250
Const Two00Scans=200
Const DataCycles=1
Const Twelve=12
Const
FRMScans=SixtyScans+Five00Scans+Two00Scans
Const Multi=1
Const Offset=0
Const Chip1Slope=1.4668
Const Chip2Slope=1.4431
Const Chip3Slope=1.4259
Const Chip1YInter=312.31
Const Chip2YInter =319.26
Const Chip3YInter =288.76
'Public Variables
Public Pre-fireCounter(2)
Public PRMCounter(2)
Public FRMCounter(2)
Public PostProcCounter
Public      Resistor(Twelve)      :      Units
Resistor()=Ohms
Public      RBaseLine(Twelve)      :      Units
RBaseLine()=Ohms
Public DeltaR(Twelve)
Public DeltaRR(Twelve)
Public DeltaRDiff(Twelve)
Public DeltaRRDiff(Twelve)
Public PRMMax(Twelve) : Units PRMMax()=Ohms
Public FRMMax(Twelve): Units FRMMax()=Ohms
Public PRMMaxD(Twelve)
Public FRMMaxD(Twelve)
Public PRMMaxDRR(Twelve)
Public FRMMaxDRR(Twelve)
Public DeltaRDiffMax(Twelve)
Public DeltaRRDiffMax(Twelve)
Public RTDOhms(3): Units RTDOhms()=Ohms
Public RTDTemp(3)
Public RTDRTempAve(3)
Public RTDTempAve(3)
Public ChipSlope(3)
Public ChipYInter(3)
Public RTDOhmsAve(3)
Public TypeT_TC
Public PanelDegC
Public Flag(8),BeginTest

'Dim
Dim i,j,k
Dim
TimeStampuSec(6),TempArray(SixtyScans,Twelve),
SumR

'Data Tables
'Pre-fire Measure Data Table
DataTable(PFRMData,True,800)'DataCycles*FRMSca
ns)
CardOut (0,10000)
Sample(Twelve,Resistor(),IEEE4)
EndTable

'Pre-fire Measure Delta Data Table
DataTable(PFMDelta,True,800)'DataCycles*FRMSca
ns)
CardOut (0,10000)
Sample(Twelve,DeltaR(),IEEE4)
Sample(Twelve,DeltaRR(),IEEE4)
Sample(6,TimeStampuSec(),IEEE4)
EndTable

'Fire Data Table
DataTable(FRMData,True,800)'DataCycles*FRMScan
s)
CardOut (0,10000)
Sample(Twelve,Resistor(),IEEE4)
EndTable

'Fire Delta Data Table
DataTable(FRMDelta,True,800)'DataCycles*FRMSca
ns)
CardOut (0,10000)
Sample(Twelve,DeltaR(),IEEE4)
Sample(Twelve,DeltaRR(),IEEE4)
EndTable

'Posprocess Data Table
DataTable(PostPro,True,800)'DataCycles*FRMScan
s)
CardOut (0,10000)
Sample(Twelve,DeltaRDiff(),IEEE4)
Sample(Twelve,DeltaRRDiff(),IEEE4)
Sample(6,TimeStampuSec(),IEEE4)
EndTable

'Baseline Data Table
DataTable(RBaseL,True,10)
CardOut (0,100)
Sample(Twelve,RBaseLine(),IEEE4)
EndTable

'RTD Data Table
DataTable(RTD,true,10)
CardOut (0,100)
Sample (3,RTDOhms(),IEEE4)
Sample (3,RTDTemp(),IEEE4)
EndTable
```

```
'Temperature Data Table
DataTable(Temp,true, 10)
CardOut (0,100)
Sample (3,RTDTempAve(),IEEE4)
Sample (3,RTDOhmsAve(),IEEE4)
Sample (1,TypeT_TC,IEEE4)
EndTable

'Max Data Table
DataTable(MaxVal,true,10)
CardOut (0,1000)
Sample (12,PRMMax(),IEEE4)
Sample (12,PRMMaxD(),IEEE4)
Sample (12,PRMMaxDRR(),IEEE4)
Sample (12,FRMMax(),IEEE4)
Sample (12,FRMMaxDRR(),IEEE4)
Sample (12,FRMMaxD(),IEEE4)
Sample (12,DeltaRDiffMax(),IEEE4)
Sample (12,DeltaRRDiffMax(),IEEE4)
EndTable

'Pre-fire Data Table (Purge Pulses)
DataTable(Pre-fire,true,100)
CardOut (0,1000)
Sample(12,Resistor(),IEEE4)
EndTable

'_____________________________
'Pre-fires to clear PC Subroutine:
Sub Pre-fire
    Flag(1)=True
    For i=1 To 5
        Pre-fireCounter(1)=Pre-
fireCounter(1)+1
       Pre-fireCounter(2)=0
       Scan(1,Sec,0,30)'SixtyScans)
           Pre-fireCounter(2)=Pre-
fireCounter(2)+1
           If     Pre-fireCounter(2)=1     Then
SW12(1)
           If     Pre-fireCounter(2)=1     Then
Flag(7)=True
           If     Pre-fireCounter(2)=1     Then
Flag(8)=False
           If     Pre-fireCounter(2)>5     Then
SW12(0)
           If     Pre-fireCounter(2)>5     Then
Flag(7)=False
           If     Pre-fireCounter(2)>5     Then
Flag(8)=True

    Resistance(Resistor(),Twelve,AutoRange,1,I
x1,3,1000,False,False,200,250,-
           1.0,0.0)
           'Move(Resistor(),Twelve,Pre-
fireCounter(2),1) 'Tracer data! Be sure to-
           remove to use real measurements.
           CallTable Pre-fire
           Call (RTDMeasure) RTDMeasure
       NextScan
    Next i
Flag(1)=False
Flag(2)=True
EndSub
'_____________________________________
'Pre-fire Resistance Measurement Subroutine:
Sub PreRMeasure
    Flag(2)=False
    Flag(3)=True
    PRMCounter(1)=0'1  Note  Mark  had  this  set
to 1
    PRMCounter(2)=0
    For i=1 to 12
        PRMMax(i)=0
        PRMMaxDRR(i)=0
    Next i
    Scan(1,Sec,SixtyScans,SixtyScans)
        PRMCounter(1)=PRMCounter(1)+1
        PRMCounter(2)=PRMCounter(2)+1

    Resistance(Resistor(),Twelve,AutoRange,1,I
x1,3,1000,False,False,200,250,1.0-
       ,0.0)

    'Move(Resistor(),Twelve,PRMCounter(2),1)
'Tracer data! Be sure to remove-
       to use real measurements.
       CallTable(PFRMData)
       For i=1 to 12
           If    Resistor(i)>PRMMax(i)    Then
PRMMax(i)=Resistor(i)

    TempArray(PRMCounter(2),i)=Resistor(i)
       Next i
    NextScan
    For i=1 To Twelve
       SumR=0
       For j=(SixtyScans-9) To SixtyScans
           PRMCounter(1)=PRMCounter(1)+0.0001
           SumR=SumR+TempArray(j,i)
       Next j
       RBaseLine(i)=SumR/(SixtyScans-
(SixtyScans-9-1))
    Next i
    For i=1 To SixtyScans
       PRMCounter(1)=PRMCounter(1)+0.0001
       For j=1 To Twelve
           DeltaR(j)=TempArray(i,j)-
RBaseLine(j)
           If DeltaR(j)<0 Then DeltaR(j)=0
           DeltaRR(j)=DeltaR(j)/RBaseLine(j)
           If    DeltaR(j)>PRMMaxD(j)    Then
PRMMaxD(j)=DeltaR(j)
           If   DeltaRR(j)>PRMMaxDRR(j)   Then
PRMMaxDRR(j)=DeltaRR(j)
       Next j
       For k=1 To 6

    TimeStampuSec(k)=PFRMData.TimeStamp(8-
k,SixtyScans+1-i)
       Next k
       CallTable(PFMDelta)
    Next i
    SW12(1)
    Flag(7)=True
    Flag(8)=False
    PRMCounter(1)=SixtyScans
    PRMCounter(2)=0
    Scan(20,mSec,Five00Scans,Five00Scans)
       PRMCounter(1)=PRMCounter(1)+1
       PRMCounter(2)=PRMCounter(2)+1

    Resistance(Resistor(),Twelve,AutoRange,1,I
x1,3,1000,False,False,200,250,1.0-
       ,0.0)

    'Move(Resistor(),Twelve,PRMCounter(2),1)
'Tracer data! Be sure to remove to
       use real measurements.
       For i=1 To Twelve
           DeltaR(i)=Resistor(i)-RBaseLine(i)
           If DeltaR(i)<0 Then DeltaR(i)=0
```

```
            DeltaRR(i)=DeltaR(i)/RBaseLine(i)
            If    Resistor(i)>PRMMax(i)    Then
PRMMax(i)=Resistor(i)
            If     DeltaR(i)>PRMMaxD(i)     Then
PRMMaxD(i)=DeltaR(i)
            If   DeltaRR(i)>PRMMaxDRR(i)   Then
PRMMaxDRR(i)=DeltaRR(i)
        Next i
        If PRMCounter(2)>250 Then SW12(0)
        If        PRMCounter(2)>250        Then
Flag(7)=False
        If PRMCounter(2)>250 Then Flag(8)=True
        CallTable(PFMDelta)
        CallTable(PFRMData)
    NextScan
    PRMCounter(2)=0
    Scan(1,Sec,Two00Scans,Two00Scans)
        PRMCounter(1)=PRMCounter(1)+1
        PRMCounter(2)=PRMCounter(2)+1

    Resistance(Resistor(),Twelve,AutoRange,1,I
x1,3,1000,False,False,200,250,1.0-
        ,0.0)

    'Move(Resistor(),Twelve,PRMCounter(2),1)
'Tracer data! Be sure to remove to-
        use real measurements.
        For i=1 To Twelve
            DeltaR(i)=Resistor(i)-RBaseLine(i)
            If DeltaR(i)<0 Then DeltaR(i)=0
            DeltaRR(i)=DeltaR(i)/RBaseLine(i)
            If    Resistor(i)>PRMMax(i)    Then
PRMMax(i)=Resistor(i)
            If     DeltaR(i)>PRMMaxD(i)     Then
PRMMaxD(i)=DeltaR(i)
            If   DeltaRR(i)>PRMMaxDRR(i)   Then
PRMMaxDRR(i)=DeltaRR(i)
        Next i
        CallTable(PFMDelta)
        CallTable(PFRMData)
    NextScan
    CallTable(RBaseL)
    For i=1 To Twelve
        RBaseLine(i)=0
        DeltaR(i)=0
        DeltaRR(i)=0
    Next i
Flag(3)=False
Flag(4)=True
EndSub
'_____________________________________
'Fire Resistance Measurement Subroutine:
Sub RMeasure
    Flag(4)=False
    Flag(5)=True
    FRMCounter(1)=0
    FRMCounter(2)=0
    For i=1 to 12
        FRMMax(i)=0
        FRMMaxDRR(i)=0
    Next i
    Scan(1,Sec,SixtyScans,SixtyScans)
        FRMcounter(1)=FRMCounter(1)+1
        FRMcounter(2)=FRMCounter(2)+1

    Resistance(Resistor(),Twelve,AutoRange,1,I
x1,3,1000,False,False,200,250,1.0-
        ,0.0)

    'Move(Resistor(),Twelve,FRMCounter(2),1)
'Tracer data! Be sure to remove to-
        use real measurements.
        CallTable(FRMData)
        For i=1 To Twelve
            If    Resistor(i)>FRMMax(i)    Then
FRMMax(i)=Resistor(i)

    TempArray(FRMCounter(2),i)=Resistor(i)
        Next i
    NextScan
    For i=1 To Twelve
        SumR=0
        For j=(SixtyScans-9) To SixtyScans
            FRMCounter(1)=FRMCounter(1)+0.0001
            SumR=SumR+TempArray(j,i)
        Next j
        RBaseLine(i)=SumR/(SixtyScans-
(SixtyScans-9-1))
    Next i
    For i=1 To SixtyScans
        FRMCounter(1)=FRMCounter(1)+0.0001
        For j=1 To Twelve
            DeltaR(j)=TempArray(i,j)-
RBaseLine(j)
            If DeltaR(j)<0 Then DeltaR(j)=0
            DeltaRR(j)=DeltaR(j)/RBaseLine(j)
            If     DeltaR(j)>FRMMaxD(j)     Then
FRMMaxD(j)=DeltaR(j)
            If   DeltaRR(j)>FRMMaxDRR(j)   Then
FRMMaxDRR(j)=DeltaRR(j)
        Next j
        For k=1 To 6

    TimeStampuSec(k)=FRMData.TimeStamp(8-
k,SixtyScans+1-i)
        Next k
        CallTable(FRMDelta)
    Next i
    SW12(1)
    Flag(7)=True
    Flag(8)=False
    FRMCounter(1)=SixtyScans
    FRMCounter(2)=0
    Scan(20,mSec,Five00Scans,Five00Scans)
        FRMCounter(1)=FRMCounter(1)+1
        FRMCounter(2)=FRMCounter(2)+1

    Resistance(Resistor(),Twelve,AutoRange,1,I
x1,3,1000,False,False,200,250,1.0-
        ,0.0)

    'Move(Resistor(),Twelve,FRMCounter(2),1)
'Tracer data! Be sure to remove to-
        use real measurements.
        For i=1 To Twelve
            DeltaR(i)=Resistor(i)-RBaseLine(i)
            If DeltaR(i)<0 Then DeltaR(i)=0
            DeltaRR(i)=DeltaR(i)/RBaseLine(i)
            If    Resistor(i)>FRMMax(i)    Then
FRMMax(i)=Resistor(i)
            If     DeltaR(i)>FRMMaxD(i)     Then
FRMMaxD(i)=DeltaR(i)
            If   DeltaRR(i)>FRMMaxDRR(i)   Then
FRMMaxDRR(i)=DeltaRR(i)
        Next i
        If FRMCounter(2)>250 Then SW12(0)
        If        FRMCounter(2)>250        Then
Flag(7)=False
        If FRMCounter(2)>250 Then Flag(8)=True
        CallTable(FRMDelta)
        CallTable(FRMData)
    NextScan
```

```
    FRMCounter(2)=0
    Scan(1,Sec,Two00Scans,Two00Scans)
        FRMcounter(1)=FRMCounter(1)+1
        FRMCounter(2)=FRMCounter(2)+1

    Resistance(Resistor(),Twelve,AutoRange,1,I
x1,3,1000,False,False,200,250,1.0,-
        0.0)

    'Move(Resistor(),Twelve,FRMCounter(2),1)
'Tracer data! Be sure to remove to
        use real measurements.
        For i=1 to Twelve
            DeltaR(i)=Resistor(i)-RBaseLine(i)
            If DeltaR(i)<0 Then DeltaR(i)=0
            DeltaRR(i)=DeltaR(i)/RBaseLine(i)
            If    Resistor(i)>FRMMax(i)    Then
FRMMax(i)=Resistor(i)
            If     DeltaR(i)>FRMMaxD(i)     Then
FRMMaxD(i)=DeltaR(i)
            If   DeltaRR(i)>FRMMaxDRR(i)   Then
FRMMaxDRR(i)=DeltaRR(i)
        Next i
        CallTable(FRMDelta)
        CallTable(FRMData)
    NextScan
    CallTable(RBaseL)
    For i=1 To Twelve
        RBaseLine(i)=0
        DeltaR(i)=0
        DeltaRR(i)=0
    Next i
Flag(5)=False
Flag(6)=True
EndSub
'_______________
Sub PostProcess
    PostProcCounter=0
    For i=1 To FRMScans
        PostProcCounter=PostProcCounter+1
        For j=1 to Twelve

    DeltaRDiff(j)=FRMDelta.DeltaR(j,FRMScans+1
-i)-PFMDelta.DeltaR-
            (j,FRMScans+1-i)

    DeltaRRDiff(j)=FRMDelta.DeltaRR(j,FRMScans
+1-i)-PFMDelta.DeltaRR-
            (j,FRMScans+1-i)
            If   DeltaRDiff(j)>DeltaRDiffMax(j)
Then DeltaRDiffMax(j)=DeltaRDiff(j)
            If       DeltaRDiff(j)<0       Then
DeltaRDiff(j)=0
            If DeltaRRDiff(j)>DeltaRRDiffMax(j)
Then DeltaRRDiffMax(j)-
            =DeltaRRDiff(j)
            If      DeltaRRDiff(j)<0      Then
DeltaRRDiff(j)=0
        Next j
        CallTable(PostPro)
    Next i
CallTable MaxVal
EndSub
'_______________
Sub RTDMeasure
    Scan(1,Sec,1,5)

    Resistance(RTDOhms(),3,AutoRange,13,Ix4,3,
2500,False,False,200,250,1.0,0.0)
        For i=1 To 3
            RTDTemp(i)=(ChipSlope(i)*RTDOhms(i))-
ChipYInter(i)
        Next i
        AvgRun(RTDOhmsAve(1),3,RTDOhms(1),5)
        AvgRun(RTDRTempAve(1),3,RTDTemp(1),5)
    NextScan
    For i=1 To 3
        RTDTempAve(i)=RTDRTempAve(i)
    Next i
    Scan(1,Sec,1,1)
        PanelTemp(PanelDegC,250)

    TCDiff(TypeT_TC,1,mV20C,20,TypeT,PanelDegC
,True,0,250,Multi,Offset)
    NextScan
    CallTable(RTD)
    CallTable(Temp)
EndSub

'Minus 270 for count times
Sub Timer1
Scan (1,Sec,3,630)
NextScan
EndSub

'Minus 60 seconds from total amount of time
'between  pulses  because  of  60  of  readings
prior to reading
Sub Timer2
Scan (1,Sec,3,840)
NextScan
EndSub
'_
BeginProg
  '_
    ChipSlope(1)=Chip1Slope
    ChipSlope(2)=Chip2Slope
    ChipSlope(3)=Chip3Slope
    ChipYInter(1)=Chip1YInter
    ChipYInter(2)=Chip2YInter
    ChipYInter(3)=Chip3YInter
    Flag(8)=True
'_______________
    Scan(20,mSec,3,0) 'Control Scan
    'Remember  1  minute  prior  to  pulse  should
be subtracted.
    If IfTime (670,1440,min) Then
        'Cycle #1
        Call (Pre-fire)
        'Minus 60 seconds from total amount of
time between pulses because of 60 of-
        readings prior to reading
        Call (Timer2)
        Call (PreRMeasure)
        'Minus 270 for count times
        Call (Timer1)
        Call (RMeasure)
        Call (PostProcess)
        FileMark(PFRMData) : FileMark(FRMData)
        FileMark(PFMDelta)                    :
FileMark(FRMDelta)
        FileMark(PostPro)

        'Cycle #2
        Call (Pre-fire)
        Call (Timer2)
        Call (RMeasure)
        Call (PostProcess)
        FileMark(PFRMData) : FileMark(FRMData)
```

```
       FileMark(PFMDelta)                    :
FileMark(FRMDelta)
       FileMark(PostPro)

       'Cycle #3
       Call (Pre-fire)
       Call (Timer2)
       Call (RMeasure)
       Call (PostProcess)
       FileMark(PFRMData) : FileMark(FRMData)
       FileMark(PFMDelta)                    :
FileMark(FRMDelta)
       FileMark(PostPro)

       'Cycle #4
       Call (Pre-fire)
       Call (Timer2)
       Call (RMeasure)
       Call (PostProcess)
       FileMark(PFRMData) : FileMark(FRMData)
       FileMark(PFMDelta)                    :
FileMark(FRMDelta)
       FileMark(PostPro)

       'Cycle #5
       Call (Pre-fire)
       Call (Timer2)
       Call (RMeasure)
       Call (PostProcess)
       FileMark(PFRMData) : FileMark(FRMData)
       FileMark(PFMDelta)                    :
FileMark(FRMDelta)
       FileMark(PostPro)
   EndIf
   NextScan
   'Timing           tests,           Control
Scan_____________________________________
   'Scan(20,mSec,3,0)      'Test      program
operation:
       If BeginTest=True Then Move(Flag(),3,-
1,1)
           If Flag(1) Then Call(Pre-fire)
           If Flag(2) Then Call(PreRMeasure)
           If Flag(3) Then
           Call(RMeasure)
           Call(PostProcess)
           FileMark(PFRMData)                :
FileMark(FRMData)
           FileMark(PFMDelta)                :
FileMark(FRMDelta)
           FileMark(Delta)
           BeginTest=False
       EndIf
   'NextScan

EndProg
```

12.2. E4 Chemiresistor Demo Program

```
;{CR10X}
;E4 Demo Program             *
;Written By: Lucas McGrath & *
;             Jerome Wright  *
;                            *
;CR10X Data logger           *
;*****************************

*Table 1 Program
  01: 1         Execution Interval (seconds)
1:  Batt Voltage (P10)
 1: 1        Loc [ Vbatt     ]

;The following instructions read the
chemiresistor E4

2:  Excite-Delay (SE) (P4);This reads PECH in
mV
 1: 1        Reps
 2: 5        2500 mV Slow Range
 3: 1        SE Channel
 4: 1        Excite all reps w/Exchan 1
 5: 0        Delay (units 0.01 sec)
 6: 2500     mV Excitation
 7: 22       Loc [ PECH      ]
 8: .0004    Mult
 9: 0        Offset

3:  BR Transform Rf[X/(1-X)] (P59)
 1: 1        Reps
 2: 22       Loc [ PECH      ]
 3: 746.9    Multiplier (Rf)

4:  Excite-Delay (SE) (P4);This reads PNVP in
mV
 1: 1        Reps
 2: 5        2500 mV Slow Range
 3: 2        SE Channel
 4: 1        Excite all reps w/Exchan 1
 5: 0        Delay (units 0.01 sec)
 6: 2500     mV Excitation
 7: 23       Loc [ PNVP      ]
 8: .0004    Mult
 9: 0        Offset

5:  BR Transform Rf[X/(1-X)] (P59)
 1: 1        Reps
 2: 23       Loc [ PNVP      ]
 3: 822.1    Multiplier (Rf)

6:  Excite-Delay (SE) (P4);This reads PIB in
mV
 1: 1        Reps
 2: 5        2500 mV Slow Range
 3: 3        SE Channel
 4: 2        Excite all reps w/Exchan 2
 5: 0        Delay (units 0.01 sec)
 6: 2500     mV Excitation
 7: 24       Loc [ PIB       ]
 8: .0004    Mult
 9: 0        Offset

7:  BR Transform Rf[X/(1-X)] (P59)
 1: 1        Reps
 2: 24       Loc [ PIB       ]
 3: 300      Multiplier (Rf)

8:  Excite-Delay (SE) (P4);This reads PEVA in
mV
 1: 1        Reps
 2: 5        2500 mV Slow Range
 3: 4        SE Channel
 4: 2        Excite all reps w/Exchan 2
 5: 0        Delay (units 0.01 sec)
 6: 2500     mV Excitation
 7: 25       Loc [ PEVA      ]
 8: .0004    Mult
 9: 0        Offset

9:  BR Transform Rf[X/(1-X)] (P59)
 1: 1        Reps
 2: 25       Loc [ PEVA      ]
 3: 823.2    Multiplier (Rf)

10:  Full Bridge w/mv Excit (P9);This reads
the RTD
 1: 1        Reps
 2: 14       250 mV Fast Ex Range
 3: 14       250 mV Fast Br Range
 4: 4        DIFF Channel
 5: 3        Excite all reps w/Exchan 3
 6: 250      mV Excitation
 7: 26       Loc [ RTDOhms   ]
 8: 261.23   Mult
 9: 0.0      Offset

;Instructions 12-13 apply the RTD
calibibration for E4

11:  Z=X*F (P37)
 1: 26       X Loc [ RTDOhms   ]
 2: 1.8156   F
 3: 59       Z Loc [ RTDOhmsM  ]

12:  Z=X+F (P34)
 1: 59       X Loc [ RTDOhmsM  ]
 2: -354.33  F
 3: 60       Z Loc [ RTDTempC  ]

;The following instructions calculate a
baseline

13:  If Flag/Port (P91)
 1: 26       Do if Flag 6 is Low
 2: 30       Then Do

;The following instruction sets the amount of
time that the countdown will take.
;Change the F value will change the amount of
time that the countdown will take.

     14:  Z=F x 10^n (P30)
```

```
 1: -165     F
 2: 00       n, Exponent of 10
 3: 74       Z Loc [ Count_Dow ]

15:  Do (P86)
 1: 27       Set Flag 7 Low

16:  Do (P86)
 1: 18       Set Flag 8 High

17:  Beginning of Loop (P87)
 1: 1        Delay
 2: 15       Loop Count

;Instructions 19-24 cause the baseline flag to
blink for the RTDM software.

          18:  If time is (P92)
           1: 0     -- Minutes (Seconds --)
into a
           2: 2     -- Interval (same units as
above)
           3: 30       Then Do

               19:  Do (P86)
                1: 18       Set Flag 8 High

          20:  End (P95)

          21:  If time is (P92)
           1: 1     -- Minutes (Seconds --)
into a
           2: 2     -- Interval (same units as
above)
           3: 30       Then Do

               22:  Do (P86)
                1: 28       Set Flag 8 Low

          23:  End (P95)

;Instructions 25-34 Read the chemiresitor and
calculate a baseline

          24:  Excite-Delay (SE) (P4)
           1: 1        Reps
           2: 5        2500 mV Slow Range
           3: 1        SE Channel
           4: 1        Excite all reps
w/Exchan 1
           5: 0        Delay (0.01 sec units)
           6: 2500     mV Excitation
           7: 47       Loc [ PECHOHM   ]
           8: .0004    Mult
           9: 0.0      Offset

          25:  BR Transform Rf[X/(1-X)] (P59)
           1: 1        Reps
           2: 47       Loc [ PECHOHM   ]
           3: 0.0      Multiplier (Rf)

          26:  Excite-Delay (SE) (P4)
           1: 1        Reps
           2: 00       Range Option
           3: 2        SE Channel
           4: 1        Excite all reps
w/Exchan 1
           5: 0        Delay (0.01 sec units)
           6: 2500     mV Excitation
           7: 48       Loc [ PNVPOHM   ]
           8: .0004    Mult
           9: 0.0      Offset

          27:  BR Transform Rf[X/(1-X)] (P59)
           1: 1        Reps
           2: 48       Loc [ PNVPOHM   ]
           3: 0.0      Multiplier (Rf)

          28:  Excite-Delay (SE) (P4)
           1: 1        Reps
           2: 5        2500 mV Slow Range
           3: 3        SE Channel
           4: 2        Excite all reps
w/Exchan 2
           5: 0        Delay (0.01 sec units)
           6: 2500     mV Excitation
           7: 49       Loc [ PIBOHM    ]
           8: .004     Mult
           9: 0.0      Offset

          29:  BR Transform Rf[X/(1-X)] (P59)
           1: 1        Reps
           2: 49       Loc [ PIBOHM    ]
           3: 0.0      Multiplier (Rf)

          30:  Excite-Delay (SE) (P4)
           1: 1        Reps
           2: 5        2500 mV Slow Range
           3: 4        SE Channel
           4: 2        Excite all reps
w/Exchan 2
           5: 0        Delay (0.01 sec units)
           6: 2500     mV Excitation
           7: 50       Loc [ PEVAOHM   ]
           8: .0004    Mult
           9: 0.0      Offset

          31:  BR Transform Rf[X/(1-X)] (P59)
           1: 1        Reps
           2: 50       Loc [ PEVAOHM   ]
           3: 0.0      Multiplier (Rf)

          32:  Running Average (P52)
           1: 4        Reps
           2: 47       First Source Loc [
PECHOHM   ]
           3: 27       First Destination Loc [
PECHavg_1 ]
           4: 15       Number of Values in Avg
Window

     33:  End (P95)

;The following instruction make sure that the
baseline flag
;is low so that it does not get stuck in the
on position.

     34:  Do (P86)
      1: 28       Set Flag 8 Low

;The following instruction sets the Flag 6
high the loop will not
;start again until Flag 6 is low.

     35:  Do (P86)
      1: 16       Set Flag 6 High

36:  End (P95)

;The following 2 instructions are for the
counter, the first adds one to the counter
```

```
;the second instruction turns the value into a
postive value that is displayed on the demo
screen.

37:  Z=Z+1 (P32)
 1: 74       Z Loc [ Count_Dow ]

38:  Z=X*F (P37)
 1: 74       X Loc [ Count_Dow ]
 2: -1       F
 3: 75       Z Loc [ Count_Do2 ]

39:  If (X<=>F) (P89)
 1: 75       X Loc [ Count_Do2 ]
 2: 1        =
 3: 0.0      F
 4: 26       Set Flag 6 Low

;Instructions 41-46 cause the reading
resistances flag to blink.

40:  If time is (P92)
 1: 0     -- Minutes (Seconds --) into a
 2: 2        Interval (same units as above)
 3: 30       Then Do

     41:  Do (P86)
      1: 17       Set Flag 7 High

42:  End (P95)

43:  If time is (P92)
 1: 1     -- Minutes (Seconds --) into a
 2: 2        Interval (same units as above)
 3: 30       Then Do

     44:  Do (P86)
      1: 27       Set Flag 7 Low

45:  End (P95)

;Instructions 47-51 calculate the delta R/Rb
values for each polymer.


46:  If (X<=>F) (P89)
 1: 27       X Loc [ PECHavg_1 ]
 2: 3        >=
 3: 1        F
 4: 30       Then Do

     47:  Beginning of Loop (P87)
      1: 0        Delay
      2: 4        Loop Count

          48:  Z=X-Y (P35)
           1: 22    -- X Loc [ PECH      ]
           2: 27    -- Y Loc [ PECHavg_1 ]
           3: 51    -- Z Loc [ NumPECH   ]

          49:  Z=X/Y (P38)
           1: 51    -- X Loc [ NumPECH   ]
           2: 27    -- Y Loc [ PECHavg_1 ]
           3: 55    -- Z Loc [ deltaPECH ]

     50:  End (P95)

51:  End (P95)

;Instructions 52-56 make a negative delta R/Rb
value equal to zero.
;A negative delta R/Rb value can adversely
effect the concentration.

52:  Beginning of Loop (P87)
 1: 0        Delay
 2: 4        Loop Count

     53:  If (X<=>F) (P89)
      1: 55    -- X Loc [ deltaPECH ]
      2: 4        <
      3: 0        F
      4: 30       Then Do

          54:  Z=F x 10^n (P30)
           1: 0        F
           2: 00       n, Exponent of 10
           3: 55    -- Z Loc [ deltaPECH ]

     55:  End (P95)

56:  End (P95)

;Instructions 57-73 calculate the y-value for
water

57:  Do (P86)
 1: 3        Call Subroutine 3

58:  Z=X*Y (P36)
 1: 55       X Loc [ deltaPECH ]
 2: 62       Y Loc [ C1        ]
 3: 66       Z Loc [ c1PECH    ]

59:  Z=X*Y (P36)
 1: 56       X Loc [ deltaPNVP ]
 2: 63       Y Loc [ C2        ]
 3: 67       Z Loc [ c2PNVP    ]

60:  Z=X*Y (P36)
 1: 57       X Loc [ deltaPIB  ]
 2: 64       Y Loc [ C3        ]
 3: 68       Z Loc [ c3PIB     ]

61:  Z=X*Y (P36)
 1: 58       X Loc [ deltaPEVA ]
 2: 65       Y Loc [ C4        ]
 3: 69       Z Loc [ c4PEVA    ]

62:  Z=X+Y (P33)
 1: 66       X Loc [ c1PECH    ]
 2: 67       Y Loc [ c2PNVP    ]
 3: 70       Z Loc [ PECHxPNVP ]

63:  Z=X+Y (P33)
 1: 68       X Loc [ c3PIB     ]
 2: 69       Y Loc [ c4PEVA    ]
 3: 71       Z Loc [ PIBxPEVA  ]

64:  Z=X+Y (P33)
```

```
 1: 70       X Loc [ PECHxPNVP ]
 2: 71       Y Loc [ PIBxPEVA  ]
 3: 72       Z Loc [ all_added ]

65:  Z=X+Y (P33)
 1: 72       X Loc [ all_added ]
 2: 61       Y Loc [ C0        ]
 3: 73       Z Loc [ y_water   ]

66:  If (X<=>Y) (P88)
 1: 73       X Loc [ y_water   ]
 2: 3        >=
 3: 80       Y Loc [ min_water ]
 4: 30       Then Do

     67:  Do (P86)
      1: 11       Set Flag 1 High

; The following instruction sets the display
ppm equal to the calculated ppm (can be
different)
     68:  Z=X (P31)
      1: 73       X Loc [ y_water   ]
      2: 76       Z Loc [ Water_ppm ]

69:  End (P95)

;The following instructions sets the water
flag low if the y-value drops below threshold
ppm and sets display value equal to zero.

70:  If (X<=>Y) (P88)
 1: 73       X Loc [ y_water   ]
 2: 4        <
 3: 80       Y Loc [ min_water ]
 4: 30       Then Do

     71:  Do (P86)
      1: 21       Set Flag 1 Low

     72:  Z=F x 10^n (P30)
      1: 0.0      F
      2: 00       n, Exponent of 10
      3: 76       Z Loc [ Water_ppm ]

73:  End (P95)

;Instructions 114-122 calculate the y-value
for acetone

74:  Do (P86)
 1: 4        Call Subroutine 4

75:  Z=X*Y (P36)
 1: 55       X Loc [ deltaPECH ]
 2: 62       Y Loc [ C1        ]
 3: 66       Z Loc [ c1PECH    ]

76:  Z=X*Y (P36)
 1: 56       X Loc [ deltaPNVP ]
 2: 63       Y Loc [ C2        ]
 3: 67       Z Loc [ c2PNVP    ]

77:  Z=X*Y (P36)
 1: 57       X Loc [ deltaPIB  ]
 2: 64       Y Loc [ C3        ]
 3: 68       Z Loc [ c3PIB     ]

78:  Z=X*Y (P36)
 1: 58       X Loc [ deltaPEVA ]
 2: 65       Y Loc [ C4        ]
 3: 69       Z Loc [ c4PEVA    ]

79:  Z=X+Y (P33)
 1: 66       X Loc [ c1PECH    ]
 2: 67       Y Loc [ c2PNVP    ]
 3: 70       Z Loc [ PECHxPNVP ]

80:  Z=X+Y (P33)
 1: 68       X Loc [ c3PIB     ]
 2: 69       Y Loc [ c4PEVA    ]
 3: 71       Z Loc [ PIBxPEVA  ]

81:  Z=X+Y (P33)
 1: 70       X Loc [ PECHxPNVP ]
 2: 71       Y Loc [ PIBxPEVA  ]
 3: 72       Z Loc [ all_added ]

82:  Z=X+Y (P33)
 1: 72       X Loc [ all_added ]
 2: 61       Y Loc [ C0        ]
 3: 78       Z Loc [ y_acetone ]

83:  If (X<=>Y) (P88)
 1: 78       X Loc [ y_acetone ]
 2: 3        >=
 3: 79       Y Loc [ min_aceto ]
 4: 30       Then Do

     84:  Do (P86)
      1: 12       Set Flag 2 High

;The following instruction assigns the display
value of acetone to the calculated value (can
be different)
     85:  Z=X (P31)
      1: 78       X Loc [ y_acetone ]
      2: 77       Z Loc [ AcetonPPM ]

86:  End (P95)

;The following 3 instructions set the Acetone
flag low if the ppm drops below threshold ppm
and sets the display value to zero.

87:  If (X<=>Y) (P88)
 1: 78       X Loc [ y_acetone ]
 2: 4        <
 3: 79       Y Loc [ min_aceto ]
 4: 30       Then Do

     88:  Do (P86)
      1: 22       Set Flag 2 Low

     89:  Z=F x 10^n (P30)
      1: 0.0      F
      2: 00       n, Exponent of 10
      3: 77       Z Loc [ AcetonPPM ]

90:  End (P95)

;Instructions 91-101 set output flag high and
stores data in area 2
;area 2 has been set to low byte compacity so
that the data logger does not
;fill up storage area 1 and cause it to run
slowly.

91:  Do (P86)
 1: 10       Set Output Flag High (Flag 0)

92:  Set Active Storage Area (P80)^20550
```

```
 1: 2        Final Storage Area 2
 2: 111      Array ID

93:  Sample (P70)^14867
 1: 4        Reps
 2: 22       Loc [ PECH      ]

94:  Sample (P70)^14405
 1: 1        Reps
 2: 60       Loc [ RTDTempC  ]

95:  Sample (P70)^29453
 1: 1        Reps
 2: 74       Loc [ Count_Dow ]

96:  If time is (P92)
 1: 1        Minutes (Seconds --) into a
 2: 60       Interval (same units as above)
 3: 10       Set Output Flag High (Flag 0)

97:  Resolution (P78)
 1: 01       High Resolution

98:  Real Time (P77)^7187
 1: 0221     Day,Hour/Minute,Seconds (midnight
= 2400)

99:  Sample (P70)^2714
 1: 4        Reps
 2: 22       Loc [ PECH      ]

100:  Sample (P70)^8978
 1: 1        Reps
 2: 26       Loc [ RTDOhms   ]

101:  Sample (P70)^1974
 1: 4        Reps
 2: 55       Loc [ deltaPECH ]

*Table 2 Program
  02: 0         Execution Interval (seconds)

*Table 3 Subroutines

1:  Beginning of Subroutine (P85)
 1: 3        Subroutine 3
;Coefficients for water
     2:  Z=F x 10^n (P30)
      1: 0        F
      2: 0        n, Exponent of 10
      3: 61       Z Loc [ C0        ]

     3:  Z=F x 10^n (P30)
      1: 0        F
      2: 00       n, Exponent of 10
      3: 62       Z Loc [ C1        ]

     4:  Z=F x 10^n (P30)
      1: 1.2      F
      2: 5        n, Exponent of 10
      3: 63       Z Loc [ C2        ]

     5:  Z=F x 10^n (P30)
      1: 0        F
      2: 00       n, Exponent of 10
      3: 64       Z Loc [ C3        ]

     6:  Z=F x 10^n (P30)
      1: 0        F
      2: 00       n, Exponent of 10
      3: 65       Z Loc [ C4        ]

7:  End (P95)

8:  Beginning of Subroutine (P85)
 1: 4        Subroutine 4
;Coefficients for acetone
     9:  Z=F x 10^n (P30)
      1: 1.23     F
      2: 2        n, Exponent of 10
      3: 61       Z Loc [ C0        ]

     10:  Z=F x 10^n (P30)
      1: 1.20     F
      2: 6        n, Exponent of 10
      3: 62       Z Loc [ C1        ]

     11:  Z=F x 10^n (P30)
      1: 2.06     F
      2: 4        n, Exponent of 10
      3: 63       Z Loc [ C2        ]

     12:  Z=F x 10^n (P30)
      1: 1.11     F
      2: 6        n, Exponent of 10
      3: 64       Z Loc [ C3        ]


     13:  Z=F x 10^n (P30)
      1: 3.66     F
      2: 4        n, Exponent of 10
      3: 65       Z Loc [ C4        ]

; Threshold limit for water

     14:  Z=F x 10^n (P30)
      1: 1.5      F
      2: 03       n, Exponent of 10
      3: 80       Z Loc [ min_water ]

; Threshold limit for acetone

     15:  Z=F x 10^n (P30)
      1: 5.0      F
      2: 3        n, Exponent of 10
      3: 79       Z Loc [ min_aceto ]

16:  End (P95)

End Program

-Input Locations-
1 Vbatt     1 0 1
2 Sen_1_mVm 1 0 0
3 Sen_2_mVm 1 0 0
4 Sen_3_mVm 1 0 0
5 Sen_4_mVm 1 0 0
6 Res_1_mVc 1 0 0
7 Res_2_mVc 1 0 0
8 Res_3_mVc 1 0 0
9 Res_4_mVc 1 0 0
10 Ref1_Kohm 1 0 0
11 uA_1c     1 0 0
12 Ref2_Kohm 1 0 0
13 uA_2c     1 0 0
14 Ref3_Kohm 1 0 0
15 uA_3c     1 0 0
16 Ref4_Kohm 1 0 0
17 uA_4c     1 0 0
18 negkohms1 1 0 0
19 negkohms2 1 0 0
20 negkohms3 1 0 0
```

```
21 negkohms4 1 0 0
22 PECH      1 4 2
23 PNVP      1 3 2
24 PIB       1 3 2
25 PEVA      1 3 2
26 RTDOhms   1 2 1
27 PECHavg_1 5 3 1
28 PNVPavg   9 0 1
29 PIBavg    9 0 1
30 PEVAavg   17 0 1
31 PECHmv_1  1 0 0
32 PNVPmv_2  1 0 0
33 PIBmv_1   1 0 0
34 PEVAmv_2  1 0 0
35 PECH_RESM 1 0 0
36 PNVP_RESM 1 0 0
37 PIB_RESM  1 0 0
38 PEVA_RESM 1 0 0
39 uA_PECH   1 0 0
40 uA_PNVP   1 0 0
41 uA_PIB    1 0 0
42 uA_PEVA   1 0 0
43 negPECH   1 0 0
44 negPNVP   1 0 0
45 negPIB    1 0 0
46 negPEVA   1 0 0
47 PECHOHM   5 2 2
48 PNVPOHM   1 2 2
49 PIBOHM    5 2 2
50 PEVAOHM   1 2 2
51 NumPECH   1 1 1
52 NumPNVP   1 0 0
53 NumPIB    1 0 0
54 NumPEVA   1 0 0
55 deltaPECH 1 4 2
56 deltaPNVP 1 3 0
57 deltaPIB  1 3 0
58 deltaPEVA 1 3 0
59 RTDOhmsM  1 1 1
60 RTDTempC  1 1 1
61 C0        1 2 2
62 C1        1 2 2
63 C2        1 2 2
64 C3        1 2 2
65 C4        1 2 2
66 c1PECH    1 2 2
67 c2PNVP    1 2 2
68 c3PIB     1 2 2
69 c4PEVA    1 2 2
70 PECHxPNVP 1 2 2
71 PIBxPEVA  1 2 2
72 all_added 1 2 2
73 y_water   1 3 1
74 Count_Dow 1 2 2
75 Count_Do2 1 1 1
76 Water_ppm 1 0 2
77 AcetonPPM 1 0 2
78 y_acetone 1 3 1
79 min_aceto 1 2 1
80 min_water 1 2 1
81 _________ 1 0 0
-Program Security-
0000
0000
0000
-Mode 4-
-Final Storage Area 2-
300
-CR10X ID-
0
-CR10X Power Up-
3
-CR10X Compile Setting-
3
-CR10X RS-232 Setting-
-1
-DLD File Labels-
0
-Final Storage Labels-
0,Day_RTM,7187
0,Hour_Minute_RTM
0,Seconds_RTM
1,PECH~22,2714
1,PNVP~23
1,PIB~24
1,PEVA~25
2,RTDOhms~26,8978
3,deltaPECH~55,1974
3,deltaPNVP~56
3,deltaPIB~57
3,deltaPEVA~58
4,111,20550
5,PECH~22,14867
5,PNVP~23
5,PIB~24
5,PEVA~25
6,RTDTempC~60,14405
7,Count_Dow~74,29453
```

12.3. CR23X Program for Chemical Waste Landfill

```
;{CR23X}
;
*Table 1 Program
  01: 60        Execution Interval (seconds)
1:  Batt Voltage (P10)
 1: 1        Loc [ Vbatt     ]

2:  Do (P86)
 1: 1        Call Subroutine 1

;The following instructions read the polymers
on E19

3:  Excite-Delay (SE) (P4)
 1: 1        Reps
 2: 15       5000 mV, Fast Range
 3: 1        SE Channel
 4: 1        Excite all reps w/Exchan 1
 5: 0        Delay (0.01 sec units)
 6: 5000     mV Excitation
 7: 34       Loc [ E19_PIB   ]
 8: .0002    Mult
 9: 0.0      Offset

4:  BR Transform Rf[X/(1-X)] (P59)
 1: 1        Reps
 2: 34       Loc [ E19_PIB   ]
 3: 132.41   Multiplier (Rf)

5:  Excite-Delay (SE) (P4)
 1: 1        Reps
 2: 15       5000 mV, Fast Range
 3: 2        SE Channel
 4: 1        Excite all reps w/Exchan 1
 5: 0        Delay (0.01 sec units)
 6: 5000     mV Excitation
 7: 35       Loc [ E19_PNVP  ]
 8: .0002    Mult
 9: 0.0      Offset

6:  BR Transform Rf[X/(1-X)] (P59)
 1: 1        Reps
 2: 35       Loc [ E19_PNVP  ]
 3: 149.70   Multiplier (Rf)

7:  Excite-Delay (SE) (P4)
 1: 1        Reps
 2: 15       5000 mV, Fast Range
 3: 3        SE Channel
 4: 1        Excite all reps w/Exchan 1
 5: 0        Delay (0.01 sec units)
 6: 5000     mV Excitation
 7: 36       Loc [ E19_PVTD  ]
 8: .0002    Mult
 9: 0.0      Offset

8:  BR Transform Rf[X/(1-X)] (P59)
 1: 1        Reps
 2: 36       Loc [ E19_PVTD  ]
 3: 299.31   Multiplier (Rf)

9:  Excite-Delay (SE) (P4)
 1: 1        Reps
 2: 15       5000 mV, Fast Range
 3: 4        SE Channel
 4: 1        Excite all reps w/Exchan 1
 5: 0        Delay (0.01 sec units)
 6: 5000     mV Excitation
 7: 37       Loc [ E19_PEVA  ]
 8: .0002    Mult
 9: 0.0      Offset

10:  BR Transform Rf[X/(1-X)] (P59)
 1: 1        Reps
 2: 37       Loc [ E19_PEVA  ]
 3: 199.25   Multiplier (Rf)

;The following instructions read E21

11:  Excite-Delay (SE) (P4)
 1: 1        Reps
 2: 15       5000 mV, Fast Range
 3: 13       SE Channel
 4: 2        Excite all reps w/Exchan 2
 5: 1        Delay (0.01 sec units)
 6: 5000     mV Excitation
 7: 204      Loc [ E25_PECH  ]
 8: .0002    Mult
 9: 0.0      Offset

12:  BR Transform Rf[X/(1-X)] (P59)
 1: 1        Reps
 2: 204      Loc [ E25_PECH  ]
 3: 199.60   Multiplier (Rf)

13:  Excite-Delay (SE) (P4)
 1: 1        Reps
 2: 15       5000 mV, Fast Range
 3: 14       SE Channel
 4: 2        Excite all reps w/Exchan 2
 5: 1        Delay (0.01 sec units)
 6: 5000     mV Excitation
 7: 205      Loc [ E25_PNVP  ]
 8: .0002    Mult
 9: 0.0      Offset

14:  BR Transform Rf[X/(1-X)] (P59)
 1: 1        Reps
 2: 205      Loc [ E25_PNVP  ]
 3: 199.00   Multiplier (Rf)

15:  Excite-Delay (SE) (P4)
 1: 1        Reps
 2: 15       5000 mV, Fast Range
 3: 15       SE Channel
 4: 2        Excite all reps w/Exchan 2
 5: 1        Delay (0.01 sec units)
 6: 5000     mV Excitation
 7: 206      Loc [ E25_PIB   ]
 8: .0002    Mult
 9: 0.0      Offset

16:  BR Transform Rf[X/(1-X)] (P59)
 1: 1        Reps
 2: 206      Loc [ E25_PIB   ]
 3: 214.92   Multiplier (Rf)

17:  Excite-Delay (SE) (P4)
 1: 1        Reps
 2: 15       5000 mV, Fast Range
 3: 16       SE Channel
```

```
 4: 2        Excite all reps w/Exchan 2
 5: 1        Delay (0.01 sec units)
 6: 5000     mV Excitation
 7: 207      Loc [ E25_PEVA  ]
 8: .0002    Mult
 9: 0.0      Offset

18:  BR Transform Rf[X/(1-X)] (P59)
 1: 1        Reps
 2: 207      Loc [ E25_PEVA  ]
 3: 174.03   Multiplier (Rf)

19:  Full Bridge w/mv Excit (P9);This reads
E19's RTD
 1: 1        Reps
 2: 14       1000 mV, Fast, Ex Range
 3: 14       1000 mV, Fast, Br Range
 4: 3        DIFF Channel
 5: 3        Excite all reps w/Exchan 3
 6: 1000     mV Excitation
 7: 31       Loc [ RTDohms   ]
 8: 261.11   Mult
 9: 0.0      Offset

20:  Full Bridge w/mv Excit (P9);This reads
E25's RTD
 1: 1        Reps
 2: 14       1000 mV, Fast, Ex Range
 3: 14       1000 mV, Fast, Br Range
 4: 9        DIFF Channel
 5: 3        Excite all reps w/Exchan 3
 6: 1000     mV Excitation
 7: 185      Loc [ E21RTDohm ]
 8: 235.76   Mult
 9: 0.0      Offset

;Instructions 10-11 calculate E19's RTD
temperature

21:  Z=X*F (P37)
 1: 31       X Loc [ RTDohms   ]
 2: .0035    F
 3: 33       Z Loc [ RTDTempM  ]

22:  Z=X+F (P34)
 1: 33       X Loc [ RTDTempM  ]
 2: 17.093   F
 3: 32       Z Loc [ RTDTempC  ]

;Instructions 12-13 calculate E21's RTD
temperature

23:  Z=X*F (P37)
 1: 185      X Loc [ E21RTDohm ]
 2: 1.7005   F
 3: 190      Z Loc [ E21RTD_M  ]

24:  Z=X+F (P34)
 1: 190      X Loc [ E21RTD_M  ]
 2: -362.96  F
 3: 191      Z Loc [ E21_TempC ]

25:  Panel Temperature (P17)
 1: 6        Loc [ T_ref     ]

;The following instuctions are for the
multiplexer

26:  Do (P86)
 1: 42       Set Port 2 High

27:  Beginning of Loop (P87)
 1: 0        Delay
 2: 2        Loop Count

     28:  Do (P86)
      1: 73       Pulse Port 3

     29:  Delay w/Opt Excitation (P22)
      1: 1        Ex Channel
      2: 0        Delay W/Ex (0.01 sec units)
      3: 1        Delay After Ex (0.01 sec
units)
      4: 0        mV Excitation

     30:  Thermocouple Temp (DIFF) (P14)
      1: 1        Reps
      2: 21       10 mV, 60 Hz Reject, Slow
Range
      3: 12       DIFF Channel
      4: 1        Type T (Copper-Constantan)
      5: 6        Ref Temp (Deg. C) Loc [
T_ref     ]
      6: 251   -- Loc [ T_Type_D3 ]
      7: 1.0      Mult
      8: 0.0      Offset

31:  End (P95)

32:  Beginning of Loop (P87)
 1: 0        Delay
 2: 2        Loop Count

     33:  Do (P86)
      1: 73       Pulse Port 3

     34:  Delay w/Opt Excitation (P22)
      1: 1        Ex Channel
      2: 0        Delay W/Ex (0.01 sec units)
      3: 1        Delay After Ex (0.01 sec
units)
      4: 0        mV Excitation

     35:  Volt (SE) (P1)
      1: 1        Reps
      2: 25       5000 mV, 60 Hz Reject, Fast
Range (same as code 45)
      3: 23       SE Channel
      4: 10    -- Loc [ PSIVolts  ]
      5: 1.0      Mult
      6: 0.0      Offset

36:  End (P95)

;The following instruction read the voltage
off of the solar panel

37:  Beginning of Loop (P87)
 1: 0        Delay
 2: 1        Loop Count

     38:  Do (P86)
      1: 73       Pulse Port 3

     39:  Delay w/Opt Excitation (P22)
      1: 1        Ex Channel
      2: 0        Delay W/Ex (0.01 sec units)
      3: 1        Delay After Ex (0.01 sec
units)
      4: 0        mV Excitation

     40:  Volt (Diff) (P2)
```

```
      1: 1        Reps
      2: 25       5000 mV, 60 Hz Reject, Fast
Range (same as code 45)
      3: 12       DIFF Channel
      4: 283      Loc [ SolarVolD ]
      5: .001     Mult
      6: 0.0      Offset

41:  End (P95)

42:  Do (P86)
 1: 52       Set Port 2 Low

;The following instruction convert the divided
solar panel voltage into its actual voltage
;and precicts the wattage

43:  Z=X*F (P37)
 1: 283      X Loc [ SolarVolD ]
 2: 4.14396  F
 3: 284      Z Loc [ SolarVolt ]

44:  Z=X*F (P37)
 1: 284      X Loc [ SolarVolt ]
 2: 1.17     F
 3: 285      Z Loc [ SolarWatt ]

45:  Z=X*F (P37)
 1: 11       X Loc [ HeatBarV  ]
 2: .001     F
 3: 11       Z Loc [ HeatBarV  ]

46:  Z=X-Y (P35)
 1: 32       X Loc [ RTDTempC  ]
 2: 251      Y Loc [ T_Type_D3 ]
 3: 99       Z Loc [ RTD_Ttype ]

;The follwoing instructions read the HX92AC
and convert the output to Rh

47:  Volt (SE) (P1)
 1: 1        Reps
 2: 25       5000 mV, 60 Hz Reject, Fast Range
(same as code 45)
 3: 22       SE Channel
 4: 9        Loc [ RHVolts   ]
 5: 1.0      Mult
 6: 0.0      Offset

48:  Z=X/Y (P38)
 1: 9        X Loc [ RHVolts   ]
 2: 118      Y Loc [ RhRefR    ]
 3: 119      Z Loc [ RhmAmps   ]

49:  Z=X+F (P34)
 1: 119      X Loc [ RhmAmps   ]
 2: -4       F
 3: 120      Z Loc [ RhAmps_mi ]

50:  Z=X*F (P37)
 1: 120      X Loc [ RhAmps_mi ]
 2: 6.25     F
 3: 14       Z Loc [ HX92RH    ]

51:  If (X<=>F) (P89)
 1: 14       X Loc [ HX92RH    ]
 2: 3        >=
 3: 100      F
 4: 30       Then Do

     52:  Z=F x 10^n (P30)
      1: 100      F
      2: 0        n, Exponent of 10
      3: 14       Z Loc [ HX92RH    ]

53:  End (P95)

54:  If (X<=>F) (P89)
 1: 14       X Loc [ HX92RH    ]
 2: 4        <
 3: 0        F
 4: 30       Then Do

     55:  Z=F x 10^n (P30)
      1: 0        F
      2: 0        n, Exponent of 10
      3: 14       Z Loc [ HX92RH    ]

56:  End (P95)

;The following Insturctions will convert the
PSI Volts into PSI

57:  Z=X/Y (P38)
 1: 10       X Loc [ PSIVolts  ]
 2: 286      Y Loc [ PSIRefR   ]
 3: 12       Z Loc [ PSIamps   ]

58:  Z=X*F (P37)
 1: 12       X Loc [ PSIamps   ]
 2: .9375    F
 3: 16       Z Loc [ PSIVoltM  ]

59:  Z=X+F (P34)
 1: 16       X Loc [ PSIVoltM  ]
 2: -3.75    F
 3: 15       Z Loc [ PX215_PSI ]

60:  Z=X*F (P37)
 1: 15       X Loc [ PX215_PSI ]
 2: 6894.76  F
 3: 253      Z Loc [ PX215_Pa  ]

;The following  instructions calculate
Saturated Vapor Pressure and
;multiply it by the humidity to calculate Vp
Pa of the system

61:  Saturation Vapor Pressure (P56)
 1: 251      Temperature Loc [ T_Type_D3 ]
 2: 128      Loc [ SatVpKpa  ]

62:  Z=X*F (P37)
 1: 128      X Loc [ SatVpKpa  ]
 2: 1000     F
 3: 129      Z Loc [ SatVpPa   ]

63:  Z=X*F (P37)
 1: 14       X Loc [ HX92RH    ]
 2: .01      F
 3: 130      Z Loc [ HX92Rh001 ]

64:  Z=X*Y (P36)
 1: 129      X Loc [ SatVpPa   ]
 2: 130      Y Loc [ HX92Rh001 ]
 3: 131      Z Loc [ Vp_Ambien ]

;Instuctions 48-54 calculate the Saturated
Vapor Pressure of TCE

65:  Polynomial (P55)
 1: 1        Reps
```

```
 2: 251      X Loc [ T_Type_D3 ]
 3: 301      F(X) Loc [ D3sTCE_Pa ]
 4: 2153.8   C0
 5: 139.53   C1
 6: 4.0333   C2
 7: .0575    C3
 8: .0003    C4
 9: 0        C5

66:  Polynomial (P55)
 1: 1        Reps
 2: 252      X Loc [ T_TypeMW2 ]
 3: 305      F(X) Loc [ MWsTCE_Pa ]
 4: 2153.8   C0
 5: 139.53   C1
 6: 4.0333   C2
 7: .0575    C3
 8: .0003    C4
 9: 0.0      C5

67:  Z=X/Y (P38)
 1: 301      X Loc [ D3sTCE_Pa ]
 2: 253      Y Loc [ PX215_Pa  ]
 3: 302      Z Loc [ D3sTCE_PX ]

68:  Z=X/Y (P38)
 1: 305      X Loc [ MWsTCE_Pa ]
 2: 253      Y Loc [ PX215_Pa  ]
 3: 306      Z Loc [ MWsTCE_PX ]

69:  Z=F x 10^n (P30)
 1: 1        F
 2: 6        n, Exponent of 10
 3: 303      Z Loc [ Million   ]

70:  Z=X*Y (P36)
 1: 302      X Loc [ D3sTCE_PX ]
 2: 303      Y Loc [ Million   ]
 3: 304      Z Loc [ D3sTCEppm ]

71:  Z=X*Y (P36)
 1: 307      X Loc [ MWsTCEppm ]
 2: 303      Y Loc [ Million   ]
 3: 307      Z Loc [ MWsTCEppm ]

;The following instructions read and calculate
the Head Ft of the CS400 Submersible Pressure
Transducer

72:  Full Bridge (P6)
 1: 1        Reps
 2: 12       50 mV, Fast Range
 3: 6        DIFF Channel
 4: 4        Excite all reps w/Exchan 4
 5: 860      mV Excitation
 6: 25       Loc [ MA_MEAS   ]
 7: .01      Mult
 8: 0.0      Offset

73:  Full Bridge (P6)
 1: 1        Reps
 2: 12       50 mV, Fast Range
 3: 5        DIFF Channel
 4: 4        Excite all reps w/Exchan 4
 5: 860      mV Excitation
 6: 26       Loc [ mv_ma     ]
 7: .5       Mult
 8: 0.0      Offset

74:  Z=X/Y (P38)
 1: 26       X Loc [ mv_ma     ]
 2: 25       Y Loc [ MA_MEAS   ]
 3: 27       Z Loc [ MV        ]

75:  Z=X*F (P37)
 1: 27       X Loc [ MV        ]
 2: 3.0241   F
 3: 28       Z Loc [ HEAD_FT   ]

76:  Z=X+F (P34)
 1: 28       X Loc [ HEAD_FT   ]
 2: -1       F
 3: 28       Z Loc [ HEAD_FT   ]

77:  Z=X+F (P34)
 1: 27       X Loc [ MV        ]
 2: -.2647   F
 3: 29       Z Loc [ MV_Minus  ]

78:  Z=X*F (P37)
 1: 29       X Loc [ MV_Minus  ]
 2: 1.3115   F
 3: 30       Z Loc [ PSIG_CS40 ]

;The following insturctions calculate the
depth of water level
;and head of water above the chemireistor

79:  Z=X-Y (P35)
 1: 258      X Loc [ D_PressFt ]
 2: 28       Y Loc [ HEAD_FT   ]
 3: 254      Z Loc [ D_GW_ft   ]

80:  Z=X*F (P37)
 1: 254      X Loc [ D_GW_ft   ]
 2: .3048    F
 3: 255      Z Loc [ D_GW_m    ]

81:  Z=X-Y (P35)
 1: 28       X Loc [ HEAD_FT   ]
 2: 259      Y Loc [ D_ChemiFt ]
 3: 256      Z Loc [ Hh2oE20ft ]

82:  Z=X*F (P37)
 1: 256      X Loc [ Hh2oE20ft ]
 2: .3048    F
 3: 257      Z Loc [ Hh20E20m  ]

;The following instructions calculate delta
R/Rb for E19 polymers

83:  If (X<=>F) (P89)
 1: 95       X Loc [ base_PIB  ]
 2: 3        >=
 3: 1        F
 4: 30       Then Do

     84:  Z=X-Y (P35)
      1: 34       X Loc [ E19_PIB   ]
      2: 95       Y Loc [ base_PIB  ]
      3: 104      Z Loc [ NumPIB    ]

     85:  Z=X/Y (P38)
      1: 104      X Loc [ NumPIB    ]
      2: 95       Y Loc [ base_PIB  ]
```

```
      3: 105      Z Loc [ deltaPIB  ]

86:  End (P95)

87:  If (X<=>F) (P89)
 1: 96       X Loc [ base_PNVP ]
 2: 3        >=
 3: 1        F
 4: 30       Then Do

     88:  Z=X-Y (P35)
      1: 35       X Loc [ E19_PNVP  ]
      2: 96       Y Loc [ base_PNVP ]
      3: 106      Z Loc [ NumPNVP   ]

     89:  Z=X/Y (P38)
      1: 106      X Loc [ NumPNVP   ]
      2: 96       Y Loc [ base_PNVP ]
      3: 107      Z Loc [ deltaPNVP ]

90:  End (P95)

91:  If (X<=>F) (P89)
 1: 97       X Loc [ base_PVTD ]
 2: 3        >=
 3: 1        F
 4: 30       Then Do

     92:  Z=X-Y (P35)
      1: 36       X Loc [ E19_PVTD  ]
      2: 97       Y Loc [ base_PVTD ]
      3: 108      Z Loc [ NumPVTD   ]

     93:  Z=X/Y (P38)
      1: 108      X Loc [ NumPVTD   ]
      2: 97       Y Loc [ base_PVTD ]
      3: 109      Z Loc [ deltaPVTD ]

94:  End (P95)

95:  If (X<=>F) (P89)
 1: 98       X Loc [ base_PEVA ]
 2: 3        >=
 3: 1        F
 4: 30       Then Do

     96:  Z=X-Y (P35)
      1: 37       X Loc [ E19_PEVA  ]
      2: 98       Y Loc [ base_PEVA ]
      3: 110      Z Loc [ NumPEVA   ]

     97:  Z=X/Y (P38)
      1: 110      X Loc [ NumPEVA   ]
      2: 98       Y Loc [ base_PEVA ]
      3: 111      Z Loc [ deltaPEVA ]

98:  End (P95)

;The following instructions calculate delta
R/Rb for E21 polymers

99:  If (X<=>F) (P89)
 1: 209      X Loc [ BlE25PECH ]
 2: 3        >=
 3: 1        F
 4: 30       Then Do

     100:  Z=X-Y (P35)
      1: 204      X Loc [ E25_PECH  ]
      2: 209      Y Loc [ BlE25PECH ]
      3: 213      Z Loc [ nE25PECH  ]

     101:  Z=X/Y (P38)
      1: 213      X Loc [ nE25PECH  ]
      2: 209      Y Loc [ BlE25PECH ]
      3: 217      Z Loc [ E25DPECH  ]

102:  End (P95)

103:  If (X<=>F) (P89)
 1: 210      X Loc [ BlE25PNVP ]
 2: 3        >=
 3: 1        F
 4: 30       Then Do

     104:  Z=X-Y (P35)
      1: 205      X Loc [ E25_PNVP  ]
      2: 210      Y Loc [ BlE25PNVP ]
      3: 214      Z Loc [ nE25PNVP  ]

     105:  Z=X/Y (P38)
      1: 214      X Loc [ nE25PNVP  ]
      2: 210      Y Loc [ BlE25PNVP ]
      3: 218      Z Loc [ E25DPNVP  ]

106:  End (P95)

107:  If (X<=>F) (P89)
 1: 211      X Loc [ BlE25PIB  ]
 2: 3        >=
 3: 1        F
 4: 30       Then Do

     108:  Z=X-Y (P35)
      1: 206      X Loc [ E25_PIB   ]
      2: 211      Y Loc [ BlE25PIB  ]
      3: 215      Z Loc [ nE25PIB   ]

     109:  Z=X/Y (P38)
      1: 215      X Loc [ nE25PIB   ]
      2: 211      Y Loc [ BlE25PIB  ]
      3: 219      Z Loc [ E25DPIB   ]

110:  End (P95)

111:  If (X<=>F) (P89)
 1: 212      X Loc [ BlE25PEVA ]
 2: 3        >=
 3: 1        F
 4: 30       Then Do

     112:  Z=X-Y (P35)
      1: 207      X Loc [ E25_PEVA  ]
      2: 212      Y Loc [ BlE25PEVA ]
      3: 216      Z Loc [ nE25PEVA  ]

     113:  Z=X/Y (P38)
      1: 216      X Loc [ nE25PEVA  ]
      2: 212      Y Loc [ BlE25PEVA ]
      3: 220      Z Loc [ E25DPEVA  ]

114:  End (P95)

;The following instructions apply the model
for predicting TCE concentration
;for the chip E19
;They calculate using the T_Type Thermocouple
in Well D3

115:  Do (P86)
 1: 3        Call Subroutine 3
```

```
116:  Z=X*Y (P36)
 1: 122      X Loc [ B1        ]
 2: 251      Y Loc [ T_Type_D3 ]
 3: 161      Z Loc [ B1X       ]

117:  Z=X*Y (P36)
 1: 123      X Loc [ B2        ]
 2: 107      Y Loc [ deltaPNVP ]
 3: 152      Z Loc [ B2PNVP    ]

118:  Z=X*Y (P36)
 1: 152      X Loc [ B2PNVP    ]
 2: 111      Y Loc [ deltaPEVA ]
 3: 162      Z Loc [ B2X       ]

119:  Z=X*Y (P36)
 1: 124      X Loc [ B3        ]
 2: 109      Y Loc [ deltaPVTD ]
 3: 153      Z Loc [ B3PVTD    ]

120:  Z=X*Y (P36)
 1: 153      X Loc [ B3PVTD    ]
 2: 251      Y Loc [ T_Type_D3 ]
 3: 163      Z Loc [ B3X       ]

121:  Z=X*Y (P36)
 1: 125      X Loc [ B4        ]
 2: 111      Y Loc [ deltaPEVA ]
 3: 154      Z Loc [ B4PEVA    ]

122:  Z=X*Y (P36)
 1: 154      X Loc [ B4PEVA    ]
 2: 251      Y Loc [ T_Type_D3 ]
 3: 164      Z Loc [ B4X       ]

123:  Z=X*Y (P36)
 1: 126      X Loc [ B5        ]
 2: 109      Y Loc [ deltaPVTD ]
 3: 155      Z Loc [ B5PVTD    ]

124:  Z=X*Y (P36)
 1: 155      X Loc [ B5PVTD    ]
 2: 131      Y Loc [ Vp_Ambien ]
 3: 165      Z Loc [ B5X       ]

125:  Z=X*Y (P36)
 1: 127      X Loc [ B6        ]
 2: 105      Y Loc [ deltaPIB  ]
 3: 156      Z Loc [ b6PIB     ]

126:  Z=X*Y (P36)
 1: 156      X Loc [ b6PIB     ]
 2: 107      Y Loc [ deltaPNVP ]
 3: 157      Z Loc [ b6PIBPNVP ]

127:  Z=X*Y (P36)
 1: 157      X Loc [ b6PIBPNVP ]
 2: 251      Y Loc [ T_Type_D3 ]
 3: 166      Z Loc [ B6X       ]

128:  Z=X*Y (P36)
 1: 151      X Loc [ B7        ]
 2: 105      Y Loc [ deltaPIB  ]
 3: 158      Z Loc [ B7PIB     ]

129:  Z=X*Y (P36)
 1: 158      X Loc [ B7PIB     ]
 2: 109      Y Loc [ deltaPVTD ]
 3: 159      Z Loc [ B7PIBPVTD ]

130:  Z=X*Y (P36)
 1: 159      X Loc [ B7PIBPVTD ]
 2: 111      Y Loc [ deltaPEVA ]
 3: 160      Z Loc [ B7PibPPEV ]

131:  Z=X*Y (P36)
 1: 160      X Loc [ B7PibPPEV ]
 2: 251      Y Loc [ T_Type_D3 ]
 3: 167      Z Loc [ B7X       ]

132:  Z=X-Y (P35)
 1: 121      X Loc [ B0        ]
 2: 161      Y Loc [ B1X       ]
 3: 169      Z Loc [ B0_B1     ]

133:  Z=X+Y (P33)
 1: 162      X Loc [ B2X       ]
 2: 163      Y Loc [ B3X       ]
 3: 170      Z Loc [ B2_B3     ]

134:  Z=X+Y (P33)
 1: 164      X Loc [ B4X       ]
 2: 165      Y Loc [ B5X       ]
 3: 168      Z Loc [ B4X_B5Xa  ]

135:  Z=X-Y (P35)
 1: 168      X Loc [ B4X_B5Xa  ]
 2: 166      Y Loc [ B6X       ]
 3: 171      Z Loc [ B4_B5_B6  ]

136:  Z=X+Y (P33)
 1: 171      X Loc [ B4_B5_B6  ]
 2: 167      Y Loc [ B7X       ]
 3: 172      Z Loc [ B4B5B6B7  ]

137:  Z=X+Y (P33)
 1: 169      X Loc [ B0_B1     ]
 2: 170      Y Loc [ B2_B3     ]
 3: 173      Z Loc [ B0B1B2B3  ]

138:  Z=X+Y (P33)
 1: 173      X Loc [ B0B1B2B3  ]
 2: 172      Y Loc [ B4B5B6B7  ]
 3: 132      Z Loc [ TCE_ppm   ]

139:  Z=X+F (P34)
 1: 132      X Loc [ TCE_ppm   ]
 2: 0.0      F
 3: 174      Z Loc [ TCE_ppmR  ]

140:  If (X<=>F) (P89)
 1: 174      X Loc [ TCE_ppmR  ]
 2: 4        <
 3: 5000     F
 4: 30       Then Do

     141:  Z=F x 10^n (P30)
      1: 0.0      F
      2: 00       n, Exponent of 10
      3: 174      Z Loc [ TCE_ppmR  ]

142:  End (P95)

143:  If (X<=>F) (P89)
 1: 174      X Loc [ TCE_ppmR  ]
 2: 3        >=
 3: 5000     F
 4: 30       Then Do

     144:  Do (P86)
      1: 115      Set Flag 15 High
```

```
145:  End (P95)

146:  If (X<=>Y) (P88)
 1: 132      X Loc [ TCE_ppm   ]
 2: 3        >=
 3: 304      Y Loc [ D3sTCEppm ]
 4: 30       Then Do

     147:  Z=X (P31)
      1: 304      X Loc [ D3sTCEppm ]
      2: 132      Z Loc [ TCE_ppm   ]

148:  End (P95)



;The following instructions apply the model
for the predicting TCE in ppm
;for the chemiresistor E25

149:  Do (P86)
 1: 5        Call Subroutine 5



;The following are multipliers for the
equation

150:  Z=X*Y (P36)
 1: 217      X Loc [ E25DPECH  ]
 2: 220      Y Loc [ E25DPEVA  ]
 3: 288      Z Loc [ dPECHxdPE ]

151:  Z=X*Y (P36)
 1: 219      X Loc [ E25DPIB   ]
 2: 220      Y Loc [ E25DPEVA  ]
 3: 289      Z Loc [ dPIBxdPEV ]

152:  Z=X*Y (P36)
 1: 220      X Loc [ E25DPEVA  ]
 2: 218      Y Loc [ E25DPNVP  ]
 3: 310      Z Loc [ dPEVAxdPN ]

153:  Z=X*Y (P36)
 1: 217      X Loc [ E25DPECH  ]
 2: 219      Y Loc [ E25DPIB   ]
 3: 309      Z Loc [ dPIBXdPEC ]


154:  Z=X*Y (P36)
 1: 222      X Loc [ C1        ]
 2: 217      Y Loc [ E25DPECH  ]
 3: 308      Z Loc [ C1_PECH   ]

155:  Z=X*Y (P36)
 1: 223      X Loc [ C2        ]
 2: 309      Y Loc [ dPIBXdPEC ]
 3: 311      Z Loc [ C2_X      ]

156:  Z=X*Y (P36)
 1: 224      X Loc [ C3        ]
 2: 288      Y Loc [ dPECHxdPE ]
 3: 312      Z Loc [ C3_X      ]

157:  Z=X*Y (P36)
 1: 225      X Loc [ C4        ]
 2: 310      Y Loc [ dPEVAxdPN ]
 3: 313      Z Loc [ C4_X      ]

158:  Z=X*Y (P36)
 1: 226      X Loc [ C5        ]
 2: 289      Y Loc [ dPIBxdPEV ]
 3: 314      Z Loc [ C5_X      ]

159:  Z=X+Y (P33)
 1: 221      X Loc [ C0        ]
 2: 308      Y Loc [ C1_PECH   ]
 3: 243      Z Loc [ C0_C1     ]

160:  Z=X+Y (P33)
 1: 311      X Loc [ C2_X      ]
 2: 312      Y Loc [ C3_X      ]
 3: 244      Z Loc [ C2_C3     ]

161:  Z=X+Y (P33)
 1: 313      X Loc [ C4_X      ]
 2: 314      Y Loc [ C5_X      ]
 3: 245      Z Loc [ C4_C5     ]

162:  Z=X+Y (P33)
 1: 243      X Loc [ C0_C1     ]
 2: 244      Y Loc [ C2_C3     ]
 3: 247      Z Loc [ C0C1C2C3  ]

163:  Z=X+Y (P33)
 1: 247      X Loc [ C0C1C2C3  ]
 2: 246      Y Loc [ C6_C7     ]
 3: 249      Z Loc [ E25TCEppm ]

164:  Z=X+F (P34)
 1: 249      X Loc [ E25TCEppm ]
 2: 0.0      F
 3: 250      Z Loc [ E25_ppm_R ]

165:  If (X<=>F) (P89)
 1: 250      X Loc [ E25_ppm_R ]
 2: 4        <
 3: 5000     F
 4: 30       Then Do

     166:  Z=F x 10^n (P30)
      1: 0.0      F
      2: 00       n, Exponent of 10
      3: 250      Z Loc [ E25_ppm_R ]

167:  End (P95)

168:  If (X<=>F) (P89)
 1: 250      X Loc [ E25_ppm_R ]
 2: 3        >=
 3: 5000     F
 4: 30       Then Do

     169:  Do (P86)
      1: 114      Set Flag 14 High

170:  End (P95)

171:  If (X<=>Y) (P88)
 1: 249      X Loc [ E25TCEppm ]
 2: 3        >=
 3: 307      Y Loc [ MWsTCEppm ]
 4: 30       Then Do

     172:  Z=X (P31)
      1: 307      X Loc [ MWsTCEppm ]
      2: 249      Z Loc [ E25TCEppm ]

173:  End (P95)
```

```
;The following instuctions check the system
for malfunctions

174:  If (X<=>F) (P89)
 1: 99       X Loc [ RTD_Ttype ]
 2: 3        >=
 3: 5        F
 4: 118      Set Flag 18 High ;Upper Limit
Check Temperature

175:  If (X<=>F) (P89)
 1: 99       X Loc [ RTD_Ttype ]
 2: 4        <
 3: -5       F
 4: 118      Set Flag 18 High;Lower Limit
Check Temperature

176:  If (X<=>F) (P89)
 1: 191      X Loc [ E21_TempC ]
 2: 4        <
 3: 24       F
 4: 112      Set Flag 12 High

177:  If (X<=>F) (P89)
 1: 191      X Loc [ E21_TempC ]
 2: 3        >=
 3: 27       F
 4: 112      Set Flag 12 High




178:  If (X<=>F) (P89)
 1: 1        X Loc [ Vbatt     ]
 2: 3        >=
 3: 11.5     F
 4: 217      Set Flag 17 Low

179:  If (X<=>F) (P89)
 1: 1        X Loc [ Vbatt     ]
 2: 4        <
 3: 11.5     F
 4: 117      Set Flag 17 High

;Checks for negative chemiresistor resistances

180:  If (X<=>F) (P89)
 1: 34       X Loc [ E19_PIB   ]
 2: 4        <
 3: 0        F
 4: 116      Set Flag 16 High

181:  If (X<=>F) (P89)
 1: 35       X Loc [ E19_PNVP  ]
 2: 4        <
 3: 0        F
 4: 116      Set Flag 16 High

182:  If (X<=>F) (P89)
 1: 36       X Loc [ E19_PVTD  ]
 2: 4        <
 3: 0        F
 4: 116      Set Flag 16 High

183:  If (X<=>F) (P89)
 1: 37       X Loc [ E19_PEVA  ]
 2: 4        <
 3: 0        F
 4: 116      Set Flag 16 High

184:  If (X<=>F) (P89)
 1: 204      X Loc [ E25_PECH  ]
 2: 4        <
 3: 0        F
 4: 113      Set Flag 13 High

185:  If (X<=>F) (P89)
 1: 205      X Loc [ E25_PNVP  ]
 2: 4        <
 3: 0        F
 4: 113      Set Flag 13 High

186:  If (X<=>F) (P89)
 1: 206      X Loc [ E25_PIB   ]
 2: 4        <
 3: 0        F
 4: 113      Set Flag 13 High

187:  If (X<=>F) (P89)
 1: 207      X Loc [ E25_PEVA  ]
 2: 4        <
 3: 0        F
 4: 113      Set Flag 13 High

;The following instructions give numerical
values to the flags


188:  If Flag/Port (P91)
 1: 112      Do if Flag 12 is High
 2: 30       Then Do

     189:  Z=F x 10^n (P30)
      1: 1        F
      2: 0        n, Exponent of 10
      3: 282      Z Loc [ E21Rtdmal ]

190:  End (P95)

191:  If Flag/Port (P91)
 1: 212      Do if Flag 12 is Low
 2: 30       Then Do

     192:  Z=F x 10^n (P30)
      1: 0        F
      2: 0        n, Exponent of 10
      3: 282      Z Loc [ E21Rtdmal ]

193:  End (P95)

194:  If Flag/Port (P91)
 1: 113      Do if Flag 13 is High
 2: 30       Then Do

     195:  Z=F x 10^n (P30)
      1: 1        F
      2: 0        n, Exponent of 10
      3: 261      Z Loc [ E21negRes ]

196:  End (P95)

197:  If Flag/Port (P91)
 1: 213      Do if Flag 13 is Low
 2: 30       Then Do

     198:  Z=F x 10^n (P30)
      1: 0        F
      2: 0        n, Exponent of 10
      3: 261      Z Loc [ E21negRes ]
```

```
199:  End (P95)

200:  If Flag/Port (P91)
 1: 114      Do if Flag 14 is High
 2: 30       Then Do

     201:  Z=F x 10^n (P30)
      1: 1        F
      2: 0        n, Exponent of 10
      3: 260      Z Loc [ E21tcedet ]

202:  End (P95)

203:  If Flag/Port (P91)
 1: 214      Do if Flag 14 is Low
 2: 30       Then Do

     204:  Z=F x 10^n (P30)
      1: 0        F
      2: 00       n, Exponent of 10
      3: 260      Z Loc [ E21tcedet ]

205:  End (P95)


206:  If Flag/Port (P91)
 1: 115      Do if Flag 15 is High
 2: 30       Then Do

     207:  Z=F x 10^n (P30)
      1: 1        F
      2: 00       n, Exponent of 10
      3: 175      Z Loc [ TCE_detec ]

208:  End (P95)

209:  If Flag/Port (P91)
 1: 215      Do if Flag 15 is Low
 2: 30       Then Do

     210:  Z=F x 10^n (P30)
      1: 0        F
      2: 0        n, Exponent of 10
      3: 175      Z Loc [ TCE_detec ]

211:  End (P95)


212:  If Flag/Port (P91)
 1: 116      Do if Flag 16 is High
 2: 30       Then Do

     213:  Z=F x 10^n (P30)
      1: 1        F
      2: 00       n, Exponent of 10
      3: 112      Z Loc [ negResist ]

214:  End (P95)

215:  If Flag/Port (P91)
 1: 216      Do if Flag 16 is Low
 2: 30       Then Do

     216:  Z=F x 10^n (P30)
      1: 0        F
      2: 0        n, Exponent of 10
      3: 112      Z Loc [ negResist ]

217:  End (P95)

218:  If Flag/Port (P91)
 1: 117      Do if Flag 17 is High
 2: 30       Then Do

     219:  Z=F x 10^n (P30)
      1: 1        F
      2: 00       n, Exponent of 10
      3: 113      Z Loc [ lowB_Volt ]

220:  End (P95)

221:  If Flag/Port (P91)
 1: 217      Do if Flag 17 is Low
 2: 30       Then Do

     222:  Z=F x 10^n (P30)
      1: 0        F
      2: 0        n, Exponent of 10
      3: 113      Z Loc [ lowB_Volt ]

223:  End (P95)

224:  If Flag/Port (P91)
 1: 118      Do if Flag 18 is High
 2: 30       Then Do

     225:  Z=F x 10^n (P30)
      1: 1        F
      2: 0        n, Exponent of 10
      3: 114      Z Loc [ Temp_Malf ]

226:  End (P95)

227:  If Flag/Port (P91)
 1: 218      Do if Flag 18 is Low
 2: 30       Then Do

     228:  Z=F x 10^n (P30)
      1: 0        F
      2: 00       n, Exponent of 10
      3: 114      Z Loc [ Temp_Malf ]

229:  End (P95)



;The following instructions turn the cell
phone on and off

230:  If time is (P92)
 1: 0        Minutes (Seconds --) into a
 2: 60       Interval (same units as above)
 3: 41       Set Port 1 High

231:  If time is (P92)
 1: 30       Minutes (Seconds --) into a
 2: 60       Interval (same units as above)
 3: 51       Set Port 1 Low


;The following instructions set the output
flag high and samples the desired data

232:  If time is (P92)
 1: 0        Minutes (Seconds --) into a
 2: 60       Interval (same units as above)
 3: 10       Set Output Flag High (Flag 0)

233:  Set Active Storage Area (P80)^16339
 1: 1        Final Storage Area 1
 2: 340      Array ID
```

```
234:  Resolution (P78)
 1: 01       High Resolution

235:  Real Time (P77)^29312
 1: 1220     Year,Day,Hour/Minute (midnight =
2400)

236:  Sample (P70)^20270
 1: 4        Reps
 2: 34       Loc [ E19_PIB   ]

237:  Sample (P70)^5399
 1: 1        Reps
 2: 31       Loc [ RTDohms   ]

238:  Sample (P70)^12677
 1: 1        Reps
 2: 32       Loc [ RTDTempC  ]

239:  Sample (P70)^27880
 1: 1        Reps
 2: 132      Loc [ TCE_ppm   ]

240:  Sample (P70)^17767
 1: 1        Reps
 2: 174      Loc [ TCE_ppmR  ]

241:  Sample (P70)^22622
 1: 1        Reps
 2: 251      Loc [ T_Type_D3 ]

242:  Sample (P70)^3217
 1: 1        Reps
 2: 131      Loc [ Vp_Ambien ]

243:  Sample (P70)^19800
 1: 3        Reps
 2: 13       Loc [ HX94Temp  ]

244:  Sample (P70)^7443
 1: 1        Reps
 2: 6        Loc [ T_ref     ]

245:  Sample (P70)^25702
 1: 1        Reps
 2: 1        Loc [ Vbatt     ]

246:  Sample (P70)^20607
 1: 1        Reps
 2: 28       Loc [ HEAD_FT   ]

247:  Sample (P70)^26641
 1: 1        Reps
 2: 30       Loc [ PSIG_CS40 ]

248:  Sample (P70)^13752
 1: 3        Reps
 2: 112      Loc [ negResist ]

249:  Sample (P70)^1084
 1: 1        Reps
 2: 175      Loc [ TCE_detec ]

250:  Sample (P70)^25590
 1: 4        Reps
 2: 204      Loc [ E25_PECH  ]

251:  Sample (P70)^5416
 1: 1        Reps
 2: 185      Loc [ E21RTDohm ]

252:  Sample (P70)^5298
 1: 1        Reps
 2: 191      Loc [ E21_TempC ]

253:  Sample (P70)^17648
 1: 1        Reps
 2: 249      Loc [ E25TCEppm ]

254:  Sample (P70)^24801
 1: 1        Reps
 2: 250      Loc [ E25_ppm_R ]

255:  Sample (P70)^15517
 1: 1        Reps
 2: 252      Loc [ T_TypeMW2 ]

256:  Sample (P70)^23308
 1: 5        Reps
 2: 253      Loc [ PX215_Pa  ]

257:  Sample (P70)^22319
 1: 2        Reps
 2: 260      Loc [ E21tcedet ]

258:  Sample (P70)^15481
 1: 1        Reps
 2: 11       Loc [ HeatBarV  ]

259:  Sample (P70)^19766
 1: 1        Reps
 2: 282      Loc [ E21Rtdmal ]

260:  Sample (P70)^21370
 1: 2        Reps
 2: 284      Loc [ SolarVolt ]

261:  Sample (P70)^12331
 1: 1        Reps
 2: 304      Loc [ D3sTCEppm ]

262:  Sample (P70)^6967
 1: 1        Reps
 2: 307      Loc [ MWsTCEppm ]



*Table 2 Program
  02: 2         Execution Interval (seconds)

;The following program calculates the water
vapor corrected baseline for E19

1:  If time is (P92)
 1: 0        Minutes (Seconds --) into a
 2: 1440     Interval (same units as above)
 3: 30       Then Do

     2:  Z=Z+1 (P32)
      1: 38       Z Loc [ Counter   ]

     3:  If (X<=>F) (P89)
      1: 38       X Loc [ Counter   ]
      2: 3        >=
      3: 7        F
      4: 211      Set Flag 11 Low

4:  End (P95)
```

```
;The following instructions calculate a
countdown to next baseline


5:  Z=X+F (P34)
 1: 38       X Loc [ Counter   ]
 2: -7       F
 3: 300      Z Loc [ DaysTillB ]

6:  Z=X*F (P37)
 1: 300      X Loc [ DaysTillB ]
 2: -1       F
 3: 300      Z Loc [ DaysTillB ]


7:  If Flag/Port (P91)
 1: 211      Do if Flag 11 is Low
 2: 30       Then Do

     8:  Beginning of Loop (P87)
      1: 1        Delay
      2: 60       Loop Count

          9:  Do (P86)
           1: 1        Call Subroutine 1

          10:  Z=F x 10^n (P30)
           1: 0        F
           2: 0        n, Exponent of 10
           3: 38       Z Loc [ Counter   ]

          11:  Excite-Delay (SE) (P4)
           1: 1        Reps
           2: 15       5000 mV, Fast Range
           3: 1        SE Channel
           4: 1        Excite all reps
w/Exchan 1
           5: 0        Delay (0.01 sec units)
           6: 5000     mV Excitation
           7: 63       Loc [ PIB_Base  ]
           8: .0002    Mult
           9: 0.0      Offset

          12:  BR Transform Rf[X/(1-X)] (P59)
           1: 1        Reps
           2: 63       Loc [ PIB_Base  ]
           3: 132.41   Multiplier (Rf)

          13:  Excite-Delay (SE) (P4)
           1: 1        Reps
           2: 15       5000 mV, Fast Range
           3: 2        SE Channel
           4: 1        Excite all reps
w/Exchan 1
           5: 0        Delay (0.01 sec units)
           6: 5000     mV Excitation
           7: 64       Loc [ PNVP_base ]
           8: .0002    Mult
           9: 0.0      Offset

          14:  BR Transform Rf[X/(1-X)] (P59)
           1: 1        Reps
           2: 64       Loc [ PNVP_base ]
           3: 149.70   Multiplier (Rf)

          15:  Excite-Delay (SE) (P4)
           1: 1        Reps
           2: 15       5000 mV, Fast Range
           3: 3        SE Channel
           4: 1        Excite all reps
w/Exchan 1
           5: 0        Delay (0.01 sec units)
           6: 5000     mV Excitation
           7: 65       Loc [ PVTD_base ]
           8: .0002    Mult
           9: 0.0      Offset

          16:  BR Transform Rf[X/(1-X)] (P59)
           1: 1        Reps
           2: 65       Loc [ PVTD_base ]
           3: 299.31   Multiplier (Rf)

          17:  Excite-Delay (SE) (P4)
           1: 1        Reps
           2: 15       5000 mV, Fast Range
           3: 4        SE Channel
           4: 1        Excite all reps
w/Exchan 1
           5: 0        Delay (0.01 sec units)
           6: 5000     mV Excitation
           7: 66       Loc [ PEVA_base ]
           8: .0002    Mult
           9: 0.0      Offset

          18:  BR Transform Rf[X/(1-X)] (P59)
           1: 1        Reps
           2: 66       Loc [ PEVA_base ]
           3: 199.25   Multiplier (Rf)

          ;The following instructions read E21

          19:  Excite-Delay (SE) (P4)
           1: 1        Reps
           2: 15       5000 mV, Fast Range
           3: 13       SE Channel
           4: 2        Excite all reps
w/Exchan 2
           5: 1        Delay (0.01 sec units)
           6: 5000     mV Excitation
           7: 278      Loc [ BlPibE21  ]
           8: .0002    Mult
           9: 0.0      Offset

          20:  BR Transform Rf[X/(1-X)] (P59)
           1: 1        Reps
           2: 278      Loc [ BlPibE21  ]
           3: 199.60   Multiplier (Rf)

          21:  Excite-Delay (SE) (P4)
           1: 1        Reps
           2: 15       5000 mV, Fast Range
           3: 14       SE Channel
           4: 2        Excite all reps
w/Exchan 2
           5: 1        Delay (0.01 sec units)
           6: 5000     mV Excitation
           7: 279      Loc [ BlPnvpE21 ]
           8: .0002    Mult
           9: 0.0      Offset

          22:  BR Transform Rf[X/(1-X)] (P59)
           1: 1        Reps
           2: 279      Loc [ BlPnvpE21 ]
           3: 199.00   Multiplier (Rf)

          23:  Excite-Delay (SE) (P4)
           1: 1        Reps
           2: 15       5000 mV, Fast Range
           3: 15       SE Channel
           4: 2        Excite all reps
w/Exchan 2
           5: 1        Delay (0.01 sec units)
```

```
 6: 5000     mV Excitation
 7: 280      Loc [ BlPvtdE21 ]
 8: .0002    Mult
 9: 0.0      Offset

24:  BR Transform Rf[X/(1-X)] (P59)
 1: 1        Reps
 2: 280      Loc [ BlPvtdE21 ]
 3: 214.92   Multiplier (Rf)

25:  Excite-Delay (SE) (P4)
 1: 1        Reps
 2: 15       5000 mV, Fast Range
 3: 16       SE Channel
 4: 2        Excite all reps
w/Exchan 2
 5: 1        Delay (0.01 sec units)
 6: 5000     mV Excitation
 7: 281      Loc [ BlPevaE21 ]
 8: .0002    Mult
 9: 0.0      Offset

26:  BR Transform Rf[X/(1-X)] (P59)
 1: 1        Reps
 2: 281      Loc [ BlPevaE21 ]
 3: 174.03   Multiplier (Rf)

;Multiplexer instructions to read the
temperature of well D3

27:  Temp (107) (P11)
 1: 1        Reps
 2: 21       SE Channel
 3: 4        Excite all reps w/E4
 4: 299      Loc [ T_RefB    ]
 5: 1.0      Mult
 6: 0.0      Offset

28:  Do (P86)
 1: 42       Set Port 2 High

29:  Beginning of Loop (P87)
 1: 0        Delay
 2: 1        Loop Count

     30:  Do (P86)
      1: 73       Pulse Port 3

     31:  Delay w/Opt Excitation
(P22)
      1: 1        Ex Channel
      2: 0        Delay W/Ex (0.01
sec units)
      3: 1        Delay After Ex
(0.01 sec units)
      4: 0        mV Excitation

     32:  Thermocouple Temp (DIFF)
(P14)
      1: 1        Reps
      2: 21       10 mV, 60 Hz
Reject, Slow Range
      3: 12       DIFF Channel
      4: 1        Type T (Copper-
Constantan)
      5: 299      Ref Temp (Deg. C)
Loc [ T_RefB    ]
      6: 179   -- Loc [ T_TypeD3V ]
      7: 1.0      Mult
      8: 0.0      Offset

33:  End (P95)

34:  Do (P86)
 1: 52       Set Port 2 Low

35:  Volt (SE) (P1)
 1: 1        Reps
 2: 25       5000 mV, 60 Hz Reject,
Fast Range (same as code 45)
 3: 22       SE Channel
 4: 100      Loc [ RHVoltVp  ]
 5: 1        Mult
 6: 0.0      Offset

36:  Do (P86)
 1: 1        Call Subroutine 1

37:  Z=X/Y (P38)
 1: 100      X Loc [ RHVoltVp  ]
 2: 118      Y Loc [ RhRefR    ]
 3: 133      Z Loc [ RhVpAmps  ]

38:  Z=X+F (P34)
 1: 133      X Loc [ RhVpAmps  ]
 2: -4       F
 3: 134      Z Loc [ RhVpAmMin ]

39:  Z=X*F (P37)
 1: 134      X Loc [ RhVpAmMin ]
 2: 6.25     F
 3: 101      Z Loc [ HX94RhVp  ]

40:  If (X<=>F) (P89)
 1: 101      X Loc [ HX94RhVp  ]
 2: 3        >=
 3: 100      F
 4: 30       Then Do

     41:  Z=F x 10^n (P30)
      1: 100      F
      2: 00       n, Exponent of 10
      3: 101      Z Loc [ HX94RhVp
]

42:  End (P95)

43:  If (X<=>F) (P89)
 1: 101      X Loc [ HX94RhVp  ]
 2: 4        <
 3: 0        F
 4: 30       Then Do

     44:  Z=F x 10^n (P30)
      1: 0        F
      2: 0        n, Exponent of 10
      3: 101      Z Loc [ HX94RhVp
]

45:  End (P95)

46:  Running Average (P52)
 1: 4        Reps
 2: 63       First Source Loc [
PIB_Base  ]
 3: 67       First Destination Loc [
PIB_AVG   ]
 4: 60       Number of Values in Avg
Window

47:  Running Average (P52)
 1: 1        Reps
```

```
           2: 101      First Source Loc [
HX94RhVp  ]
           3: 102      First Destination Loc [
RhVpavg   ]
           4: 60       Number of Values in Avg
Window

          48:  Running Average (P52)
           1: 1        Reps
           2: 179      First Source Loc [
T_TypeD3V ]
           3: 180      First Destination Loc [
T_TypeD3A ]
           4: 60       Number of Values in Avg
Window

          49:  Running Average (P52)
           1: 4        Reps
           2: 278      First Source Loc [
BlPibE21  ]
           3: 209      First Destination Loc [
BlE25PECH ]
           4: 60       Number of Values in Avg
Window

     50:  End (P95)

     51:  Z=X*F (P37)
      1: 102      X Loc [ RhVpavg   ]
      2: .01      F
      3: 103      Z Loc [ RhVpavgM  ]

     52:  Saturation Vapor Pressure (P56)
      1: 180      Temperature Loc [ T_TypeD3A
]
      2: 74       Loc [ VPKPaCamp ]

     53:  Z=X*F (P37)
      1: 74       X Loc [ VPKPaCamp ]
      2: 1000     F
      3: 73       Z Loc [ VP_PaCamp ]

     54:  Z=X*Y (P36)
      1: 73       X Loc [ VP_PaCamp ]
      2: 103      Y Loc [ RhVpavgM  ]
      3: 72       Z Loc [ VP_Pa     ]

     55:  Do (P86)
      1: 2        Call Subroutine 2

     56:  Z=X^Y (P47)
      1: 72       X Loc [ VP_Pa     ]
      2: 75       Y Loc [ PIBVpExp  ]
      3: 79       Z Loc [ VPxPIB    ]

     57:  Z=X^Y (P47)
      1: 72       X Loc [ VP_Pa     ]
      2: 76       Y Loc [ PNVPVpExp ]
      3: 80       Z Loc [ VPxPNVP   ]

     58:  Z=X^Y (P47)
      1: 72       X Loc [ VP_Pa     ]
      2: 78       Y Loc [ PVTDVpExp ]
      3: 81       Z Loc [ VPxPVTD   ]

     59:  Z=X^Y (P47)
      1: 72       X Loc [ VP_Pa     ]
      2: 77       Y Loc [ PEVAVpExp ]
      3: 82       Z Loc [ VPxPEVA   ]

     60:  Z=X*Y (P36)
      1: 79       X Loc [ VPxPIB    ]
      2: 83       Y Loc [ PIB_mult  ]
      3: 87       Z Loc [ VP_Pib    ]

     61:  Z=X*Y (P36)
      1: 80       X Loc [ VPxPNVP   ]
      2: 84       Y Loc [ PNVP_mult ]
      3: 88       Z Loc [ VP_Pnvp   ]

     62:  Z=X*Y (P36)
      1: 81       X Loc [ VPxPVTD   ]
      2: 85       Y Loc [ PVTD_mult ]
      3: 89       Z Loc [ Vp_Pvtd   ]

     63:  Z=X*Y (P36)
      1: 82       X Loc [ VPxPEVA   ]
      2: 86       Y Loc [ PEVA_mult ]
      3: 90       Z Loc [ Vp_Peva   ]

     64:  Z=X+F (P34)
      1: 87       X Loc [ VP_Pib    ]
      2: 1        F
      3: 91       Z Loc [ VP_PibDen ]

     65:  Z=X+F (P34)
      1: 88       X Loc [ VP_Pnvp   ]
      2: 1        F
      3: 92       Z Loc [ VP_PnvpDe ]

     66:  Z=X+F (P34)
      1: 89       X Loc [ Vp_Pvtd   ]
      2: 1        F
      3: 93       Z Loc [ Vp_PvtdDe ]

     67:  Z=X+F (P34)
      1: 90       X Loc [ Vp_Peva   ]
      2: 1        F
      3: 94       Z Loc [ Vp_PevaDe ]

     68:  Z=X/Y (P38)
      1: 67       X Loc [ PIB_AVG   ]
      2: 91       Y Loc [ VP_PibDen ]
      3: 135      Z Loc [ b_PIB_Vp  ]

     69:  Z=X/Y (P38)
      1: 68       X Loc [ PNVP_AVG  ]
      2: 92       Y Loc [ VP_PnvpDe ]
      3: 136      Z Loc [ b_PNVP_Vp ]

     70:  Z=X/Y (P38)
      1: 69       X Loc [ PVTD_AVG  ]
      2: 93       Y Loc [ Vp_PvtdDe ]
      3: 137      Z Loc [ b_PVTD_Vp ]

     71:  Z=X/Y (P38)
      1: 70       X Loc [ PEVA_AVG  ]
      2: 94       Y Loc [ Vp_PevaDe ]
      3: 138      Z Loc [ b_PEVA_Vp ]

;The following instructions correct for
temperature

     72:  Z=X+F (P34)
      1: 149      X Loc [ T_TypeVpA ]
      2: -8.83    F
      3: 139      Z Loc [ DeltaTcor ]

     73:  Do (P86)
      1: 4        Call Subroutine 4

     74:  Z=X*Y (P36)
```

```
 1: 139      X Loc [ DeltaTcor ]
 2: 140      Y Loc [ PIB_m     ]
 3: 144      Z Loc [ PIBmXDelt ]

75:  Z=X*Y (P36)
 1: 139      X Loc [ DeltaTcor ]
 2: 141      Y Loc [ PNVP_m    ]
 3: 145      Z Loc [ PnpvmXDel ]

76:  Z=X*Y (P36)
 1: 139      X Loc [ DeltaTcor ]
 2: 142      Y Loc [ PVTD_m    ]
 3: 146      Z Loc [ PvtdmXDel ]

77:  Z=X*Y (P36)
 1: 139      X Loc [ DeltaTcor ]
 2: 143      Y Loc [ PEVA_m    ]
 3: 147      Z Loc [ PevamXDel ]

78:  Z=X-Y (P35)
 1: 135      X Loc [ b_PIB_Vp  ]
 2: 144      Y Loc [ PIBmXDelt ]
 3: 95       Z Loc [ base_PIB  ]

79:  Z=X-Y (P35)
 1: 136      X Loc [ b_PNVP_Vp ]
 2: 145      Y Loc [ PnpvmXDel ]
 3: 96       Z Loc [ base_PNVP ]

80:  Z=X-Y (P35)
 1: 137      X Loc [ b_PVTD_Vp ]
 2: 146      Y Loc [ PvtdmXDel ]
 3: 97       Z Loc [ base_PVTD ]

81:  Z=X-Y (P35)
 1: 138      X Loc [ b_PEVA_Vp ]
 2: 147      Y Loc [ PevamXDel ]
 3: 98       Z Loc [ base_PEVA ]

82:  Do (P86)
 1: 111      Set Flag 11 High


83:  End (P95)

84:  If time is (P92)
 1: 5        Minutes (Seconds --) into a
 2: 1440     Interval (same units as above)
 3: 10       Set Output Flag High (Flag 0)

85:  Set Active Storage Area (P80)^29708
 1: 1        Final Storage Area 1
 2: 440      Array ID

86:  Resolution (P78)
 1: 01       High Resolution

87:  Real Time (P77)^8875
 1: 1220     Year,Day,Hour/Minute (midnight =
2400)

88:  Sample (P70)^19257
 1: 4        Reps
 2: 95       Loc [ base_PIB  ]

89:  Sample (P70)^21890
 1: 4        Reps
 2: 209      Loc [ BlE25PECH ]

90:  Sample (P70)^12750
 1: 1        Reps
 2: 300      Loc [ DaysTillB ]

91:  Sample (P70)^6118
 1: 1        Reps
 2: 38       Loc [ Counter   ]


*Table 3 Subroutines

1:  Beginning of Subroutine (P85)
 1: 1        Subroutine 1

     2:  Z=F x 10^n (P30)
      1: 236.83   F
      2: 00       n, Exponent of 10
      3: 115      Z Loc [ TempRefR  ]

     3:  Z=F x 10^n (P30)
      1: 236.44   F
      2: 00       n, Exponent of 10
      3: 118      Z Loc [ RhRefR    ]

     4:  Z=F x 10^n (P30)
      1: 236.83   F
      2: 00       n, Exponent of 10
      3: 286      Z Loc [ PSIRefR   ]

     5:  Z=F x 10^n (P30)
      1: 511.76   F
      2: 00       n, Exponent of 10
      3: 258      Z Loc [ D_PressFt ]

     6:  Z=F x 10^n (P30)
      1: 13.4     F
      2: 00       n, Exponent of 10
      3: 259      Z Loc [ D_ChemiFt ]

7:  End (P95)

8:  Beginning of Subroutine (P85)
 1: 2        Subroutine 2
;The following are exponents for the Vapor
Pressure calibration of VP vs Delta R/Rb

     9:  Z=F x 10^n (P30)
      1: .9584    F
      2: 00       n, Exponent of 10
      3: 75       Z Loc [ PIBVpExp  ]

     10:  Z=F x 10^n (P30)
      1: 1.7798   F
      2: 00       n, Exponent of 10
      3: 76       Z Loc [ PNVPVpExp ]

     11:  Z=F x 10^n (P30)
      1: 1.1034   F
      2: 00       n, Exponent of 10
      3: 78       Z Loc [ PVTDVpExp ]

     12:  Z=F x 10^n (P30)
      1: 1.3308   F
      2: 0        n, Exponent of 10
      3: 77       Z Loc [ PEVAVpExp ]
;The following fixed values are multipliers
for the Vapor Pressure calibration of VP vs
Delta R/Rb

     13:  Z=F x 10^n (P30)
      1: 3        F
      2: -6       n, Exponent of 10
      3: 83       Z Loc [ PIB_mult  ]
```

```
     14:  Z=F x 10^n (P30)
      1: 6        F
      2: -7       n, Exponent of 10
      3: 84       Z Loc [ PNVP_mult ]

     15:  Z=F x 10^n (P30)
      1: 3        F
      2: -6       n, Exponent of 10
      3: 85       Z Loc [ PVTD_mult ]

     16:  Z=F x 10^n (P30)
      1: 4        F
      2: -7       n, Exponent of 10
      3: 86       Z Loc [ PEVA_mult ]

17:  End (P95)

18:  Beginning of Subroutine (P85)
 1: 3        Subroutine 3
;The following values are for the ppm
concentration prediction

     19:  Z=F x 10^n (P30)
      1: 2256.86  F
      2: 0        n, Exponent of 10
      3: 121      Z Loc [ B0        ]

     20:  Z=F x 10^n (P30)
      1: 219.123  F
      2: 0        n, Exponent of 10
      3: 122      Z Loc [ B1        ]

     21:  Z=F x 10^n (P30)
      1: 3.8234   F
      2: 5        n, Exponent of 10
      3: 123      Z Loc [ B2        ]

     22:  Z=F x 10^n (P30)
      1: 2395.25  F
      2: 0        n, Exponent of 10
      3: 124      Z Loc [ B3        ]

     23:  Z=F x 10^n (P30)
      1: 1430.62  F
      2: 0        n, Exponent of 10
      3: 125      Z Loc [ B4        ]

     24:  Z=F x 10^n (P30)
      1: 29.88    F
      2: 00       n, Exponent of 10
      3: 126      Z Loc [ B5        ]

     25:  Z=F x 10^n (P30)
      1: 47466    F
      2: 0        n, Exponent of 10
      3: 127      Z Loc [ B6        ]

     26:  Z=F x 10^n (P30)
      1: 8068     F
      2: 00       n, Exponent of 10
      3: 151      Z Loc [ B7        ]

27:  End (P95)

28:  Beginning of Subroutine (P85)
 1: 4        Subroutine 4
;Slopes of the polymers temperature dependence
     29:  Z=F x 10^n (P30)
      1: .2279    F
      2: 00       n, Exponent of 10
      3: 140      Z Loc [ PIB_m     ]

     30:  Z=F x 10^n (P30)
      1: .167     F
      2: 00       n, Exponent of 10
      3: 141      Z Loc [ PNVP_m    ]

     31:  Z=F x 10^n (P30)
      1: .3871    F
      2: 00       n, Exponent of 10
      3: 142      Z Loc [ PVTD_m    ]

     32:  Z=F x 10^n (P30)
      1: .624     F
      2: 00       n, Exponent of 10
      3: 143      Z Loc [ PEVA_m    ]

33:  End (P95)

34:  Beginning of Subroutine (P85)
 1: 5        Subroutine 5
;Constants for the TCE model of E21

     35:  Z=F x 10^n (P30)
      1: -3.4468  F
      2: 0        n, Exponent of 10
      3: 221      Z Loc [ C0        ]

     36:  Z=F x 10^n (P30)
      1: 1.5566   F
      2: 5        n, Exponent of 10
      3: 222      Z Loc [ C1        ]

     37:  Z=F x 10^n (P30)
      1: 3.8221   F
      2: 7        n, Exponent of 10
      3: 223      Z Loc [ C2        ]

     38:  Z=F x 10^n (P30)
      1: -1.8800  F
      2: 6        n, Exponent of 10
      3: 224      Z Loc [ C3        ]

     39:  Z=F x 10^n (P30)
      1: 5.7900   F
      2: 5        n, Exponent of 10
      3: 225      Z Loc [ C4        ]

     40:  Z=F x 10^n (P30)
      1: 4.6246   F
      2: 7        n, Exponent of 10
      3: 226      Z Loc [ C5        ]

41:  End (P95)

End Program

-Input Locations-
1 Vbatt     1 3 1
2 Sen_1_mVm 1 0 0
3 Sen_2_mVm 1 0 0
4 Sen_3_mVm 1 0 0
5 Sen_4_mVm 1 0 0
6 T_ref     1 2 1
7 T_type    1 0 0
8 TempVolts 1 0 0
9 RHVolts   1 1 1
10 PSIVolts  7 1 1
11 HeatBarV  19 2 1
12 PSIamps   1 1 1
13 HX94Temp  1 1 0
```

```
14 HX92RH    1 4 3
15 PX215_PSI 1 2 1
16 PSIVoltM  1 1 1
17 Res_1_mVc 1 0 0
18 Res_2_mVc 1 0 0
19 Res_3_mVc 1 0 0
20 Res_4_mVc 1 0 0
21 uA_1c     1 0 0
22 uA_2c     1 0 0
23 uA_3c     1 0 0
24 uA_4c     1 0 0
25 MA_MEAS   1 1 1
26 mv_ma     1 1 1
27 MV        1 2 1
28 HEAD_FT   1 4 2
29 MV_Minus  1 1 1
30 PSIG_CS40 1 1 1
31 RTDohms   1 2 1
32 RTDTempC  1 2 1
33 RTDTempM  1 1 1
34 E19_PIB   1 4 2
35 E19_PNVP  1 4 2
36 E19_PVTD  1 4 2
37 E19_PEVA  1 4 2
38 Counter   1 3 2
39 PECH_Br   1 0 0
40 PNVP_Br   1 0 0
41 PVTD_Br   1 0 0
42 PEVA_Br   1 0 0
43 Ref1_ohm  1 0 0
44 Ref2_ohm  1 0 0
45 Ref3_ohm  1 0 0
46 Ref4_ohm  1 0 0
47 negohms1  1 0 0
48 negohms2  1 0 0
49 negohms3  1 0 0
50 negohms4  1 0 0
51 PIB_Bmv   1 0 0
52 PNVP_Bmv  1 0 0
53 PVTD_Bmv  1 0 0
54 PEVA_Bmv  1 0 0
55 PIB_uA    1 0 0
56 PNVP_uA   1 0 0
57 PVTD_uA   1 0 0
58 PEVA_uA   1 0 0
59 negPIBb   1 0 0
60 negPNVPb  1 0 0
61 negPVTDPb 1 0 0
62 negPEVAb  1 0 0
63 PIB_Base  1 2 2
64 PNVP_base 1 2 2
65 PVTD_base 1 2 2
66 PEVA_base 1 2 2
67 PIB_AVG   5 1 1
68 PNVP_AVG  9 1 1
69 PVTD_AVG  9 1 1
70 PEVA_AVG  17 1 1
71 RTDTempVP 1 0 0
72 VP_Pa     1 4 1
73 VP_PaCamp 1 1 1
74 VPKPaCamp 1 1 1
75 PIBVpExp  1 1 1
76 PNVPVpExp 1 1 1
77 PEVAVpExp 1 1 1
78 PVTDVpExp 1 1 1
79 VPxPIB    1 1 1
80 VPxPNVP   1 1 1
81 VPxPVTD   1 1 1
82 VPxPEVA   1 1 1
83 PIB_mult  1 1 1
84 PNVP_mult 1 1 1
85 PVTD_mult 1 1 1
86 PEVA_mult 1 1 1
87 VP_Pib    1 1 1
88 VP_Pnvp   1 1 1
89 Vp_Pvtd   1 1 1
90 Vp_Peva   1 1 1
91 VP_PibDen 1 1 1
92 VP_PnvpDe 1 1 1
93 Vp_PvtdDe 1 1 1
94 Vp_PevaDe 1 1 1
95 base_PIB  1 4 1
96 base_PNVP 1 3 1
97 base_PVTD 1 3 1
98 base_PEVA 1 3 1
99 RTD_Ttype 1 2 1
100 RHVoltVp  1 1 1
101 HX94RhVp  1 3 3
102 RhVpavg   1 1 1
103 RhVpavgM  1 1 1
104 NumPIB    1 1 1
105 deltaPIB  1 2 1
106 NumPNVP   1 1 1
107 deltaPNVP 1 2 1
108 NumPVTD   1 1 1
109 deltaPVTD 1 3 1
110 NumPEVA   1 1 1
111 deltaPEVA 1 3 1
112 negResist 1 1 2
113 lowB_Volt 1 1 2
114 Temp_Malf 1 1 2
115 TempRefR  1 0 1
116 TempAmps  1 0 0
117 TAmps_Min 1 0 0
118 RhRefR    1 2 1
119 RhmAmps   1 1 1
120 RhAmps_mi 1 1 1
121 B0        1 1 1
122 B1        1 1 1
123 B2        1 1 1
124 B3        1 1 1
125 B4        1 1 1
126 B5        1 1 1
127 B6        1 1 1
128 SatVpKpa  1 1 1
129 SatVpPa   1 1 1
130 HX92Rh001 1 1 1
131 Vp_Ambien 1 2 1
132 TCE_ppm   1 3 2
133 RhVpAmps  1 1 1
134 RhVpAmMin 1 1 1
135 b_PIB_Vp  1 1 1
136 b_PNVP_Vp 1 1 1
137 b_PVTD_Vp 1 1 1
138 b_PEVA_Vp 1 1 1
139 DeltaTcor 1 4 1
140 PIB_m     1 1 1
141 PNVP_m    1 1 1
142 PVTD_m    1 1 1
143 PEVA_m    1 1 1
144 PIBmXDelt 1 1 1
145 PnpvmXDel 1 1 1
146 PvtdmXDel 1 1 1
147 PevamXDel 1 1 1
148 T_typeVp  1 0 0
149 T_TypeVpA 1 1 0
150 TrefVp    1 0 0
151 B7        1 1 1
152 B2PNVP    1 1 1
153 B3PVTD    1 1 1
154 B4PEVA    1 1 1
155 B5PVTD    1 1 1
```

```
156 b6PIB     1 1 1
157 b6PIBPNVP 1 1 1
158 B7PIB     1 1 1
159 B7PIBPVTD 1 1 1
160 B7PibPPEV 1 1 1
161 B1X       1 1 1
162 B2X       1 1 1
163 B3X       1 1 1
164 B4X       1 1 1
165 B5X       1 1 1
166 B6X       1 1 1
167 B7X       1 1 1
168 B4X_B5Xa  1 1 1
169 B0_B1     1 1 1
170 B2_B3     1 1 1
171 B4_B5_B6  1 1 1
172 B4B5B6B7  1 1 1
173 B0B1B2B3  1 1 1
174 TCE_ppmR  1 3 2
175 TCE_detec 1 1 2
176 TempVoltV 1 0 0
177 TempAmpsV 1 0 0
178 TAmpsMinV 1 0 0
179 T_TypeD3V 1 1 1
180 T_TypeD3A 1 1 1
181 E21_1_mVm 1 0 0
182 E21_2_mVm 1 0 0
183 E21_3_mVm 1 0 0
184 E21_4_mVm 1 0 0
185 E21RTDohm 1 2 1
186 E21Ref1oh 1 0 0
187 E21Ref2oh 1 0 0
188 E21Ref3oh 1 0 0
189 E21Ref4oh 1 0 0
190 E21RTD_M  1 1 1
191 E21_TempC 1 3 1
192 E21Res1mC 1 0 0
193 E21Res2mC 1 0 0
194 E21Res3mC 1 0 0
195 E21Res4mC 1 0 0
196 E21uA_1c  1 0 0
197 E21uA_2c  1 0 0
198 E21uA_3c  1 0 0
199 E21uA_4c  1 0 0
200 E21negoh1 1 0 0
201 E21negoh2 1 0 0
202 E21negoh3 1 0 0
203 E21negoh4 1 0 0
204 E25_PECH  1 4 2
205 E25_PNVP  1 4 2
206 E25_PIB   1 4 2
207 E25_PEVA  1 4 2
208 baseE21PI 1 0 0
209 BlE25PECH 5 4 1
210 BlE25PNVP 9 4 1
211 BlE25PIB  9 4 1
212 BlE25PEVA 17 4 1
213 nE25PECH  1 1 1
214 nE25PNVP  1 1 1
215 nE25PIB   1 1 1
216 nE25PEVA  1 1 1
217 E25DPECH  1 3 1
218 E25DPNVP  1 1 1
219 E25DPIB   1 2 1
220 E25DPEVA  1 3 1
221 C0        1 1 1
222 C1        1 1 1
223 C2        1 1 1
224 C3        1 1 1
225 C4        1 1 1
226 C5        1 1 1
227 C6        1 0 0
228 C7        1 0 0
229 C1xPVTD   1 0 0
230 C2xPEVA   1 0 0
231 PNVPxPVTD 1 0 0
232 C3xPoly   1 0 0
233 PNVPxPEVA 1 0 0
234 C4xPoly   1 0 0
235 PVTDxPEVA 1 0 0
236 C5xPoly   1 0 0
237 PIBxPNVP  1 0 0
238 PibPVTDPN 1 0 0
239 C6xPoly   1 0 0
240 PIBPNPVPV 1 0 0
241 PBPNPVPEV 1 0 0
242 C7xPoly   1 0 0
243 C0_C1     1 1 1
244 C2_C3     1 1 1
245 C4_C5     1 0 1
246 C6_C7     1 1 0
247 C0C1C2C3  1 1 1
248 C4C5C6C7  1 0 0
249 E25TCEppm 1 3 2
250 E25_ppm_R 1 3 2
251 T_Type_D3 7 9 1
252 T_TypeMW2 19 2 0
253 PX215_Pa  1 3 1
254 D_GW_ft   1 2 1
255 D_GW_m    1 1 1
256 Hh2oE20ft 1 2 1
257 Hh20E20m  1 1 1
258 D_PressFt 1 1 1
259 D_ChemiFt 1 1 1
260 E21tcedet 1 1 2
261 E21negRes 1 1 2
262 E21_1_mVb 1 0 0
263 E21_2_mVb 1 0 0
264 E21_3_mVb 1 0 0
265 E21_4_mVb 1 0 0
266 E21Res1mV 1 0 0
267 E21Res2mV 1 0 0
268 E21Res3mV 1 0 0
269 E21Res4mV 1 0 0
270 E21_1uAb  1 0 0
271 E21_2uAb  1 0 0
272 E21_3uAb  1 0 0
273 E21_4uAb  1 0 0
274 E21PIBneg 1 0 0
275 E21PNVPne 1 0 0
276 E21PVTDne 1 0 0
277 E21PEVAne 1 0 0
278 BlPibE21  1 2 2
279 BlPnvpE21 1 2 2
280 BlPvtdE21 1 2 2
281 BlPevaE21 1 2 2
282 E21Rtdmal 1 1 2
283 SolarVolD 1 1 1
284 SolarVolt 1 2 1
285 SolarWatt 1 0 1
286 PSIRefR   1 1 1
287 dPIBxdPVN 1 0 0
288 dPECHxdPE 1 1 1
289 dPIBxdPEV 1 1 1
290 MdPolymer 1 0 0
291 C1_PIB    1 0 0
292 C2_PVTD   1 0 0
293 C3_PIBPNV 1 0 0
294 C4_PIBPEV 1 0 0
295 C5_PVTDPE 1 0 0
296 C6_poly   1 0 0
297 C4_C5_C6  1 0 0
```

```
298 C4C5C6    1 0 0
299 T_RefB    1 1 1
300 DaysTillB 1 2 2
301 D3sTCE_Pa 1 1 1
302 D3sTCE_PX 1 1 1
303 Million   1 2 1
304 D3sTCEppm 1 3 1
305 MWsTCE_Pa 1 1 1
306 MWsTCE_PX 1 0 1
307 MWsTCEppm 1 4 1
308 C1_PECH   1 1 1
309 dPIBXdPEC 1 1 1
310 dPEVAxdPN 1 1 1
311 C2_X      1 1 1
312 C3_X      1 1 1
313 C4_X      1 1 1
314 C5_X      1 1 1
-Program Security-
0000
0000
0000
-Mode 4-
-Final Storage Area 2-
0
-CR10X ID-
0
-CR10X Power Up-
3
-CR10X Compile Setting-
3
-CR10X RS-232 Setting-
-1
-DLD File Labels-
0
-Final Storage Labels-
0,Year_RTM,29312
0,Day_RTM
0,Hour_Minute_RTM
1,E19_PIB~34,20270
1,E19_PNVP~35
1,E19_PVTD~36
1,E19_PEVA~37
2,RTDohms~31,5399
3,negResist~112,13752
3,lowB_Volt~113
3,Temp_Malf~114
4,HX94Temp~13,19800
4,HX92RH~14
4,PX215_PSI~15
5,TCE_ppm~132,27880
6,T_Type_D3~251,22622
7,Vbatt~1,25702
8,HEAD_FT~28,20607
9,PSIG_CS40~30,26641
10,RTDTempC~32,12677
11,T_ref~6,7443
12,TCE_ppmR~174,17767
13,Vp_Ambien~131,3217
14,TCE_detec~175,1084
15,E25_PECH~204,25590
15,E25_PNVP~205
15,E25_PIB~206
15,E25_PEVA~207
16,E21RTDohm~185,5416
17,E21_TempC~191,5298
18,E25TCEppm~249,17648
19,E25_ppm_R~250,24801
20,T_TypeMW2~252,15517
21,PX215_Pa~253,23308
21,D_GW_ft~254
21,D_GW_m~255
21,Hh2oE20ft~256
21,Hh20E20m~257
22,E21tcedet~260,22319
22,E21negRes~261
23,HeatBarV~11,15481
24,E21Rtdmal~282,19766
25,340,16339
26,SolarVolt~284,21370
26,SolarWatt~285
27,440,29708
28,Year_RTM,8875
28,Day_RTM
28,Hour_Minute_RTM
29,base_PIB~95,19257
29,base_PNVP~96
29,base_PVTD~97
29,base_PEVA~98
30,BlE25PECH~209,21890
30,BlE25PNVP~210
30,BlE25PIB~211
30,BlE25PEVA~212
31,DaysTillB~300,12750
32,Counter~38,6118
33,D3sTCEppm~304,12331
34,MWsTCEppm~307,6967
```

12.4. Deployment/Chronology of Events at Chemical Waste Landfill

1/30/03

Chemiresistor E19, an HX94 temperature/relative-humidity probe, a PX213 barometric pressure transducer, and a T-Type thermocouple were all wired to the CR23X and deployed at well CWL D3, 60 ft from the top of the well casing.

2/19/03

The submersible pressure transducer CS400 was pulled up from well MW2BL (it had been originally deployed several months earlier). The cable for the CS400 was tethered to a 650-ft length of chemiresistor cable and a T-Type thermocouple using cable ties. The chemiresistor cable containing the chemiresistor E20 was wired to the CR23X. The chemiresistor was positioned 13.4 ft above the submersible pressure transducer. The goal was to have the chemiresistor under 5 ft of water. The three tethered sensors were then deployed at well MW2BL. The constant voltage device was adjusted to yield a constant temperature of 25 ºC. The sensors all appeared to work well for about a week. The voltage applied to E20 was steady, and the RTD temperature and chemiresistor readings were also steady.

2/25/03

The voltage on the 24Ahr battery was dropping to low levels. The T-Type thermocouple and the HX94 temperature sensor in well D3 were reading high temperatures. The PX213 pressure transducer and the HX94 humidity sensor were also reading improperly. We replaced the 24Ahr battery with an 80Ahr Deep Cycle Marina Battery from Interstate. The sensors in well D3 were pulled up for inspection. Rain from precipitation had entered the surface of the well and flowed along the cable, breaching the back of the PX213 sensor and causing a short. The short resulted in the malfunction of the PX213 as well as causing it to heat up. The PX213 and HX94 were removed from the cable and taken back to the lab to troubleshoot.

2/27/03

The PX213 was replaced with a PX215 0-30psi probe. A newly calibrated HX94 was also deployed at this time. The probes were wired to the CR23X and tethered to the chemiresistor cable and T-Type thermocouple.

3/7/03

The HX94 temperature and humidity were not reading accurately. The probe was replaced with an HX92 relative humidity probe. The sensor in the saturated zone in MW2BL (chemiresistor E20) began to read erratic resistances and the RTD temperatures were increasing to above 100 ºC. The E20 chemiresistor (and the other sensors) were pulled up from MW2BL for visual inspection of the chip. Upon visual inspection it was discovered that water had breached the sensor housing. Visual inspection of the actual chip revealed that corrosion had taken place on Pin 1 of the chemiresistor E20. This is the pin that the voltage for the heater bar is supplied.

In order to facilitate the drying of the housing and chip, E20 was removed. Upon removing E20, Pin 1 had become separated from the dual inline package (DIP). Then the cables were separated in order to bring the chemiresistor cable back to the lab for improvements. The CS400 submersible pressure transducer was tethered to the T-Type thermocouple and lowered back down the well.

3/13/03

A new housing was placed on the chemiresistor cable and it was sprayed with Rustoleium to prevent potential rusting, and silicone seal was placed on the seams to prevent water from entering the housing. Epoxy was placed around the leads of the 16-pin socket to provide additional support and to prevent the exposed wires from touching each other. Then the chemiresistor E21 was placed inside the housing and was deployed at MW2BL to approximately 1 ft below the water table (~493 feet deep). Readings were taken on site. The RTD on the chemiresistor was reading high and the polymers all seemed to be behaving erratically. It was suspected that water had breached the sensor housing.

3/17/03

Some slight corrosion had begun to take place on Pin 9 of the DIP.

The chemiresistor sensor was allowed to dry off in the sun and then it was redeployed. Once the chemiresistor dried off, it began to read accurate resistances. The sensor was moved up 6 ft to place it above the water table. However, once the chemiresistor was deployed it began to read erratically. It was suspected that we miscalculated the depth of the ground water and the sensor was indeed in the water again. The sensor was then pulled up some additional feet to ensure that it was not in the water table. It was situated at approximately 483 ft from the top of the well casing.

3/20/03

The chemiresistor cable was pulled up from well MW2BL and E21 was visually inspected. Water had breached the housing again.

There was also more extensive corrosion on the DIP Pin 9. Pin 9 had become separated from the DIP.

The cable was visually inspected while it was pulled up and it was dry, meaning that the sensor was in fact above the water table. Chemiresistor E25 was placed in the socket and resistances were reading for all of the polymers with the exception of PEVA. Using the Fluke multimeter it was determined that corrosion had occurred within the socket. The cable was taken back to the lab to be refurbished.

3/26/03

The sensor housing was tested over a period of six days in a 2-ft high graduated cylinder. No leaking was observed. The chemiresistor E25 was placed in the housing and deployed down

well MW2BL. The sensor is approximately 483 ft from the top of the well casing. The applied voltage, RTD temperature, and chemiresistor resistances all appear to be working properly.

The chemiresistor sensors were successfully deployed at two wells at a remote site. The data is posted to the web in a near real time manner. The program will trip a warning to the website post to the website if a chemical concentration higher then 5000-ppm TCE is detected. Once the malfunctions of the sensors were addressed the sensors have been continuously reading with out incident.

Distribution

External

Dr. Timothy L. Porter
Northern Arizona University
Department of Physics and Astronomy
NAU Box 6010
Flagstaff, AZ 86011-6010
tim.porter@nau.edu

Internal

1	MS-0323	H. Westrich, 1011
1	MS-1079	M. Scott, 1700
1	MS-1425	S. Martin, 1707
1	MS-1425	R. Hughes, 1744
1	MS-1425	S. Casalnuovo, 1744
1	MS-1425	C. Davis, 1744
1	MS-1425	M. Thomas, 1744
1	MS-0892	R. Cernosek, 1764
1	MS-0886	M. Alam, 1812
1	MS-0886	D. Rivera, 1812
1	MS-0865	R. Stinnett, 1903
1	MS-0701	P. Davies, 6100
1	MS-0735	R. Finley, 6115
5	MS-0735	C. Ho, 6115
1	MS-0735	L. McGrath, 6115
1	MS-0735	J. Wright, 6115
1	MS-0735	A. Kooser, 6115
1	MS-0750	M. Walck, 6116
1	MS-0706	D. Borns, 6113
1	MS-0751	L. Costin, 6117
1	MS-0750	T. Hinkebein, 6118
1	MS-1087	F. Nimick, 6132
1	MS-1088	D. Miller, 6134
1	MS-0755	W. Einfeld, 6233
1	MS-0701	W. Cox, 6233
1	MS-1395	Y. Wang, 6822
1	MS-9018	Central Technical Files, 8945-1
2	MS-0899	Technical Library, 9616